DESIGN OPTIMIZATION AND FE ANALYSIS OF AUTOMOBILE BUMPER TO IMPROVE ENERGY ABSORPTION

EYOB SISAY YESHANEW

A thesis Submitted to

Department of Mechanical Engineering

School of Mechanical, Chemical and Materials Engineering

Presented in Partial Fulfillment of the Requirement for Master of Science in Automotive Engineering

Office of Graduate Studies

Adama Science and Technology University

June, 2022

Adama, Ethiopia

DESIGN OPTIMIZATION AND FE ANALYSIS OF AUTOMOBILE BUMPER TO IMPROVE ENERGY ABSORPTION

Eyob Sisay Yeshanew
Advisor: Dr. G. M. Sayeed Ahmed

A thesis Submitted to
Department of Mechanical Engineering
School of Mechanical, Chemical and Materials Engineering

Presented in Partial Fulfillment of the Requirement for Master of Science in Automotive Engineering

Office of Graduate Studies
Adama Science and Technology University

June, 2022
Adama, Ethiopia

DECLARATION

I hereby declare that this Master Thesis entitled “Design Optimization and FE analysis of Automobile Bumpers to Improve Energy Absorption” is my original work. That is, it has not been submitted for the award of any academic degree, diploma or certificate in any other university. All sources of materials that are used for this thesis have been duly acknowledged through citation.

____________________	____________	____________
Name of Student	Signature	Date

RECOMMENDATION

I, the advisor of this thesis, hereby certify that I have read the revised version of the thesis entitled “Design Optimization and FE analysis of Automobile Bumper to Improve Energy Absorption “prepared under my guidance by Eyob Sisay Yeshanew submitted in partial fulfillment of the requirements for the degree of masters of science in Automotive Engineering.

Therefore, I recommend the submission of revised version of the thesis to the department following the applicable procedures.

____________________________	______________	______________
Advisor	Signature	Date
__________________________	______________	______________
Co-Advisor	Signature	Date

APPROVAL PAGE

I, the advisors of the thesis entitled "**Design Optimization and FE analysis of Automobile Bumper to Improve Energy Absorption**" and developed by Eyob Sisay; hereby certify that the recommendation and suggestions made by the board of examiners are appropriately incorporated into the final version of the thesis.

______________________	______________________	______________________
Advisor	Signature	Date

I, the undersigned, members of the Board of Examiners of the thesis by Eyob Sisay have read and evaluated the thesis entitled "**Design Optimization and FE analysis of Automobile Bumper to Improve Energy Absorption**" and examined the candidate during open defense. This is, therefore, to certify that the thesis is accepted for partial fulfillment of the requirement of the degree of Master of Science in Automotive Engineering.

______________________	______________________	______________________
Chairperson	Signature	Date
______________________	______________________	______________________
Internal Examiner	Signature	Date
______________________	______________________	______________________
External Examiner	Signature	Date

Finally, approval and acceptance of the thesis is contingent upon submission of its final copy to the Office of Postgraduate Studies (OPGS) through the Department Graduate Council (DGC) and School Graduate Committee (SGC).

______________________	______________________	______________________
Department Head	Signature	Date
______________________	______________________	______________________
School Dean	Signature	Date
______________________	______________________	______________________
Office of Postgraduate Studies, Dean	Signature	Date

ACKNOWLEDGMENT

First and foremost, thank you to my god, helping me through existence to begin and finish my work. I would like to express my special thanks of gratitude to my instructor and advisor Dr. Gulam Mohammed Sayeed for his valuable advice in carrying out this wonderful project and his help in many research activities. He always helps me resolve the confusion and guide me to the final result of my thesis. He is also a friendly and open-minded person and seems to be a good friend to me. Without his encouragement, and guidance this project would not have materialized and finished. Finally Apart from my efforts, the success of the project depends heavily on the encouragement and guidance of many others. I take this opportunity to express my gratitude to the people who have been instrumental in the successful completion of this project. Specifically I would like to thank my parents and friends who helped me a lot in finalizing this thesis.

TABLE OF CONTENTS

Contents **page**

LIST OF TABLES

LIST OF FIGURES

LIST OF ACRONYMS

ASTM	American society of testing materials
CAD	Computer-Aided Design
CAE	Computer-aided engineering
CATIA	Computer aided three dimensional interactive applications
CFRP	Carbon fiber reinforced polymer
FEA	Finite Element Analysis
FEM	Finite Element Method
FMVSS	The federal motor vehicle safety standard
GMT	Glass Mat Thermoplastic
IGES	Initial graphics exchange specification model
KMPH	Kilometres per hour
LS-DYNA	Liver more dynamic simulation
MPH	Miles per hour
NHTSA	National highway traffic safety administration
PCF	Peak crushing force
SWR	Strength to weight ratio
mm	Millimetre

LIST OF ABBREVIATIONS

mi	Mass of impactor
mv	Total mass of the vehicle
mh	Average mass of humans
E_i	Internal energy
E_h	Hourglass energy
E_d	Damping energy
W_{ext}	Work done by the external forces
E_{ke}	Kinetic energy
E_S	Interface sliding (dissipated contact energy)
E_i^0	Initial internal energy
E_{ke}^o	Initial kinetic energy
Fmean	Average force
Fpeak	Peak of the force
E_{11}	Transversal Young's modulus (GPa)
E_{22}	Longitudinal Young's modulus (GPa)
G_{12}/G_{31}	Transversal Shear modulus (GPa)
G_{23}	Longitudinal Shear modulus (GPa)
ρ	Mass density(kg/m^3)
XC	Longitudinal compressive strength (GPa)
XT	Longitudinal tensile strength (GPa)
YC	Transverse compressive strength (GPa)
YT	Transverse tensile strength (GPa)
η	Crush force efficiency (%)

ABSTRACT

*Bumper is one of the main parts which are used as protection for passengers from front and rear collisions. The emission of harmful gases and fuel efficiency of vehicles are two important issues in these days. The best practice to improve fuel economy is to reduce the weight of vehicle parts. Bumper is one of the parts that have slightly more weight. This thesis was aimed to improve the crashworthiness of the existing automobile bumper to minimize crash injuries. The automobile bumper was analyzed for frontal collision. Based on the analysis results obtained from the existing model of automobile bumper then modifications are made by means of changing the geometry, using a composite material and optimizing the thickness of bumper. Then the modified bumper was analyzed under the same condition as the existing one. Software's like that of CATIA and SOLIDWORKS was used for 3D modeling and LS-DYNA for simulation and FEM analysis. The result of the simulations shows that the weight of the carbon polyamide bumper is reduced as compared with the existing steel bumper by 9.7 kg or 52.5%, with this reduction in weight 42% increase in fuel economy*___;___ *the energy absorption capability of carbon polyamide bumper is improved from the existing steel and aluminum bumper by 11.15% and 16.3% respectively and with this modification, the impact force is reduced from the existing steel bumper, which has 9.78 kN and aluminum alloy bumper, which has 4.10 kN to 1.86 kN. the crashworthiness parameter result analysis showed that the corrugated bumper geometry had a structural energy absorption (SEA), total energy absorption (TEA) and crush force efficiency (CFE) of 103.28J/kg, 911J and 77.99%, which is higher than the hallow bumper geometry of 102.4J/kg,847J and 65.83% respectively. In addition to that, as the thickness of carbon polyamide bumper reduced from 4mm to 3.5mm, 3mm and 2.5mm, deformation increased with a small rate from 13.5 mm to 16.7, 18.52 and 22.04 respectively, this does not mean that a bumper with less thickness is always better because more deformation means that there is probability of intrusion in to the vehicle main compartments. So it can be concluded that a bumper with 3mm thickness* is *the optimized model, the safety and crashworthiness of the automobile bumper was greatly improved without affecting the appearance and safety of the existing models.*

Keywords: *Automobile bumper, Crash worthiness, Finite element analysis, LS-DYNA.*

CHAPTER ONE

1. INTRODUCTION

1.1 Background

One of the biggest challenges we face in the world today is to provide optimal, efficient, cost-effective and environmentally friendly transportation services. Designing a car that is economical, safe and aesthetically pleasing has been a major challenge for designers. Today's automotive structures suffer from a fundamental drawback: short shatter zones to absorb impact energy. By using a good bumper, it is possible to ensure the safety of the occupants to some extent in the event of a vehicle accident (Sonawane & Shelar, 2018).

An automobile bumper is the most critical structural component placed at the front and the rear end of the vehicle which is a highly exposed area during low-speed accidents. Bumpers are not capable of reducing injury to vehicle occupants in high-speed impacts, but advanced-level bumpers are being designed to mitigate injury to pedestrians hit by cars. The main habit of vehicle driven on streets bumper search out make less the impact all the while accident and enhance the management and efficiency level of the means of attaining end(G Keni et al., 2021).

A bumper is a productive element made up of well-known materials such as aluminum, plastic, and steel, etc., which is locating on both the ends of the automotive vehicle. The prime aim of the bumper is to provide the safety and security to the passengers by absorbing the impact energy when low speed collision occurs in the car. The existing bumper has capable to withstand high amount load with more weight. More pressure intensely reduces the fuel efficiency and by that influences the effectiveness of the vehicle driven on streets. Hence, the reduction in the weight with high withstanding capability is the fundamental need of the future vehicle’s bumper (Raj Kumar et al., 2019).

In the case of a crash accident, a bumper is expected to be collapsed with absorbing crash energy before other body parts so that the damage to the main body frame is reduced and passengers are saved. Energy generated from the collision of vehicle has been absorbed mainly by the plastic deformation of the bumper material(Muhammad Nasiruddin, Hambali, Rosidah, Widodo, & Ahmad, 2017).

Figure 1.1 shows the schematic view of vehicle front structure which mainly includes a cover, absorber, coolant and crash bracket. The absorber is arranged below to the cover and mounting elements is used to connect a cover and absorber to the vehicle body whereas the crush brackets and metal bumper supports during slow impact and protect nearby engines parts. The automotive bumper protects the grill, hood, fuel and exhaust systems, cooling system and helps in towing capabilities of the vehicle.

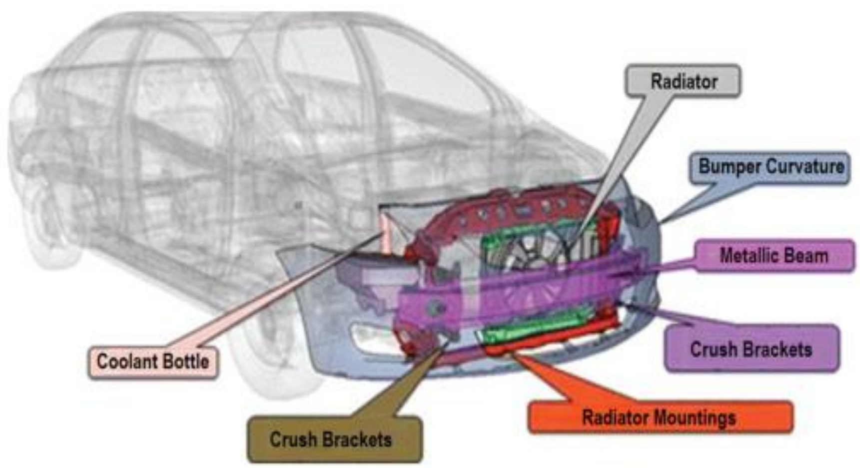

Figure 1.1: Vehicle front structure(Sonawane & Shelar, 2018).

The introduction of composite materials will make it possible to reduce the weight of the bumper without any reduction on load carrying capacity and stiffness. Since this material has more elastic strain energy, can withstand high amount of load, durability, corrosion resistance, design flexibility, resiliency and high strength-to-weight ratio as compared to those of steel and will offer the opportunity for substantial weight saving (Raj Kumar et al., 2019).

A composite material is a combination of two or more materials that results in better properties than those of the individual components used alone. Composite materials have been used for decades starting in the ancient Mesopotamia and Egyptians, where wood strips were used to make a plywood and straw to reinforce mud bricks. Nowadays, composite materials are commonly used in several field of engineering, especially in the aerospace and automotive industries.

Comparing to metals, composite materials have extreme substance to weight percentage. In addition, composites have high corrosion and wear resistance, good fatigue life and thermal conductivity. These mechanical properties make composite materials attractive in engineering applications that require high strength and stiffness while maintaining low weight. Composite fabric usage fashionable in aerospace, military, machine used for transportation, transportation, transport construction, infrastructure, playful personal possessions and the power manufacturing exist increasing occurring every day (Yalkın, Karakuzu, & Alpyıldız, 2020).

The study will focus on design analysis for absorbing kinetic energy during the collision and sudden accident, considers different reinforcement materials to withstand the impact of the crash, that causes serious damage and also investigate the most suitable optimized design for Toyota Camry automobile bumpers using Computer-Aided Engineering. In addition to the bumper's mechanical properties, the improved bumper has increased and improved performance when compared to the existing one. The main objectives envisaged from this thesis are to improve the energy absorption of the bumper model during a crash while also reducing the damage suffered by the engines and occupants.

1.2 Statement of the problem

Nowadays traffic accident rate of automobile vehicle is becoming higher and higher. Due to a much less energy absorption capability of the existing automobile bumper, engine, radiator and other front most components of a vehicle are fully damaged. Customers also blame to the manufacturer that the bumpers are easily damaged even with slight collision. Hence, vehicle safety is an important research area to protect the occupants as well as the structures of the vehicle during an impact. So, to alleviate traffic accident, injuries, causalities and damage of vehicle components, developing the best energy absorbing bumper model, using a 3D-printed carbon polyamide composite bumper, employing suitable bumper geometry design is necessary to protect the vehicle structure as well as minimizing the severity of human injuries.

1.3 Objectives

1.3.1 General objective

The general objective of this thesis is to optimization and improvement of automobile bumper energy absorption for Toyota Camry vehicles using FE Analysis.

1.3.2 Specific objectives

The main objective of this research is achieved through the following specific objectives:

- ✓ Crashworthiness studies of the existing bumper including structural details and materials overview in the bumper system
- ✓ Model and analyse the stuctures of the existing bumper
- ✓ Modify the bumper geometry with crashworthiness features and analyze it
- ✓ Optimizing the newly design bumper geometry
- ✓ Compare the newly design with the existing bumper

1.4 Significance of the Study

In order to protect natural resources and economize energy, weight decline has been the main focus and something that begins concerning this carbon poly amid composite materials will manage likely to reduce the weight of the bumper without any reduction on load carrying capacity and stiffness. Since this material has more elastic strain energy, flexibility, cost benefit, features crumple zones (which allows the material to flex upon collision in order to absorb the impact and returns to its original shape) and high strength-to-weight ratio as compared to those of steel and will offer the opportunity for substantial weight saving. In this work, estimation of stress and deformation of carbon poly amid material by static analysis is done and check whether the design is safe or not.

1.5 Scope of the Study

The study focus on existing design performance, advantage, and limitations. Based on observations, design improvements and optimization was made in terms of shape, size and/or material based on design modification objectives. Toyota Camry 2012 model car front bumper design was tested using FEM software for impact loads and strength analysis as per international standards. Finally comparison of the modified bumper with the existing one is done.

1.6 Limitations

Through conducting this study the following challenges were encountered;

- Due to high cost of experimental crashworthiness test, this thesis work focuses only on the numerical aspects of automobile bumper crashworthiness improvement.

- The usage of numerical method also required a high performance computer and original software package. Since it was very challenging to get such kind of machines, so with the use of low performance computer and cracked version of software the required results were obtained by waiting for more than a week.

1.7 Organization of the thesis

This thesis consists six chapters. The first chapter is an introduction to the study. It includes the background of the study, statement of the problem, objectives, significant of the study, scopes, limitation and structure of the thesis. Chapter two focuses on different kinds of literature that emphasize on study of automobile bumper design optimization and crashworthiness analysis. Chapter three describes materials and methods used to complete this work. Chapter four explains the detail of the modeling and analysis procedures used for analyzing the existing and modified automobile bumper. It also described the methods and material used for developing the safety development of automobile bumper. Chapter five presented the result of different computational simulation were imported and discussed. It shows the result and discussion of the modifications, existing and modified model of automobile bumper. Finally, conclusion and recommendation is included in chapter six.

CHAPTER TWO

2. LITERATURE REVIEW

Reviewing of the existing literature provides insight for creating a better design and reduction of injury in automobiles during accident in Ethiopia. Different researches were done on different bumper analysis in different material, method and experiment in the world in terms of cost effectiveness and reasonable for uses. This is done by using different approaches;

2.1 Bumper system Construction

In most crash events, the vehicle's front and rear bumper systems collide first (Davoodi et al., 2011). Instead of the simple rubber and plastic covers of the last few years, modern bumper systems have been made up of many sub-components.

Figure 2.1 below shows a modern car bumper system assembly located at the front and rear of the car. Bumper fascia made from polyurethane material was intended to provide better aerodynamics at low speed impacts and to serve the purpose of absorbing energy. Polystyrene foam inserted into the back of the bumper fascia to absorb most of the impact energy during low speed impacts. Both absorb another high level of impact energy dissipation from the cross member made of structural steel and the energy absorber located behind it. The mainframe is constructed of ultra-high-strength steel (UHSS), which acts as a force-applying channel and sends excessive impact force to the compartment. Nevertheless, it also provides an engine or transmission mounting point.

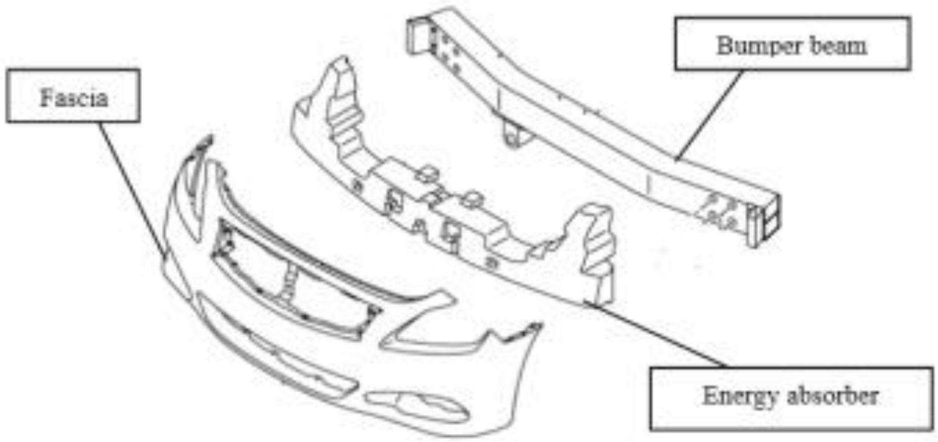

Figure 2.1 Components of automobile bumper(Muhammad Nasiruddin et al., 2017).

The collision safety performance of the entire bumper system is expected regardless of the collision speed. “The front end of the car is sturdy enough with foam inserts and bumper fascia to absorb a small amount of energy at low speed impacts without further damage to the critical components behind such as radiators, intercoolers, condensers, etc. In high speed crashes, the foam inserts and fascia direct the impact force around the bumper, but the cross members and energy absorbers also need to be fully deformed to dissipate large amounts of impact energy in the event of an impact. This led to the belief that there were many improvements in the design of the bumper car system. This theory has been proved by many previous types of research, including: Uses of composite material to replace traditional metal bumper parts and improve both impact resistance and light weight” (Belingardi, Beyene, Koricho, & Martorana, 2015). “In addition to all the above investigations, we also explored the possibility of hybrid material replacement to improve collision safety for the frame elements and energy absorbers behind the bumper beam” (Zhong, Ding, Song, & Geng, 2019).

2.2 Requirements of Bumper Material

Determining the right material during the selection process is very important. The material chosen for the bumper must meet the expectations of the engineer. The material should prove to be mechanically feasible and economical. Apart from this the materials selected should be more convincing than the materials currently in use.

The proposed material properties help material engineers to select the right material in the selection stage (Prabhakaran, Chinnarasu, & Kumar, 2012).

The selection of material for automotive bumper depends on the following factors and Requirements:-

- Able to absorb more energy while in collision
- High resistance to rust
- Low cost
- Light in weight
- availability of the material
- environmental condition
- Easy for large scale manufacturing, and others (Ezekwem, 2016).

2.3 Types of bumpers

2.3.1 Carbon Fiber Bumpers:

Carbon fiber reinforced polymers, or often carbon fiber, are very strong and lightweight fiber reinforced plastics that contain carbon fiber. “The polymers commonly used for bonding are primarily thermosetting resins. Epoxy is one of the thermosetting resins. Other thermosetting or thermoplastic polymers may also be used. Such polymers are polyester, vinyl ester or nylon. The strength and stiffness required for carbon fiber reinforced polymers are achieved by reinforcement as measured by stress and modulus, respectively. Unlike isotropic materials such as steel and aluminum, CFRP is directional” (GV, Reddy, Manoj, & Bhaskar, 2014).

CFRP has excellent corrosion resistance. Exposure to moisture over a wide temperature range can reduce the mechanical properties of CFRP, especially at the matrix-fiber interface. Carbon fiber bumpers are lighter than traditional steel bumpers. Carbon fiber bodywork is usually that of supercars, but many automakers and special modifiers are starting to use it instead of everyday car body panels (Gao, Liang, Shi, & Cao, 2019).

2.3.2 Aluminum Honeycomb Sandwich Panel Bumpers:

The geometry of a honeycomb minimizes the amount of material used. So, it minimizes costs and weight. This aluminum honeycomb is made by an expansion process. This type of structure consists of two thin skins separated by a core material. Aluminum honeycomb panel ensures lightweight, high rigidity and high structural stability (Ryan, Hedman, & Christiansen, 2009).

2.3.3 Steel Bumpers:

Originally, plated steel was used for the entire body including the bumper. This material worked well because it was so powerful at the time of the crash, but it was very heavy and dented performance. “Due to the improved engine design of the car, all steel bumpers except classic cars has almost disappeared. To replace one, need to clean a lot of scrapped cars or have one custom made” (Smith, Szyniszewski, Hajjar, Schafer, & Arwade, 2012).

2.3.4 Plastic Bumpers:

Most present day modern cars use a strengthened thermoplastic bumper, as they're reasonably-priced to manufacture, smooth to match and soak up greater strength for the duration of a crash. “A majority of automobile bumpers are custom made for a particular model, so in case you are seeking to update a cracked bumper with a comparable one, you will have to shop from a consultant dealer. However, many agencies now provide opportunity designs in thermoplastic, with various fittings designed for exceptional models” (GV et al., 2014).

2.3.5 Metal Foam Bumpers:

Foam metal is an ultra-lightweight material because it has a bubble structure consisting of solid metal and pores. Aluminum and its alloys are used as foam metals due to their low density. Foam metal bumpers have high compressive strength. There are generally two types of foam metal, open type and closed type. “In the automotive industry, closed types are mainly used to manufacture bumpers that provide optimal energy absorption” (Pandey, Singh, Khanna, & Murtaza, 2021).

2.4 Composite overview

Nowadays, almost every part of an automobile has been tested with various materials such as composite materials, and it is also used boldly for bumpers. Composites are preferred over traditional steel bumpers for weight savings. Composite bumper absorbs more collusion energy than steel bumper (Sarfraz, Hong, & Kim, 2021).

One of the most beneficial reasons to consider using composites over steel is:

- weight reduction
- Absorb more collision energy
- Excellent corrosion resistance
- High impact strength
- Material properties of composite bumper allow rapid response to induced or release stress (Ezekwem, 2016).

2.4.1 Glass Fiber

Glass Fibers are among the most adaptable industrial materials known today. They are willingly manufactured from raw materials, which are available in virtually unlimited supply. Glass fiber is manufactured by blending raw materials, melting them in a three-stage furnace, extruding the molten glass through a nozzle at the bottom of the fore hearth, cooling the filament with water, and applying chemical sizing. "The filaments then are gathered and wound into a package. All glass fibers described in this article are derived from compositions containing silica. They exhibit useful bulk properties such as hardness, transparency, resistance to chemical attack, stability, and inertness, as well as desirable fiber properties such as strength, flexibility, and stiffness. Glass fibers are used in the manufacture of structural composites, printed circuit boards and a wide range of special-purpose products. Over 95% of the fibers used in reinforced plastics are glass fibers, as they are inexpensive, easy to manufacture and possess high strength and stiffness with respect to the plastics with which they are reinforced. Their low density, resistance to chemicals, insulation capacity are other bonus characteristics, although the one major disadvantage in glass is that it is prone to break when subjected to high tensile stress for a long time" (KHAN, 2021).

Some of the fundamental properties of glass fiber are:

- Specific Strength
- Low density
- Corrosion resistance
- Impact resistance
- Electrical properties (Ezekwem, 2016).

Glass is the most usually used fibers in polymer matrix composites. The most frequently used fiberglass is E-glass, S-glass, R-glass, C-glass and D-glass fiber. E in E-glass put for electricity outline for electrical applications. E-glass Fiber is a favorable standard glass fiber that is used as a qualify strengthening for all resin systems and also meets the need of mechanical properties.

Thus E-glass fiber was found suitable for many applications. “In S-glass S stands for higher content of silica. It retains its strength at high temperature and has higher fatigue strength. It is used mainly in aerospace applications. In C-glass C stand for corrosion, it is designed to give improved surface finish. It is available usually in the form of a surface tissue for the reinforcement of corrosive barriers in chemical plant. In D-glass D stands for dielectric used for applications requiring low electric constants” (Prabhakaran et al., 2012).

Glass fiber is most widely used as reinforcement for all composites due to the following advantages:

- Molten glass easily drawn into high-strength fibers
- Readily available/easy to fabricate
- Relatively strong fibers produce very high strength in composite form
- Chemically insert in plastics

These materials are limited to low temperature applications where strength is important without the need for high rigidity. Typical uses for this material are boat hulls, flooring materials and automobile bodies. “The main type of glass used is E-glass. However, it is used for many other purposes now such as decorations and structural applications” (Prabhakaran et al., 2012).

2.4.2 Epoxy Resin

Epoxy resin is the highest performance resin currently available. For a composite material, epoxy material is most utilized. Epoxy has extremely good properties and it acts as very good adhesive, it has high strength, low shrinkage and it is a very fine anti corrosive material. "They generally function more effectively in the joining process than other resin types in terms of mechanical properties and resistance to environmental degradation, making them almost exclusive for use in aircraft technology components. As a laminated resin, it has improved adhesiveness and water resistance, making it ideal for applications such as marine engineering. For this reason, epoxies are often used as the main building material for its high performance behavior" (Mohan, 2013).

The main reasons for epoxy being the most used polymer matrix materials are

- Good compatibility with Glass fiber
- High strength
- Low viscosity and low flow rates, which allow good wetting of fibers and misalignment of fibers during processing
- Low shrink rates which reduce the tendency of gaining large shear stresses of the bond between epoxy and its reinforcement
- Available in more than 20 grades to meet specific property and processing requirements

2.4.3 Carbon polyamide

- ✓ Fiber-reinforced polymer (FRP)

FRP consists of two material phases: fiber and polymer matrix. Fibers are impregnated into the polymer matrix to form a macroscopically orthotropic layer of material with significantly higher mechanical properties along the fiber direction compared to the transverse directions. The advantages of using FRP are the high strength and stiffness-to-weight ratio along the fiber direction, ease of application in construction due to its light weight, corrosion resistance, electromagnetic inertness, and design versatility in which high strength and stiffness (fibers) may be oriented where needed in design. "Continuous fibers become extremely strong and stiff as fiber diameter becomes smaller due to the reduction and sometimes elimination of defects in the microstructure.

On the other hand, small-diameter fibers are not capable of carrying axial compression or shear stresses due to the lack of shear transfer medium between them. Thus, the fibers are embedded into a polymeric matrix that binds them together and allows load transfer by shear among the fibers" (Abbood, aldeen Odaa, Hasan, & Jasim, 2021).

- ✓ Carbon fibers

Carbon fiber has been used to reinforce both aliphatic and aromatic polyamides. Aliphatic polyamides are called nylons, and aromatic polyamides are often called aramids. Among the aliphatic polyamides, polyamide 6, polyamide 11, polyamide 12, and polyamide 10 have been used as a matrix of carbon fibers. Where the numbers indicates for the number of carbon atoms. "Factors affecting the properties of polyamide/carbon fiber composites are: fiber amount, fiber length, fiber orientation, matrix viscosity, matrix-fiber interactions, matrix-fiber adhesion, and conditions encountered during manufacturing processes. Polyamide/carbon fiber composites are lightweight and exhibit high strength, modulus, fatigue resistance, wear resistance, corrosion resistance, gear, electrical conductivity, thermal conductivity, chemical inertness, and thermal stability. Incorporation of oxidized or modified carbon fiber and nanoparticle modified carbon fiber into polyamide matrices have been found to further enhance their physical properties. Applications of polyamide/carbon fiber composites in aerospace, automobile, construction, and others" (Kausar, 2019).

- ✓ Polyamide Matrix

Polyamide (PA) is an engineering thermoplastic material (a class of polymer that can be softened through heating and then processed using methods such as extrusion, injection molding and others). "Polyamides have been frequently used in fibers, films, and sheets owing to fine mechanical and thermal properties. Polyamides exits in both the aliphatic and aromatic forms" (Kutz, 2011).

- ✓ Polyamide (pa, Nylon 6/6, Nylon 6)

Nylon 6/6 is a general-purpose nylon that can be both molded and extruded. "Nylon 6/6 has god mechanical properties and wear resistance and frequently used when a low cost, high mechanical strength, rigid and stable material is required. Nylon is highly water absorbent and will swell in watery environments" (Meng et al., 2019).

Applications: gears, bushes, cams, bearings, weather proof coatings.

Polyamide has excellent transparency, high strength, elastic modulus, rigidity, hardness, Chemical resistance, heat resistance, hygroscopicity (moisture absorption capacity) (Amintowlieh, Sardashti, & Simon, 2012).

Table 2.1 Mechanical properties of carbon poly amid material (Kausar, 2019)

Materials	Elastic Modulus (GPa)	Strength (MPa)
CF (carbon fibers)	230	4000
PA6	2.4	82
PA6/CF	8.2	1308

2.4.4 Polyurethane material (PUR)

Two new polyurethane-based polymer materials were used in the design of automobile bumpers. (1) Rigid Polyurethane 60 (RPU60); (2) Flexible Polyurethane 40 (FPU40). We tested the impact strength of flexible polyurethane elastomers. The polymer showed hyper elastic behavior and showed great elongation, but recovered completely upon unloading. RPUs are commonly used for insulation applications. Several composite foams made from RPUs fortified with the polyhedral oligomer silsesquioxane have been developed and characterized, and improvements in bending and compressive strength have been observed with the composite foams. Therefore, it was determined that it was worth studying the use of FPU and RPU in the structural applications of automobiles. Rigid polyurethane is a versatile material that is inherently rigid. Its applications are widespread in industries including industrial products, automobiles and consumer goods. RPU has high rigidity, high strength, and maximum tensile strength of 48MPa. Flexible polyurethane provides high impact resistance and excellent surface finish, making it an ideal raw material for 3D printing or additive manufacturing applications.

Table 2.2 Mechanical properties of flexible and rigid polyurethane (Begum, Ahmed, Badruddin, Tirth, & Algahtani, 2019).

Tensile properties	RPU	FPU
Tensile modulus	1600 MPa	860 MPa
Ultimate tensile strength	48 MPa	30 MPa
Yield strength	42 MPa	21 MPa
Yield point elongation (%)	6	8

2.4.5 ABS

Acrylonitrile-butadiene-styrene is a copolymer made by polymerizing styrene and acrylonitrile in the presence of poly-butadiene. Styrene gives the plastic a glossy, impermeable finish and butadiene, a rubbery substance, provides elasticity at low temperatures. Various changes can be easily made to improve impact strength, heat resistance and toughness.

Applications: automobile body parts, dashboards, wheel cover.

2.4.6 Polypropylene (PP)

Polypropylene is a thermoplastic polymer utilized in many of applications. As a saturated addition polymer made from the monomeric propylene, it is robust and highly resistant to many chemical solvents, bases and acids.

Applications: car bumpers, chemical tanks, cable insulation, petrol cans, carpet fibers.

Table 2.3 Mechanical properties of the ABS Plastic and polypropylene (Uddandapu, 2013)

Thermoplastic materials	Density (kg/m^3)	Youngus modulus (MPa)	Poisons ratio
ABS	1020	2240	0.39
Polypropylene (PP)	940	3500	0.42

The main purpose of bumper is to absorb shock in case of the collision. Several materials have been used to develop these shock-absorbing capabilities, such as steel, aluminum, glass mat thermoplastics and long fiber thermoplastic. In this research we choose carbon poly-amid composite material to compare the performance of the materials during impact testing. The purpose of this document is to design bumpers aimed at improving the impact resistance of bumpers. Collision safety is the bumper's ability to prevent occupant injuries in the event of an accident. This is achieved by minimizing the impact force in the event of a collision. Some of the mechanical properties of the bumper materials are shown in table 2.4 below:

Table 2.4 Mechanical Property of Bumper Materials(Jeyanthi, Paul ChandraKumar, Rajesh Kumar, Dhinakaran, & Hari Prasad, 2014)

Materials	Young's Modulus, (GPa)	Poisson Ratio	Yield Strength (MPa)	Density (kg/m³)
Steel	210	0.3	700	7850
Al	70	0.33	480	2710
GMT	12	0.41	230	1280
CFRP	140	0.3	1550	1950

2.5 vehicle safety standard for bumper

The National Highway Traffic Safety Administration (NHTSA) has created several bumper standards for light passenger cars to know the performance requirements of passenger cars in low-speed front and rear collisions. It is applied to the front and rear bumpers of passenger cars to prevent damage to the vehicle body and safety-related equipment. All bumper manufacturers must meet the following criteria:

- Passenger car front and rear bumpers are designed to prevent damage to the car body.
- Components such as radiators, headlights, etc. that are placed immediately after the bumper should work the same as before and after the impact.
- The bumper must withstand the impact force generated by a parked vehicle with a full width of 4.023 km / h (2.5 mph) and a corner impact of 1.609 km / h (1.609 km / h).
- The bumper placement is 16 to 20 inches above the road surface (Prabhakaran et al., 2012).
- According to the ECE standard, the impactor collides with the bumper system in a straight direction. “The velocity of the impactor is 4 km/h, and the height of the impactor baseline is 445 mm away from the ground at the same time the baseline keeps horizontal” (Wang & Li, 2015).

All bumpers must meet the above criteria. European carmaker case studies track bumper safety parameters.

- Low speed impact test: Impact test on longitudinal pendulum by 4 km/h, and corner pendulum impact test by 1.0 km/h with visual, functional and safety damage to the bumper.
- high speed impact test: “No bumper damage or yielding after 8kmph (full impact) frontal impact into a flat, rigid barrier” (Motgi, Naik, & Kulkarin, 2013).

The Insurance Institute for Highway Safety (IIHS) front-crash tests are quite different from NHTSA's in that they’re designed to emphasize the structural integrity and restraint performance of the vehicle. Vehicles are rated as good, acceptable, marginal, or bad based on the structure of the vehicle and the forces acting on the dummy.

During the full overlap head-on collision test, the vehicle is given an initial speed of 10 km/h. The front part of the lower end of the impact barrier is 457 mm above the ground. In the event of a collision, the vehicle centerline will coincide with the barrier centerline. The vehicle collides with the barrier at 10 km / h. After the vehicle has stopped, the damage to the vehicle is analyzed.

In the front corner impact test, the vehicle's initial velocity is 5 km / h. The guardrail is installed so that the front part of the lower end of the guardrail is 406 mm from the ground. In a collision, the vehicle overlaps the side edge of the barrier by 15% of Vehicle width as Measured from the wheel wall of the relevant axle, including moldings and sheet metal overhangs. That is, Front axle for front corner test and rear axle for rear corner test. The vehicle collides with the barrier at 5 km / h. After the vehicle has stopped, the damage to the vehicle is analyzed.

It is important to note that the assumptions used during the impact test are: A material that is considered isotropic; all welds, bolts and rivets are considered safe; buckling fracture is not considered, and the work hardening effect of the material by stamping the parts being manufactured is not considered.

Figure 2.2 Full frontal impact and front corner impact (Sonawane & Shelar, 2018).

2.6 Vehicle Crashworthiness

The concept of collision safety aims to determine the level of protection a vehicle can achieve. Crashworthiness types, conditions, and parameters were developed primarily by automakers to reduce the potential for damage to the vehicle itself, reduce occupant injuries, and meet vehicle safety standards. Ideally, to obtain post-impact behavior and relevant data, perform physical impact strength tests to improve on the original design. This means how to destroy a prototype vehicle by hitting it against a hard impact object such as a concrete wall or pole. The impact process produces crash records and relevant data for engineers to assess and further improve the safety of the vehicle. Due to the complexity of the crash safety process, preparing for each crash test is expensive and time consuming, and the data is only useful in a particular category (front, back, or side). To fine-tune a vehicle's collision safety performance, multiple collision safety tests are required to understand the vehicle's comprehensive post-collision behavior and tests must be performed in each categories to achieve comprehensive security objectives. As a result, it is inevitable that prototypes will be partially or completely destroyed during testing and discarded, and more prototypes will be needed for further testing. This adds cost and time to the development process. Therefore, crash tests are very expensive.

Compared to high speed crash tests, collision test speed ranges such as low speed and medium speed occurred more frequently than in high speed scenarios. Therefore, a bumper system is specially installed on the front of the vehicle to alleviate this problem.

The bumper system is designated to be sacrificed to dissipate at least some of the impact energy without transmitting a significant amount to other parts of the vehicle and causing more damage. “Because such a system is located at very front of the vehicle, and most likely in contact with the impact object regardless of the impact type and speed. Thus, it is essential to have good crashworthiness performance on a bumper system” (Zhang, 2020).

2.6.1 Crashworthiness Test Dynamic

The impact resistance of bumper tests is primarily dominated by either physical impact analysis or computer-assisted finite element crash test simulations. Prior to the advent of computer simulation, material impact testing was the only option. Material testing is a simple and objective crash test of an automobile during the research and design stages. Manufacturers need a specific crash environment to perform actual crash tests. Different types of impact targets with different weights. On the other hand, special equipment is required because the car needs to be pulled or pushed at different angles with respect to a particular speed or impact object. In addition, electronic devices such as sensors and computers are essential to measure all correct readings of the vehicle after being affected by post-collision analysis, style changes, and other improvements. Manufacturers also mass-produce car parts or assemblies and consider many scenarios that need to be repeatedly tested to determine the optimal combination. Therefore, it is possible to optimize the part or assembly in this way to find the best combination. In physical crash tests, the test vehicle can only be used once at a time. Test samples such as parts, assemblies and finished vehicles are discarded after testing. Therefore, the test sample loses its commercial value. Development cycles, crash tests, redesigns and retests are also quite time consuming and costly. As a result, physical impact safety appears to be less efficient in terms of time, cost, and labor.

2.6.2 Crashworthiness test FEA simulation

Computer-aided engineering (CAE) and finite element analysis (FEA) were used by supported automakers. During the early development of Computer Aided Simulation for crash tests, simulation results were limited due to low computational power. As a result, fully automated simulations are difficult to perform, and local designs can perform less complex simulations, which impacts the speed and accuracy of the simulation process and is almost unsuccessful. Therefore, the overall benefits of CAE and FEA simulations have not been fully investigated and demonstrated and did not meet the manufacturer's requirements. Due to the breakthroughs in computer science and the dramatic expansion of hardware and software functionality over the last decade, this upward trend has led to widespread and accepted CAE and FEA simulations for automobiles in the automotive industry. It has become a very viable solution for impact resistance testing.

CAE and FEA simulation techniques have many advantages over traditional physics testing. First and foremost, the model computer drawings reproduce the model involved in the crash test on a 1: 1 scale. Materials and historical details are also created and further manipulated to suit individual needs based on design parameters. Second, it saves time and money because you don't have to present a physical device. Third, all aspects of testing are performed early in the development cycle, significantly reducing lead times for new products. The design team can gain a wide range of background knowledge without having to create a large number of prototypes. Therefore, the quality of the final product is expected. “In addition, all parameters are highly customizable, and the design team can iteratively fine-tune certain parameters until they meet the design objectives, so the progress of the simulation is reproducible” (Costas, Díaz, Romera, & Hernández, 2014).

2.7 Finite Element Analysis

Many engineering problems are dominated by differential or integral equations. The solutions of these equations provide an exact closed-form solution of these equations for the particular problem under study. However, the complexity of geometry and boundary conditions inherent in most real-world problems usually means that impossible to get an accurate solution or get it in real time. But current product design cycle times imply that engineers need to get design solutions in a short amount of time. They are happy to get an approximate solution that can be easily achieved with reasonable effort in a reasonable time frame. The FEM is one such approximate solution (Andersson, Schedin, Magnusson, Ocklund, & Persson, 2002).

The function of the method is to analyze the performance of the structure. It is also a calculation method that predicts how the product will respond to actual forces, vibrations, stresses, heat, fluid flow, and other physical effects. “Finite Element Analysis (FEA) is a numerical method to find an approximate solution to a partial differential equation. Widely used in the field of mechanical system design which can explained the behavior of individual element with simple equation, and this set equation described the behavior of the whole structure when combine with big set of equation” (Costas et al., 2014).

The finite element method works by discretizing the continuum, selecting interpolated functions, finding the properties of the elements, constructing the element equations, solving the global system of equations, and computing additional results. The finite element method

(FEM) is a numerical method like the finite difference method, but it is more general and powerful in its application to real problems. “By using FEM for the machine structure in analysis, it was possible to generate values of stresses and displacements for both situations which allowed the choice of suitable design for structural components of a machine coffee harvester”(da Silva, da Silva, & Magalh, 2014).

Finite element analysis was performed in three steps: pre-processing, resolution, and post-processing. “Equivalent von Miss stress, total deflection, and impact force plots can be easily calculated using FEA analysis” (Purohit, Khitoliya, & Koli, 2014).

2.8 Basic Governing Equations

Many practical design systems are required to absorb energy in the event of a collision. An energy absorber (in the context of impact resistance) is a device that converts dynamic impact energy into another form of energy, thereby reducing the peak damage transmitted to the structure protected by it. Energy is completely or partially absorbed. The ideal energy absorber is defined as maintaining the maximum permissible deceleration force over the entire stroke.

The integration of the force-deformation curve provides the energy absorption of the corresponding deformation. Some concepts and terminology related to energy absorption and its measurement are described below.

- **Mean or average crush load (F_{avg})**: It is defined as the absorbed energy divided by the current deformation. It is better to use mean crushing load to compare different energy absorbers. This is an important parameter used in all analysis throughout this research.

$$\mathrm{Favg} = \frac{EA\,(absorbed\ energy)}{deformation} \qquad \text{Eq (2.1)}$$

- **Peak crushing force (PCF) (F_{max}):** It is the maximum force which occurs during folding of tubes. This force should be kept equal to/preferably below a certain level in case of automobile crash safety design as a large Peak Crushing Force generally leads to high acceleration of the passenger.

$$\mathrm{Fmax} = Curb\ weight\ of\ thebumper\ (Kg) \times gravity(m/s^2) \qquad \text{Eq (2.2)}$$

- **Crush force efficiency (CFE):** It is the ratio between the average crushing load (F_{avg}) and the maximum crushing load (F_{max}), and it can be obtained from the equation:

$$\text{CFE}\ (\eta) = \frac{\text{Favg}}{\text{Fmax}} \times 100 \qquad \text{Eq (2.3)}$$

This is a very important parameter to evaluate the performance of the structure during the crushing process. It is a useful measure of the uniformity of collapse load; for the ideal energy absorber, $\eta = 1$.

$$\text{Total energy absorbed (TEA)} = \int_0^l F(x)dx \qquad \text{Eq (2.4)}$$

Where l is the effective crush stroke and $F(x)$ is instantaneous crush force applied.

- Structural energy absorption (SEA) is the ratio of total energy absorbed (TEA) by the structure through plastic deformation to the total mass (m) of the structure. The ideal requirement is to absorb a maximum amount of impact energy with a minimum possible mass of the EA structure. In today's automotive industry, structures with superior performance-to-weight ratio are highly appreciated. The SEA is expressed as:

$$\text{SEA} = \frac{\text{TEA}}{\text{m}} \qquad \text{Eq (2.5)}$$

2.9 Impact Theory

Moving vehicles have enormous kinetic energy and impact force, and in the event of an accident, they must absorb that enormous impact force, which can be extremely deadly and disastrous. "The amount depends on the speed and mass of the car, and the speed and mass of what collides. The heavier the vehicle, the faster the speed and the more impulse energy it absorbs in the event of a collision" (Pawlus, Karimi, & Robbersmyr, 2014).

If a car is traveling at high speed and abruptly stops whilst it hits another object, the impact force will have a much greater impact, resulting in more damage to the vehicle and injury to the body of the occupant. If there is a possibility of slowing down before hitting an object, or if it takes time for the vehicle to reach the stop point, the effect of momentum will be lessened, resulting in damage to the vehicle or injury to the occupant's body will be less. In a head-on collision with another vehicle, or in a collision with a building, concrete structure, or a stationary object such as a large rock or tree, the impact force will be stronger.

If a vehicle collides with another vehicle at the same opposite angle and speed, the larger and heavier vehicle will do more damage to the smaller and lighter vehicle because of the higher impulse power. Large and heavy vehicles can push small and light vehicles backwards and even crush smaller vehicles. In general, the best way to reduce the initial force with a given mass and velocity impact is to slow down the collision.

If you know the force acting on an object, you only need to integrate the equations of motion to solve the impact problem. The movement of an object during a collision must always follow the momentum equation, the energy equation, and the third law of motion. These are sufficient to determine all movements except those that occur during impact.

The second law of motion, formulated by Sir Isaac Newton (1642-1727), is the basic law of most vehicle dynamics analysis.

$$Force\ (F) = m\ a \qquad \text{Eq (2.6)}$$

Where F is the applied vehicle force; a is the resulting acceleration of the vehicle and m is the mass of vehicle.

In most collisions, the vehicle produces high forward momentum. This can be defined as the degree of difficulty in stopping a moving object, called momentum (M).

$$Momentum\ (M) = m\ v \qquad \text{Eq (2.7)}$$

Where m is mass of vehicle and v is the vehicle travelling velocity. Also, the applied vehicle motion converts potential energy (PE) to kinetic energy (KE) and depends only on the mass and velocity of the vehicle.

$$Kinetic\ Energy\ (KE) = 1/2\, m\, v^2 \qquad \text{Eq (2.8)}$$

Where m is the mass of vehicle and size and v is the vehicle travelling velocity.

When a vehicle collides with another vehicle, some of its kinetic energy is absorbed as internal energy in the vehicle's deformed structure, and the remaining energy is the sum of the vehicle's kinetic energy. In a head-on collision between two vehicles, the total initial kinetic energy before the collision can be determined as follows:

$$KE_{Before} = \left(1/_2 \left(m_A v_{A_1}{}^2\right) + m_B v_{B_1}{}^2\right)\Big)_{intial} \qquad \text{Eq (2.9)}$$

Where m_A, v_{A_1} and m_B,v_{B_1} are the mass and speed for vehicle A and B are respectively. Also, the total kinetic energy after collision can be determined as:

$$KE_{After} = \left(1/_2 \left(m_A v_{A_2}{}^2 + m_B v_{B_2}{}^2\right)\right)_{after} \qquad \text{Eq (2.10)}$$

Where m_A, v_{A_2} and m_B,v_{B_2} are the mass and speed for vehicle A and B are respectively.

Figure 3.3 Vehicle impact with different velocity

According to conservation of energy, the following equation can be written after collision:

$$\left(1/_2 \left(m_A v_{A_1}{}^2\right) + m_B v_{B_1}{}^2\right)\Big)_{before} = \left(1/_2 \left(m_A v_{A_2}{}^2 + m_B v_{B_2}{}^2\right)\right)_{after} + E_{absorbed} \qquad \text{Eq (2.11)}$$

Assuming that after crashing the two vehicles is moving together with the same residual speed v3;

$$1/_2 \left(m_A v_{A_1}{}^2 + m_B v_{B_1}{}^2\right) = 1/_2 \left(m_A + m_B\right) v_3^2 \qquad \text{Eq (2.12)}$$

From the conservation of momentum principle, the following equation can be written:

$$\left(m_A V_{A1} + m_B V_{B1}\right)_{before} = \left(m_A V_{A2} + m_B V_{B2}\right)_{after} \qquad \text{Eq (2.13)}$$

Assuming that after collision the two vehicles are moving together with the same residual speed v3;

$$\left(m_A V_{A_1} + m_B V_{B_1}\right)_{before} = (m_A + m_B) V_3 \ \text{ Implies that}$$

$$V_3 = \frac{m_A V_{A_1} + m_B V_{B_1}}{(m_A + m_B)} \qquad \text{Eq (2.14)}$$

From these three equations, we can calculate the dissipative energy used to deform both vehicles. This is equal to the difference between the initial energy and the residual energy

$$\Delta E = KE_{Before} - KE_{After}$$

$$\Delta E = \frac{m_A m_B}{m_A + m_B} \left(v_{A_1} + v_{B_1}\right)^2 \qquad \text{Eq (2.15)}$$

Work done by the average force arising during collision of car is given by;

$$\Delta E = F.S$$

Where: F is average force acting during the impact (N) and s is car crush distance (m).This implies that:

$$F = \frac{\Delta E}{s} = \frac{m_A m_B}{(m_A + m_B)s}\left(v_{A_1} + v_{B_1}\right)^2 \qquad \text{Eq (2.16)}$$

This shows that the average force acting during the impact is function of vehicle masses, closing speed and car crush distance and Energy dissipated can be estimated as;

$$E_d = \frac{1}{2} F_{max} d_{max} \qquad \text{Eq (2.17)}$$

Where: F_{max}, is maximum force and d_{max} is a maximum deflection (Al-Graitti, 2019).

The velocities after impact may be determined with the coefficient of restitution (e). The coefficient of restitution (COR) is the ratio of speed of separation to speed of approach in a collision.

$$e = \frac{(V_{B_1} - V_{A_1})after}{(V_{A_1} - V_{B_1})before} \qquad \text{Eq (2.18)}$$

Objects with a COR of 1 will elastically collide, while objects with a COR of 0 will elastically collide and effectively attach to the colliding object without any bounce. “The coefficient of restitution is a numerical value that indicates how much kinetic energy (kinetic energy) remains after two objects collide. A high factor (very close to 1) means that little kinetic energy was lost during the collision. If the coefficient is low (close to 0), this indicates that much of the kinetic energy has been converted to heat or absorbed by deformation” (Dange, Buktar, & Raykar, 2015a).

2.10 Previous Investigations on Related Topics

2.10.1 Literature review related to experiments

(R. Patil, Lande, Tadamalle, & Reddy, 2017) investigated the impact performance of the bumper designed using a sandwich panel with a honeycomb structure made from Aluminum in three plies. The aim was also to improve the strength to weight ratio along with a 40% improvement in energy absorbed.

(Wei et al., 2016) used the finite element method (FEM) to design the structure of bumper with different structures and materials. The aim was to take advantage of plastic deformation of the bumper material to absorb maximum energy during a crash. The collision of the bumper was evaluated using simulation. The results indicate that the crashworthiness was best in the Aluminum bumper with honeycomb structure with maximum energy absorption at minimum deflection. But the Aluminum material is a soft material and many composite materials do offer better strength to weight ratio.

(Aseer & Sankaranarayanasamy, 2017) studied the effect of fiber on retention of tensile properties and degradation of polyester based polymer composites prepared by compression molding and reinforced with biodegradable Hibiscus Sabdariffa (HS) cellulose microfibers. They found 7.5% improvement in the mechanical properties and higher modulus and tensile strength in the composites compared with polyester, the resistance to microorganism attack was better but the tensile strength of the composites was deteriorated after water absorption and concluded that the bio composites are environmentally friendly bumper material.

(Magalhaes, Fontes, & de Melo, 2012) designed a front bumper surface to eliminate the problems of stress concentration and used the boundary element method (BEM) for stress analysis and validated the results with FEM. They found an improvement of 28% in yield strength using BEM while an improvement of 25% was estimated by FEM. The time required to analyze each design by BEM was 37.5% and without the requirement of a workstation or special skills, compared with the time taken for same analysis by FEM, which required high configuration computing facilities and skilled workers.

2.10.2 Literatures related to materials and impact behavior

(Zhu, Wang, Cheng, & Li, 2017) developed a carbon fiber reinforced plastic (CFRP) beam for bumper with a variable cross-section to predict the impact behavior at low velocity and found that the composite beam is better than the metallic beam in terms of weight and crashworthiness. Among the prevalent materials, the GMT is the most common bumper material but SMC composite, as well as the GMT composite, have better performance, properties, and safety.

(Bohra, Pawar, & Bargat, 2014) in this review, the front bumper was designed and analyzed during impact, the materials used were ABS (Acrylonitrile Butadine Styrene) and PEI (Polyetherimide). ABS plastic is very tough and resilient, has high impact strength, good chemical resistance, nontoxic and taint free. ABS plastic has low density compared to PEI. Hence, ABS material has been chosen and comparatively best than the PEI.

(Motgi et al., 2013) studied about the Impact Analysis of Front Bumper. In this review, the material used for this analysis were aluminum and composite fascia, where aluminum having higher density than fascia. Finally, it is found that composite fascia is suitable from impact point of view.

(Dange, Buktar, & Raykar, 2015b) proposed about the design and analysis of an automotive front bumper. The materials used were M220 (Martinsite 220 min tensile strength) formed in carbon steels. It can minimize the bumper deflection, impact force and stress distribution and also maximize the elastic strain energy. However, it also has some disadvantages such as high material cost compared to fiber glass, difficulty in mass production and has high density.

(Jacob & Arunkumar, 2016) emphasized about improving crashworthiness of an automobile bumper. This review suggests a new bumper model that has more crashworthiness than the existing. They aim is to improve crashworthiness of an automobile bumper. They selected TOYOTA CAMRY MODEL released in 2012. The bumper of the existing model had steel bumper. Two new designs were proposed in this review Model containing Honeycomb inside the bumper exists in the first individual and foam included design as the second. The newly designed models namely foam and honeycomb incorporated bumpers show better impact absorption capacity. The absorption capacity of the Honeycomb model is 11.26% and of foam model capacity is 6%.

(John & Nidhi, 2014) in this review, the materials used were aluminum 390 alloy, chromium coated mild steel and carbon composite. The analysis under dynamic loading showed that carbon composite had the maximum Stress value, high strength to weight ratio and producing deformation. From all these analyses it can be conclude that carbon composite is the best material and it can be used.

(Ramyasree, Venkataramaniah, & Kumar, 2015) in this review the material used was long fiber reinforced thermoplastics. It is then compared to conventional material. The purpose of this project is to design a bumper which is to improve crashworthiness of bumper. From the above analysis it is concluded that long fiber reinforced thermoplastic material based is good. Then it is compared with other materials and natural fibers have good energy absorption capacity.

(Uddandapu, 2013) in this review materials used were ABS plastic and PEI. The aim of this study is to analyze and study the structure and material. In this research analysis is done for speed according to regulations and also by changing speed in this analysis. The density of ABS plastic and PEI is less than that of steel therefore the overall weight of car bumper is reduced. In this conclusion, comparing the results of ABS plastic and PEI with steel, the stress values are less for ABS plastic and for the other two materials, therefore ABS plastic is better for utilization comparing PEI.

(Ezekwem, 2016) studied and analyzed about the use of composite materials in frontal car bumper. Materials in the way that nylon-6 nano composite and polyethylene/palm essence covering-iron filings composites were used and the mechanical feature of these composite materials distinguished with common car bumper materials like Aluminum and Steel. This comparison showed a reduction in weight, cost and environmental impact and also has some disadvantages such as difficulty in mass production and sophistication (quality) of the production process was also noted.

(Marzbanrad, Alijanpour, & Kiasat, 2009) discussed about the ultimate influential parameters such as material, density, shape and impact condition used for design, examination and determination of an automotive front bumper to make or become better the crashworthiness design fashionable for low-speed impact. The simulation of original bumper under condition impact done according to the low-speed standard of automotive stated in E.C.E. United Nations Agreement Regulationno.42, 1994. In this research, a front bumper made of three materials such as: aluminum, glass mat thermoplastic (GMT) and high-strength sheet molding compound(SMC) were studied by impact modeling to determine the deflection, impact force, stress distribution and energy-absorption behavior. The above mentioned characteristics were compared to each other to find best choice of material, shape and thickness. The results showed that a modified SMC bumper beam can minimize the bumper deflection, impact force and stress distribution and maximize the elastic strain energy. In addition, the effect of passengers in the impact behavior was also examined.

(Zhu, Liao, Sun, & Li, 2020) showed in their study that honeycomb structure also had a cell geometry which is capable of elastic buckling, which gives the honeycomb structure to recover their shape and properties after collision. Aluminum honeycomb structure if deformed in collision then they have to be changed or repaired. Actually, most of the bumpers have to be changed or repaired if possible after its first collision. CFRP is the costliest one because of its long and arduous manufacturing process. The honeycomb structure has strength and absorbs more energy which insures passenger safety. Foam bumper made by Age-hardening of aluminum shows the improvement of foam with large void sizes but not with small sizes. Mostly steel bumpers are used in heavy vehicles and rests of the bumpers are used in almost all types of vehicles.

2.11 Summary from Literature Survey

From all the above literature survey, we come to know that weight reduction, cost and low impact are the three major aspects considered in designing of a car bumper. Various authors had done analysis for different materials and given their results and conclusions. Based on their work the following review used to identify the research areas which will need further studies.

- Different researches were done on automobile bumper analysis using different materials, methods and experiment in the world in terms of cost effective and reasonable for uses.
- NO studies were done on using carbon poly amid material developed by 3D printing selective leather sintering method for different geometries of Toyota Camry automobile bumper.
- Studies related to modifications and crash analyzing aspects were not satisfactory to protect engines and occupants at the event of crash.
- There is no systematic study which explains design and analysis of front bumpers in the presence of solid mechanics using advanced FEA tools.
- After reviewing for the existing literatures, it is observed that there is no enough research work was done on design modification, optimization and FEA of automobile bumpers using carbon poly amid composite material for Toyota Camry vehicle.

2.12 Research Gaps

The prime issue currently involves that traffic accident rate of automobile vehicles is becoming higher and higher and most of its bumpers are made from materials such as aluminum alloy and steel, which have a low energy absorption capability. This low level of energy absorption has led the bumpers easily to damage even with slight collision. In order to conserve natural resources and economize energy, weight reduction has been the main focus and the introduction of composite materials will make it possible to reduce the weight of the bumper without any reduction on load carrying capacity and stiffness. However, the primary limitations involve the fact that using the advanced level of composite material for automobile bumpers requires higher financial values than that of metals such as steel. Therefore, the choice of composites maybe established as adjustment middle from two points cost and performance and also the use of composite materials for automobile bumper is found to be more efficient than steel (P. R. Patil & Kadam, 2017).

High-speed automobiles require lightweight body parts and thus maximum focus should be given to the use of composite materials. Furthermore, these composite materials have high melting point, good corrosion resistance and have high energy absorption that can withstand possible accidents while minimizing damage to automobile body parts, drivers and passengers. From that point of view, we will do design optimization for Toyota Camry automobile front bumper using carbon poly amid material and do the FE analysis i.e. optimization in terms of (geometry, material and thickness) analysis and static analysis (impact, stress, and strength analysis). In addition, it is then compared with the conventional bumper material which is steel and aluminum alloy. The formulated results obtained from the strength analysis for the materials will then compared. Finally, from the results we will check that whether or not the design is safe.

CHAPTER THREE

3. MATERIALS AND METHODS

3.1 Introduction

The main aim of this research focuses on the minimization of damage on the vehicle components as well as humans during accident. For such an accident the best way of minimizing the injuries is through optimizing the bumper design, suitable material selection and testing using software's.

The data collection has been done from local automobile assembling company manuals and modeling of the bumper done using SOLIDWORK software from the existing bumper model specification. Once the CAD model of automobile bumper is designed, it is imported into LSDYNA software simulation environment to perform frontal crash simulation at the captured speed and also explicit dynamic has been performed for different bumper geometry.

3.2 Materials

This section provides insights into the materials selected for testing and implementations in modern automobile bumpers. To test the most efficient material with high energy absorption capacity, the carbon composites have been taken into account for the test. This test can help to analyze the efficiency of using carbon composites for automobile bumper instead of steel and aluminum alloy that currently most Toyota Camry automobile bumpers are made from and also considering the possible accidents that may lead to further damage on the vehicle components as well as humans during accident. Therefore, to conduct materials test and interpret the numerical analysis of the automobile bumper the following software's are used;

SOLID-WORK

SOLIDWORK is a computer-aided design (CAD) and computer-aided engineering (CAE) computer program for solid modeling that runs on Microsoft Windows. SOLIDWORK is a solid modeler that uses a parametric, feature-based approach to create models and assemblies. The parameter refers to a constraint whose value determines the shape or geometry of the model or assembly. Parameters can be either numerical parameters such as line length or circle diameter, or geometric parameters such as tangent, parallel, concentric, horizontal, or vertical (Gouasmi, Ouali, Fernini, & Meghatria, 2012). "Numerical parameters can be linked together through the use of a relation, which allows them to capture the design intent. SOLIDWORK can analyze linear studies including buckling, drop testing, dynamic analysis, fatigue, frequency, harmonic analysis, optimization, pressure vessel design, random vibration, static, thermal, and transient heat. SOLIDWORK also used in robot modeling which used to scrutinize the theory and its motion simulation with generalized to a 3-R robot (Lad & Rao, 2014).

Stages in the Process

- ✓ Create a New part document: New parts can be created in inch, millimeter or other units. Parts are used to create and hold the solid model
- ✓ Sketch the profile: Sketches are collections of 2D geometry that are used to create solid features. These include lines, circles and rectangles
- ✓ Applying Sketch relations and dimensions: Geometric relationships such as horizontal and vertical are applied to the sketch geometry. Dimension size the geometry while the relations restrict the movement of the entities
- ✓ Extruding the sketch: Extruding uses the 2D sketch to create a 3D solid feature.

CATIA

CATIA (Computer Aided 3D Interactive Applications) software is a full multi-platform solution for computer-aided design, manufacturing and various field of engineering. The software sold by the manufacturer Dassault System's is ideal for creating solids, surfaces, assemblies, drawings, manufacturing, and analysis. Like Solid Work, this program provides powerful parametric modeling and photorealistic rendering tools. However, CATIA provides advanced features for interfaces and modules in various industries.

CATIA offers many workbenches that can be loosely termed as modules. A few of the important workbenches and their brief functionality description is given below:

- ✓ Part Design: The most essential workbench needed for solid modeling. This CATIA module makes it possible to design precise 3D mechanical parts with an intuitive and flexible user interface, from sketching in an assembly context to iterative detailed design.

- ✓ Generative Shape: Design**:** allows you to quickly model both simple and complex shapes using wireframe and surface features. It provides a large set of tools for creating and editing shape designs. Though not essential, knowledge of Part Design will be very handy in better utilization of this module.
- ✓ **Assembly:** The basics of product structure, constraints, and moving assemblies and parts can be learned quickly. This is the workbench that allows connecting all the parts to form a machine or a component.

LS DYNA

LSDYNA is an advanced general purpose metaphysics simulation software package developed by the former Livermore Software Technology Corporation (LSTC), which was acquired by ANSYS in 2019. While this package continues to extend the ability to compute many complex real-world problems, its origin and core competence is highly non-linear transient dynamic finite element analysis using explicit time integrals. "LS-DYNA allows switching between explicit and different implicit time stepping schemes. Disparate disciplines, such as coupled thermal analyses, Computational Fluid Dynamics (CFD), fluid-structure interaction, Smooth Particle Hydrodynamics (SPH), Element Free Galerkin (EFG), Corpuscular Method (CPM), and the Boundary Element Method (BEM) can be combined with structural dynamics" (Gholipour, Zhang, & Mousavi, 2020).

LS-DYNA emerged from the 3D FEA program DYNA3D, developed by Dr. John O. Hallquist at Lawrence Livermore National Laboratory (LLNL) in 1976. DYNA3D was designed to simulate the impact of a full fusing option (FUFO) or "Dialayield" nuclear bomb for low altitude emission (impact rate is approximately 40 m / s). At that time, 3D software that simulated the effects was not available, and 2D software was inadequate. "Though the FUFO bomb was eventually canceled, development of DYNA3D continued. DYNA3D used explicit time integration to study nonlinear dynamic problems, with the original applications being mostly stress analysis of structures undergoing various types of impacts. The program was initially very simple largely due to the lack of adequate computational resources at the time. The program is extensively used by many top automobile, aerospace and research organizations. A wide range of material types and interfaces enable the efficient mathematical modeling of many engineering problems" (Abedini & Zhang, 2021).

3.3 Methods

In order to address the general and specific objectives of this work a well-designed methodology was followed. Various steps which are included in the methodology are listed below.

3.3.1 Literature review and problem identification

A literature review of different types of automobile bumper materials and design analysis was the main methodology of this thesis, that helped to know about what others were doing and where the restrictions were. Therefore, this thesis was based on research gaps.

3.3.2 Data collection

The required data was collected through primary or secondary data collection by visiting various websites and using a data collector for the Toyota Camry Car Bumper in Addis Ababa. The data is collected from:

1. Federal police commission
2. Medhine insurance company
3. Federal transport minister
4. Nuru general automobile assembly company

3.3.3 Overview of composite materials

Compare and evaluate the different composites to choose the one with the highest impact energy absorption capacity.

3.3.4 Modeling and analysis of the existing model

After reviewing the literature, the appropriate Toyota Camry bumper geometry modeling and model quality performed by SOLIDWORKS software was checked by ANSYS and Ls-pre Post, and finally analyzed by the LSDYNA processor.

3.3.5 Modify and analysis of the different bumper geometry

After careful observation of the collision behavior of the existing model, corrections and designs were made at the critical point of the bumper and analyzed separately.

3.3.6 Decision

At this point, the behavior of the change is investigated using engineering analysis and decision-making methods. If the results are satisfactory, the next phase of the project will be performed, otherwise the changes will be redesigned.

3.3.7 Optimizing and analysis of the new model

Finally, the modified automobile bumper which increases the crashworthiness of vehicles are fitted in to the existing model and further optimized using LS-DYNA.

3.3.8 Numerical Analysis

Numerical comparison between of the existing, modified and optimized bumper under different loading conditions using the different crashworthiness determinant parameters such as energy absorption, impact force ,deformation and so on using LS-DYNA software.

3.3.9 Verification parameters

In the absence of experimental data, the validity of the values obtained in the computational model is accurately represented throughout the validation process. “For LS DYNA simulations, the most common and logical validation parameters are:

- Energy balance
- Energy Ratio
- Ratio of hourglass energy (HE) to IE” (Gulavani, Hughes, & Vignjevic, 2014).

Energy Balance Curve

The energy balance of the system in the event of an impact follows the law of conservation of energy. From the law of conservation of energy, energy neither be created nor destroyed, but it can be transformed from one form of energy to another. Applying the same principle to impact analysis, the amount of kinetic energy missing during a collision must be transformed to other forms of energy such as internal energy, sliding energy and hourglass energy.

Kinetic energy is the work input and internal energy is the work output. Internal energy is the energy absorbed by the system and is directly proportional to the product of force and deformation. It is also note that there may be negligible errors in the calculation of the energy ratio, because all the processes in this universe are irreversible and some losses are always included. The energy ratio is slightly off from 1.

- ❖ The total energy applied should be constant throughout the simulation.
- ❖ Total energy is the sum of kinetic energy and potential energy of the entire system.
- ❖ The kinetic energy should decrease and internal energy should increase; and ideally the sum of kinetic energy and internal energy should be equal to total energy.
- ❖ The energy of the hourglass should be less than 5% of the total energy.

Energy ratio

The ratio of 'total energy' to the sum of 'initial total energy' and 'external work done' is called energy ratio. The total energy of the system $=E_i + E_s + E_d + E_{ke} + E_h$ and Initial total energy plus work done by the external forces (W_{ext}) = $W_{ext} + E_i^0 + E_{ke}^o$.

The energy ratio is also known as 'energy balance' and is given by:

$$e = \frac{E_i + E_s + E_d + E_{ke} + E_h}{W_{ext} + E_i^0 + E_{ke}^o}$$

Energy ratios with a value of 1 give more stable and reliable FEA results, but in most cases it is difficult to reach such values. This is due to modeling errors that can increase or decrease the total energy. When checking the energy ratio, there are two causes that matter:

If e>1, which mean that artificially energy is added in the model and rises the total energy values, as a results instability occur, most of the time the rises of total energy is due to a numerical instability or through initial penetration.

If e<1, which mean that the total energy reduces because of artificially absorbed energy, either by excessive hour-glassing or during stabilization of an ill-conditioned contact surface (Samuel, Asadi, Tarda, Simbotin, & Markopoulos, 2021).

In general, “the energy ratio is simply different from 1 and is more likely to produce FE results with errors. Since it is difficult to equalize the energy ratio to 1, the permissible value for this ratio is 1.00 +/- 0.07. The ratio mismatch is due to system-generated spurious energy and simulation errors” (Rackauskaite, Kotsovinos, & Rein, 2017).

Ratio of TE/HE:

Through analyzing the energy curves, the validity of the finite element model can also be determined using the ratio between the total energy to hourglass energy. Hourglass energy can cause a zero-energy model. If the hourglass Energy is less than 5% of the total energy, the finite element model is reliable (Gulavani et al., 2014).

The above mentioned verification method are implemented at each simulation result report. The accuracy of the FEA model is checked by examining the different pattern exhibited by the simulation results. Following checkpoints are considered for simulation.

1) The results of Simulations for the existing automobile front bumper is imported and discussed.
2) Modification and analysis of the different bumper geometries are presented.
3) Optimization and analysis of the new model for the respective optimization parameters are imported and discussed.

At each section the main parameter which are going to be examined are the energy balance, absorbed energy, impact force, deformations and structural response. The simulation results at each optimizing parameters are presented below.

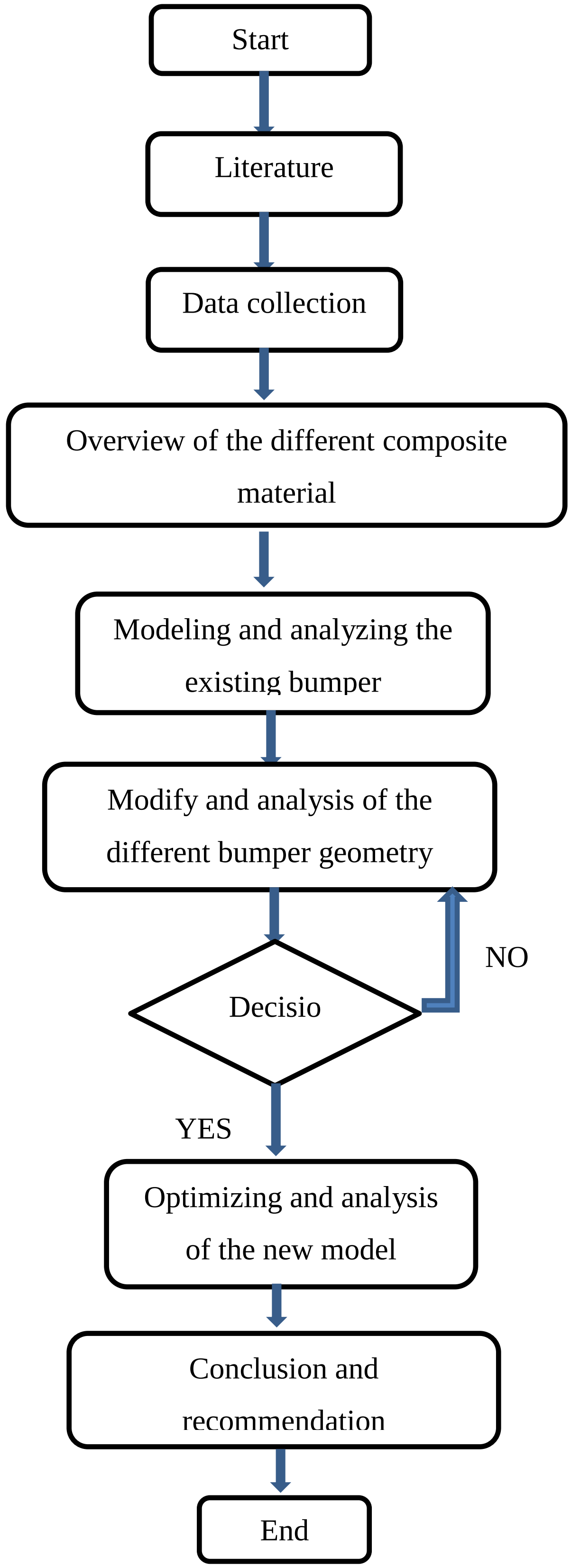

Figure 3.1: Flowchart of methodology

3.3.10 Finite element method

The finite element method (FEM) is a simplified approximate solution for many engineering systems through subdividing them into components or elements. System response analysis is described by complex differential equations, that is, a response involving many unknowns. The system accuracy of the solution can be controlled by changing the number of unknowns and the number of elements. The steps in the analysis of the systems are as follows:

- Model geometry: Model geometry represented by elements and nodes.
- Material definitions, which are usually associated with parts of the geometry.
- Parts and assembly: Geometry can be divided into parts that are relative to each other within an assembly.
- Initial conditions: non-zero initial conditions such as initial stresses, INITIAL keyword interface and velocities can be specified.
- Boundary conditions: Zero value boundary conditions (symmetry constraints, impact velocities, control chards, database cards, etc.) can be imposed on the model.
- Constraints: linear constraint equations or multi-point constraints can be defined.
- Contact interactions: contact conditions between surfaces or parts can be defined.
- Output control: options for controlling model definition output to the data file
- Analysis continuation: it is possible to write restart data or to use the results from a previous analysis and continue the analysis with new model or history data

CHAPTER FOUR

4. MODELING AND ANALYSIS

4.1 Introduction

Finite element analysis (FEA) develops computer models for structural analysis that are used in product design to improve the performance of existing product models. Finite element analysis gives designers the ability to know the design performance of the required specifications before manufacturing the product. There are two types of finite element analysis:

- 2D modeling analysis
- 3D modeling analysis

2D modeling analysis is simple, computationally efficient and less accurate, but 3D modeling gives more accurate results. Finite element analysis considers the system as linear or non-linear. Modeling linear systems is less complex and usually does not consider plastic deformation, while nonlinear systems do.

4.2 Survey Findings

Collection of the necessary data about Toyota Camry existing bumpers is helpful for numerical analysis. Various data have been collected to understand the current state and methodology of car bumper research, which also helps in the development and modification of car bumper structural impact resistance.

4.2.1 Toyota Camry Car specification

Technical specification and necessary data of the existing Toyota Camry vehicle has been collected from the vehicle manual itself and carfolio car specifications. All necessary information of Toyota Camry vehicle is shown in Table 4.1. In addition to this, when dealing with crash worthiness, the mass of the vehicle parts plays vital role (Kokate, Uttekar, Karandikar, & Holmukhe, 2020).

Table 4.1 Toyota Camry 2.5 (2012) specifications (carfolio.com/Camry model, 2012).

Specifications	
Seating Capacity	4/5 seater sedan/saloon
Number Of Doors	4
Kerb Weight	1447 kg
Cylinders	Straight 4
Engine Type	naturally aspirated petrol
Drag Coefficient	0.28
Fuel Tank Capacity	64.4 litres
Maximum Torque	230 Nm at 4100 rpm
Maximum Power Output	133 kW at 6000 rpm
Engine Position	Front
Drive Wheels	front wheel drive
Gearbox	6 speed automatic
Compression Ratio	10.4:1
Capacity	2494 cc
Ground Clearance	155 mm

4.2.2 Dimension of Toyota Camry vehicle

The model has been done using the overall dimension of length, width and height of the vehicle structure.

Table 4.2 Over all dimensions of the vehicle

Over all dimensions (mm)	
Length	4806
Width	1821
Height	1471

Figure 4.1 2012 Toyota Camry overview

4.3 Modelling of the existing automobile bumper structure

The car bumper geometry model is prepared on the basis of data acquisition specifications as shown in figure 4.3. Perform a few steps before attaching the geometry to LSDYNA Modeling in CATIA and SOLIDWORK.

Sketch tracer generation is an early stage of modeling and is formed by tracing a basic profile or part of a car bumper from an image. The surface was then generated and the appropriate extrusion thickness was set. Finally, all parts of the vehicle are assembled and the vehicle is modeled.

Table 4.3 Dimension of the bumper model

Front Bumper Model			
Parameters		Effective	Total
Over all Dimension (mm)	Length	1230	1800
	thickness		2.5
	Height		460

4.3.1 Modeling

Use CATIA v5 and SOLIDWORKS 2015 to create a 3D model of the vehicle bumper and the entire vehicle structure. The front bumper of the car is designed to be 2mm thick, 1800mm long and 460mm high. The bumper creation part is as shown in figure 4.2:

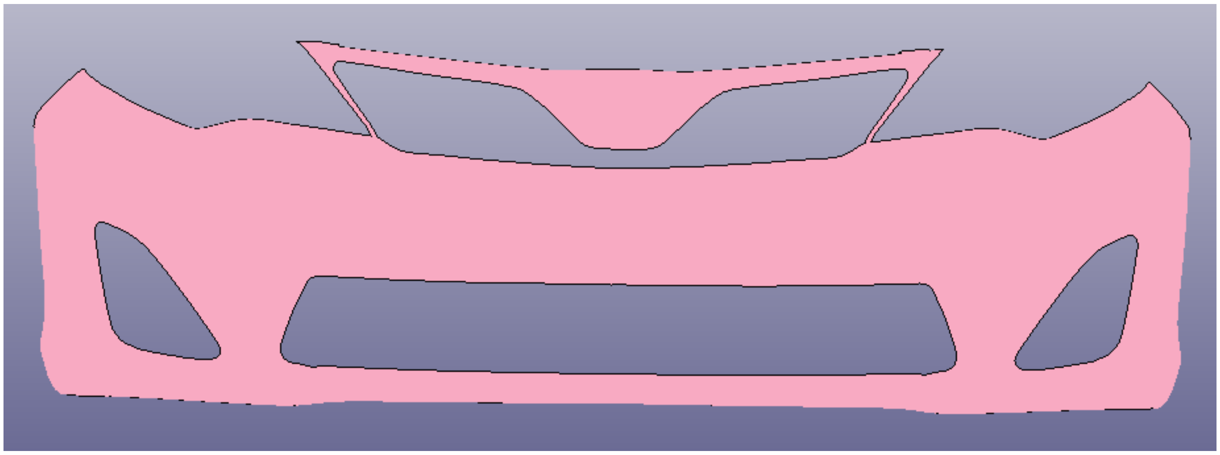

Figure 4.2 Front Toyota Camry bumper model

Computational vehicle model

Computer Aided Design (CAD) model of Toyota Camry 2012 from SOLIDWORKS software was imported to LS DYNA in form of Initial Graphics Exchange Specification (IGES) model format. Then, the FE model was created by LS DYNA software using dimensions from the real vehicle, as shown in Figure 4.3:

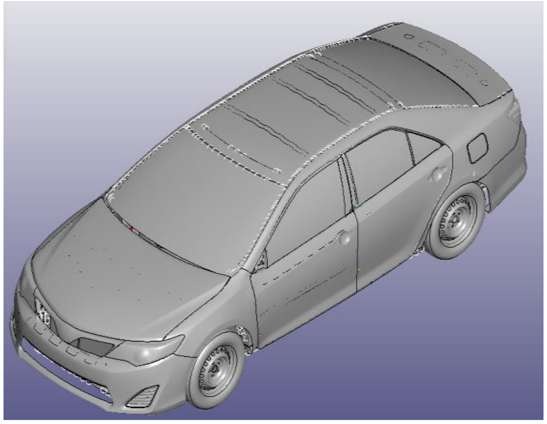

a)

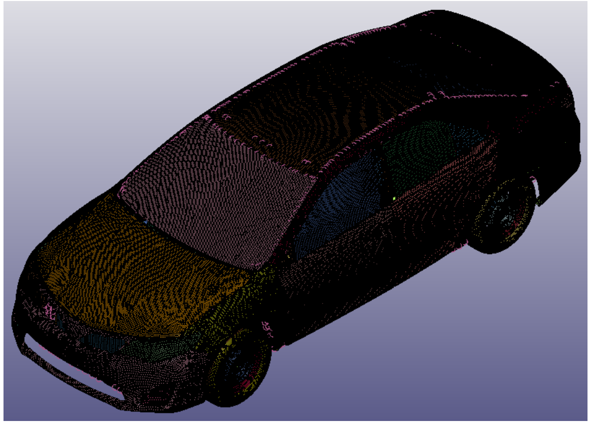

b)

Figure 4.3 a) Isometric view of Toyota Camry model b) meshed model of the vehicle

4.3.2 Model cheek and surface clean

Model checking consists of three basic phases: pre-analysis, during analysis, and post-analysis.

- ✓ Pre-analysis check: A check to perform before performing an analysis on LSDYNA.
- ✓ During the analysis: Checks while the model is running.
- ✓ Post-Analysis validation: validate the model after the analysis is complete. This includes feedback on accessing initial model data.

1. **Pre-analysis review**

The computer-aided design (CAD) of a car bumper model has been converted to an STL (Standard Triangulation Language) model by SOLIDWORKS software. Next, checking the model to see if any modeling errors such as overlapping faces, unwanted lines, edges, and intersections between parts were cropped and removed from the imported model. The next step is to export the model to LSDYNA Pre-post Meshing. Use LSDYNA Pre-Analysis Checking to check the depth further.

Check the cross edges

The first thing to check is that there are no overlapping edges. If the edge of an element intersects the surface of another shell element or solid, it is not an intersection in the classical LSDYNA sense. However, it is very important to avoid such modeling, as these mesh errors can cause serious problems when performing analysis on LSDYNA.

Initial Penetration

Initial penetration is often used to describe the degree of penetration that occurs between a node and its closest main segment or between two interacting segments and it's a term that needs to be taken care of. The most obvious recommendation is not to make any initial intrusions. However, this is very difficult due to the nature of the modeling process and the number of design changes that typically occur throughout the product life cycle.

"Penetrations are checked for shell and solid elements in LS DYNA, Penetration check by "Select Parts" and check by CONTACT" (Singh & Singh, 2015).

Keyword check

Another way to deal with problems in the modeling process is to search for cheek keywords. Here, the model is queried for input errors in keywords such as cuts, materials, and constraints. Figure 4.4 below shows a model keyword report with all errors removed and some warnings remaining.

Model Checking

Element Quality | Keyword Check | Contact Check | Model Check Setting

Total	Error(0)	Warning(192)	UnRef(0)	UnDefined(0)
BOUNDARY(1)	Error(0)	Warning(0)	UnRef(0)	UnDefined(0)
CONSTRAINED(64)	Error(0)	Warning(128)	UnRef(0)	UnDefined(0)
CONTACT(2)	Error(0)	Warning(0)	UnRef(0)	UnDefined(0)
CONTROL(3)	Error(0)	Warning(0)	UnRef(0)	UnDefined(0)
DATABASE(4)	Error(0)	Warning(0)	UnRef(0)	UnDefined(0)
ELEMENT(39710)	Error(0)	Warning(0)	UnRef(0)	UnDefined(0)
HOURGLASS(2)	Error(0)	Warning(0)	UnRef(0)	UnDefined(0)
INCLUDE(2)	Error(0)	Warning(0)	UnRef(0)	UnDefined(0)
INITIAL(1)	Error(0)	Warning(0)	UnRef(0)	UnDefined(0)
KEYWORD(3)	Error(0)	Warning(0)	UnRef(0)	UnDefined(0)
MAT(2)	Error(0)	Warning(0)	UnRef(0)	UnDefined(0)
NODE(43821)	Error(0)	Warning(64)	UnRef(0)	UnDefined(0)
PART(2)	Error(0)	Warning(0)	UnRef(0)	UnDefined(0)
SECTION(2)	Error(0)	Warning(0)	UnRef(0)	UnDefined(0)
SET(65)	Error(0)	Warning(0)	UnRef(0)	UnDefined(0)
TITLE(2)	Error(0)	Warning(0)	UnRef(0)	UnDefined(0)

Figure4.4 Keyword cheeks pic

2. **During analysis**

Intrusions, modeling errors, and other errors are reported in this section. The user can fix the problem by reading the warning in the message file or in the running LSDYNA command window.

```
Beginning of keyword reader                                05/21/22 06:22:05

*** Error 10125 (KEY+125)
    Checking PART and SECTION definition input.
    PART ID 2 with
    SECTION ID 0 does not exist.
    This is PART 1 in the order of input.

*** Error 10133 (KEY+133)
    input data failed with: 1 errors

E r r o r   t e r m i n a t i o n                          05/21/22 06:22:08
```

(a)

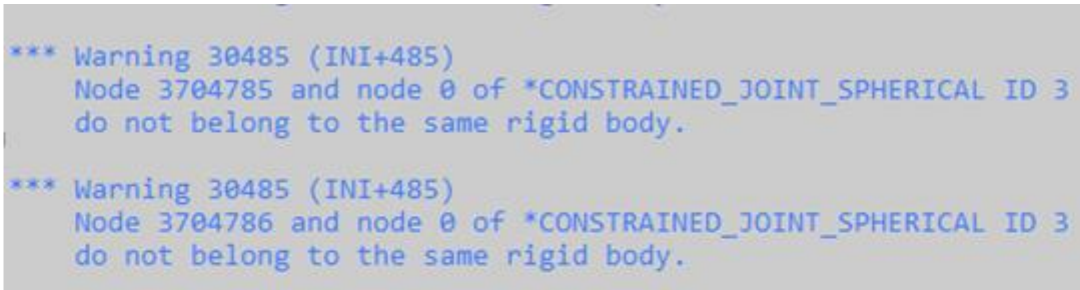

(b)

Figure 4.5 (a) Error terminations and (b) Warning during analysis

3. **Post-analysis review**

Post-checking provide information about model deformation, energy absorption, various stresses, and other consequences. All this information is useful for model checking, especially for parts with large permanent deformation and low energy absorption.

4.3.3 Mesh generation

The Mesh module provides a variety of tools that allows specifying different mesh characteristics, such as mesh density, element shape and element type. The total number of elements in the entire mesh model was 35295 and the number of nodes was 38392. Therefore, as shown in Figure 4.6, the entire mesh model is very complex and computationally intensive.

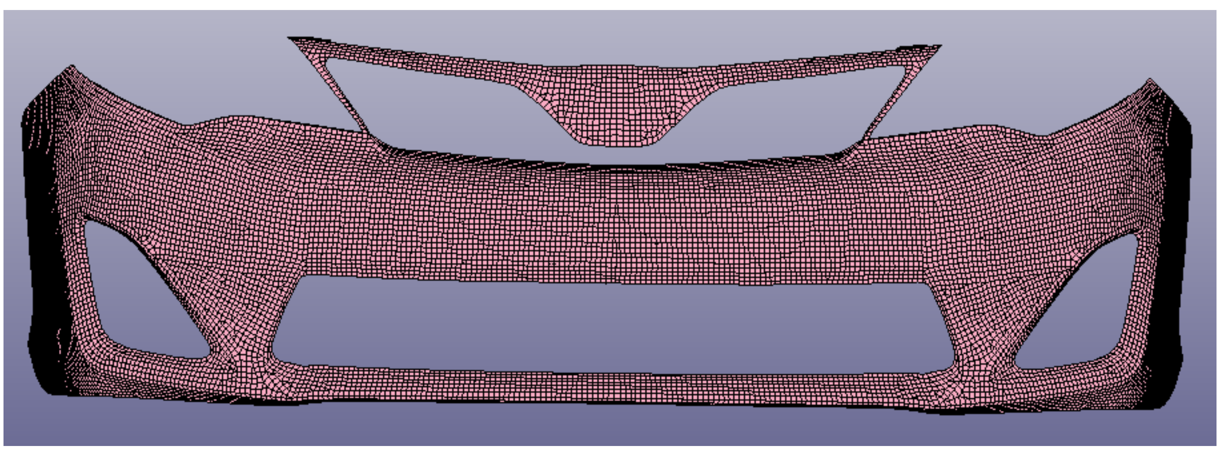

Figure 4.6 Meshed model for Toyota Camry bumper

Quality check

Various quality parameters such as skewness, aspect ratio, included angles and Jacobean stretch are the measures of how much a particular element deviates from ideal shape. “Some of the quality checks are based on angles (like skew, included angles) while others are based on aspect to area ratios" (Rahman & Babu, 2019). Figure 4.7 shows the quality for the existing automobile bumper model.

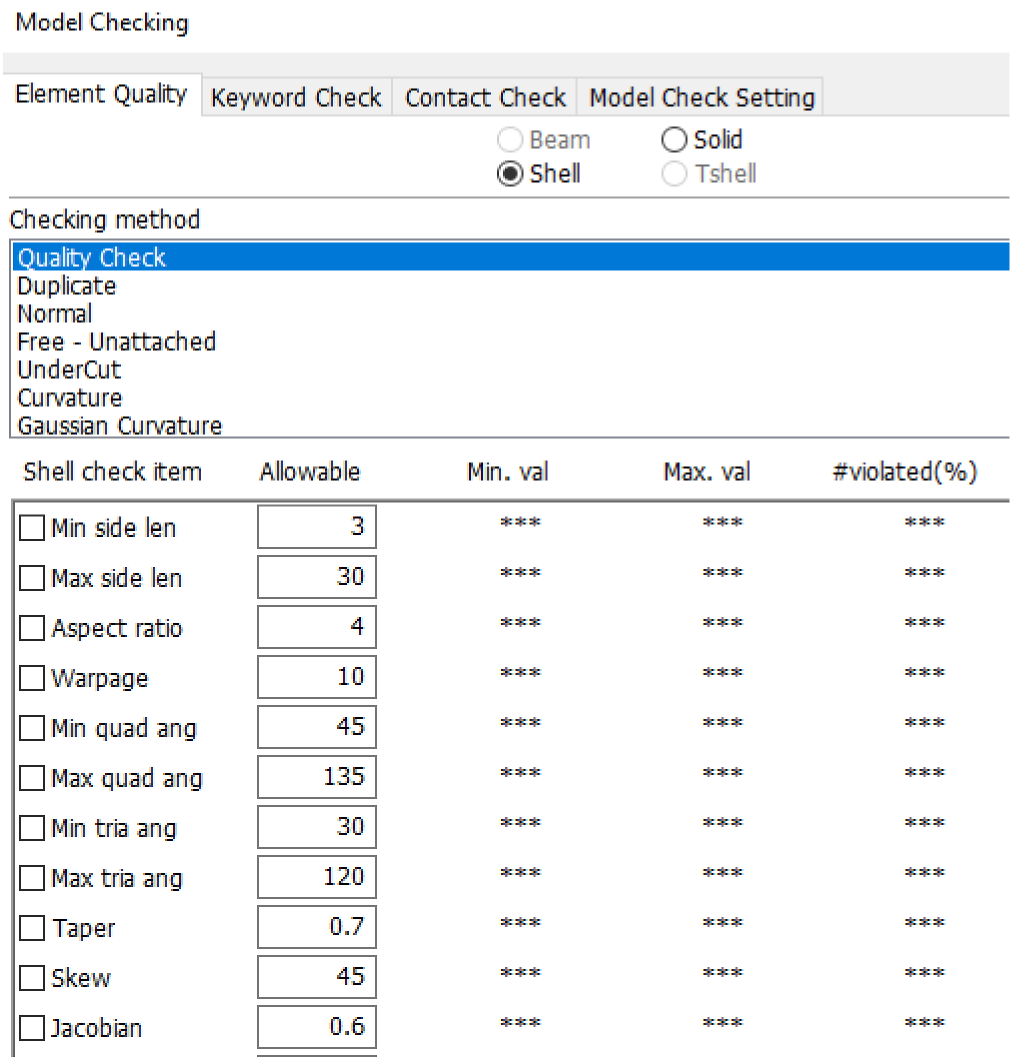

Figure 4.7 Element quality check summary table from LSDYNA

4.3.4 Definition of material properties on LSDYNA workbench

Currently, there are two kinds of materials used for manufacturing automotive bumper, namely, metal materials such as high-strength steel, aluminum alloy, and magnesium alloy and non-metallic materials such as glass mat thermoplastic (GMT) and sheet molding compound (SMC). To attain lightweight as well as strength requirements, one way of automotive bumper lightweight design is to vary the structure of high-strength steel bumper and another is to replace traditional metal materials with light materials. In fact, aluminum alloy and other light metal have some disadvantages such as high cost, low press formability, adhesion (welding) problems, and difficulty with surface treatment.

Conversely, composite materials, as another kind of important lightweight automobile materials by virtue of excellent properties, have gradually extended their application in many vehicle models (Hu, Liu, Zhang, Ding, & Wu, 2015).

The vehicle component material was selected from the LSDYNA material library. The keyword for existing car bumper materials is MAT_PIECEWISE_LINEAR_PLASTICITY, and in case of impactor, this part is un-deformed and is modeled with MAT_RIGID.

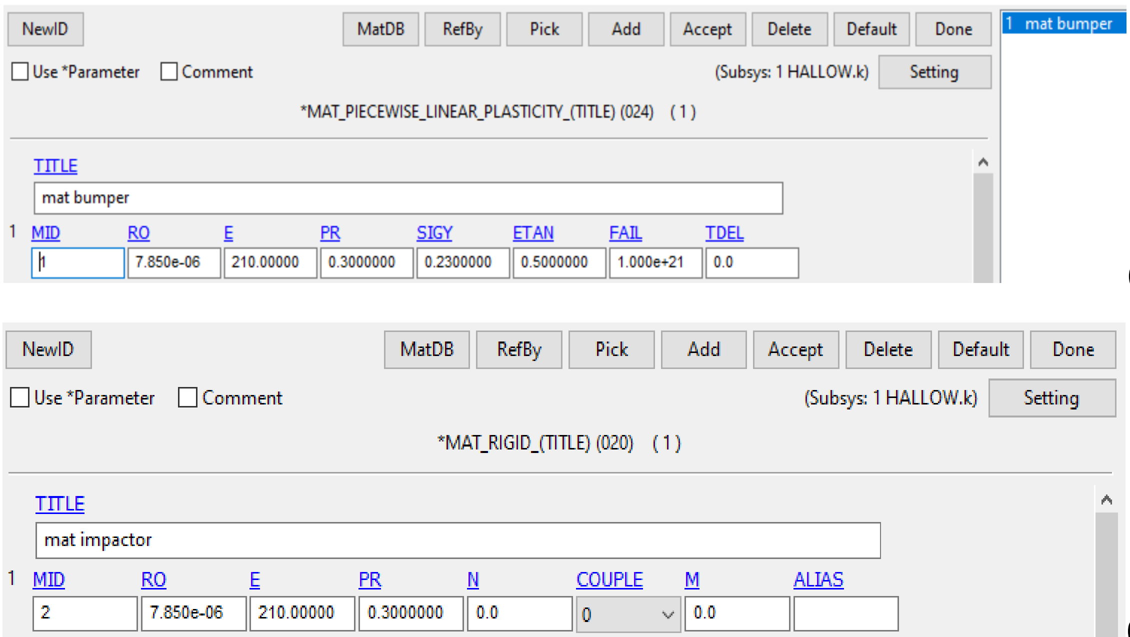

Figure 4.8 Material properties for (a) existing bumper and (b) for impactor

The thickness of most vehicle components was defined by the section shell and the rest by the volume element. For shell elements, the thickness value is determined based on the density and mass values listed in the data collection.

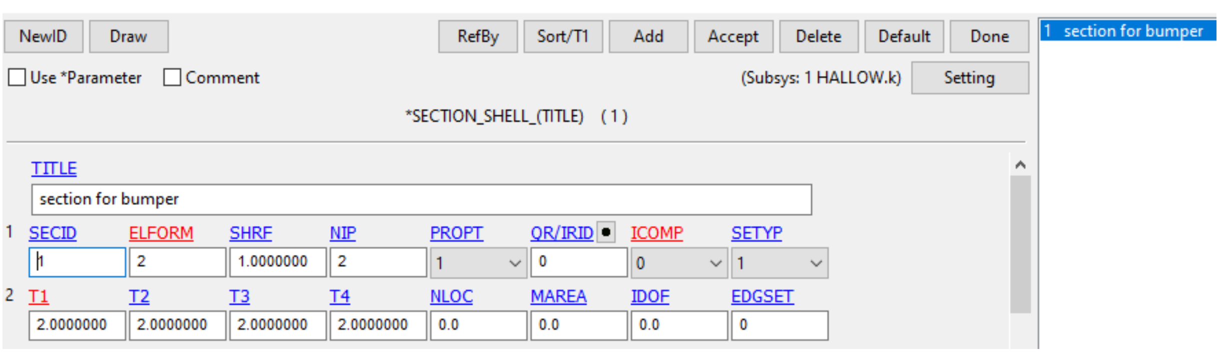

Figure 4.9 Section shell for the existing bumper

4.3.5 Inertia considerations

To simplify the model, whole components of the car are not modeled, but are represented as point masses and rigid bodies. The components worked primarily in series, traveling from the front to the center of the car, all interconnected. The representation of this component was made to maintain the inertial properties of these components. This is very important for creating an accurate collision simulation of the vehicle. According To (Hu et al., 2015), the mass of impactor should be Equal to the whole vehicle; thus, a gross mass of the vehicle was given to the impactor. These point masses were created in LS-DYNA by creating a single node, and adding a mass using ELEMENT TOOL_MASS PART and the node is connected at the center of mass of the rigid body (impactor) in the model using *CONTRAINED_EXTRA NODE SET. Hence,

- the initial mass of impactor while modeling and defining material has default mass $mi = 78.5\ kg$
- Total mass of the vehicle , $mv = 1447\ kg$
- Average weight of humans is 62 kg and the vehicle has 5 seats, implies $mh = 5 \times 62 = 310$ kg
- Therefore the gross mass added to the rigid impactor to consider inertia becomes:

$$mass\ added = mh + mv - mi$$
$$= 310kg + 1447kg - 78.5\text{kg}$$
$$= 1678.5\ kg$$

4.3.6 Constrained

After meshing individual parts, the interactions between them were defined. These interactions are defined between the surfaces of different parts and control the transmission of forces and moments between individual members. Kinematic connections have been defined for different parts of the vehicle. In LSDYNA, the constraint between the two deformable parts was specified by the CONSTRAINED_NODAL_RIGID_BODY keyword when the object was created.

4.3.7 Contacts

Many contact types are available in LSDYNA Keyword Manager. Between two parts, master (initial velocity is zero) and slave (initial velocity is defined), to prevent intrusion in case of collision with CONTACT_AUTOMATIC_SURFACE_TO_SURFACE and to define interaction with parts using CONTACT_AUTOMATIC_SINGLE_SURFACE.

4.3.8 Boundary condition

The function of boundary conditions is to create and define constraints and loads for finite element models. To simulate automobile bumper or the entire vehicle collision, it needs to model all the loads and boundary conditions that occur in a real collision event.

Friction can be defined as resistance to the relative motion of an object in contact. It is currently known that the coefficient of friction of each class of material is constant. The various operating parameters that change friction are the applied load or contact pressure, wear rate, and surface roughness. Contact is the investigation of a deformable object that touches at least one point in space. In general, contact pairs frequently experience non-linear plastic and permanent deformation Depending on the deformable body shape and material properties, and thus LSDYNA comes with a selection contact computational algorithms to deal with contact definitions with a contact interaction property between the bumper and the rigid impactor with static and dynamic friction of 0.3 and 0.2 respectively.

The input for the finite element analysis is the velocity of the rigid pole. This input is applied during operation. There are also different inputs in case of analysis steps that act on the vehicle model and the fixed rigid pole. When the analysis is carried the back edge of the bumper is constrained as shown in figure 4.10.

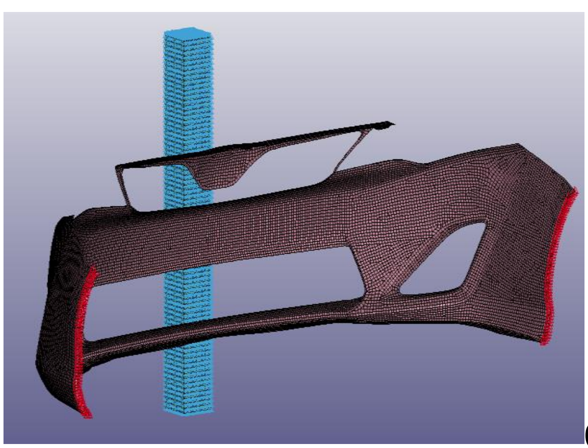
(a)
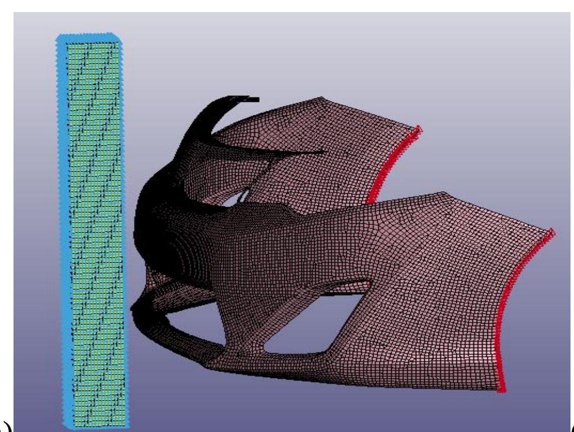
(b)

Figure 4.10 Boundary condition given to rigid pole and bumper (a) front and (b) back view

4.3.9 Impact velocity

Create boundary conditions that minimally constrain the movement of the back edge of the bumper and define some initial velocity to the rigid pole, so initial boundary conditions and the predefined velocity in the longitudinal direction (in x-direction) is applied at this step. According to National highway traffic safety administration (NHTSA), “the bumper should withstand at a speed of 2.5 mph (4.023kmph) across the full width and 1 mph (1.609kmph) on the corners. No bumper damage or yielding after 8 kmph (full impact) frontal impact into a rigid barrier” (Motgi et al., 2013).

The boundary condition are created using the displacement along the z-direction is constrained, the bumper movement is fixed so ($U_1=U_2=U_3=UR_1=UR_2=UR_3=0$) as boundary condition and in the predefined field with a varying velocity of 4 kmph, 5 kmph and 6 kmph in the x-axis and for the whole vehicle model initial velocity is given to the vehicle of 8 kmph that means:

Case 1: Vx= -1.11mm/ms for bumper- pole impact and,

Case 2: V_x= -2.22mm/ms for vehicle- pole collision.

4.3.10 Control termination

Control has a significant impact on the stability and accuracy of the simulation. CONTROL_TERMINATION was used to define the end time of the simulation. It is used to control the time step and execution time of the file. The file execution time is 300 milliseconds. DT min is the interval at which D3plot code is generated when processing files with LSDYNA and is also used when drawing diagrams i.e. for every 0.005.

Control Energy: Provides control of power consumption options.

Control Hourglass: controls zero energy generation.

4.3.11 Database cards

The database map is provided to receive the output, that is, to generate the results and interpret the chart. The database was used to define the expected results according to the American Standard Code for Information Exchange (ASCII) for information exchange, and to define specific characteristics such as GLAST, RBDOUT, RCFORC, and DEFORC.

4.4 Modification on the existing automobile bumper

Vehicle owners make changes to give them a unique look, improve performance, add the features they need, change the engine and suspension, and add long-range fuel tanks. However, some people modify their vehicles to suit specific individual purposes. Excessive changes can impair the handling of the vehicle. I.e. Too much weight and other safety measures can affect stability and the fuel economy and lead to inaccurate legal and insurance site violations. Therefore, it is very important to remain safe and legal while modifying the car. The following additional criteria must also be met for car bumper improvements:

- Has little or no impact on vehicle compliance with specified vehicle standards
- Does not compromise the safety, strength, or reliability of critical systems (Fagnant & Kockelman, 2015)
- Vehicles must not show rust or defects in areas that have changed or have already changed
- The vehicle must be structurally sound and able to support / adjust the necessary adjustments without the need for mechanical repairs (Anderson et al., 2014).

4.4.1 Bumper geometry

The bumper is responsible for protecting the engine, fuel tank, and exhaust systems as well as other safety related components at event of crush. This can be achieved by reducing any intrusion into the vehicles compartment. The front bumper has functionality of reduce kinetic energy, lessening the stress and absorb more impact energy.

The first thing to keep in mind when doing modification is that the driver and passengers need to be protected as much as possible from direct contact with obstacles and freed from uncontrolled flight. In other words, the driver and passenger must receive the modest withdrawal force or momentum generated by the collision. To achieve this goal, the vehicle structure should be designed as safe as possible with some crushing zones to absorb more energy. The location of mountings is based on the study done on the existing bumper model, this paper achieves this aim by means of adding corrugated reinforcement at the back side of the existing automobile bumper (energy absorbing component) as shown in fig 4.11:

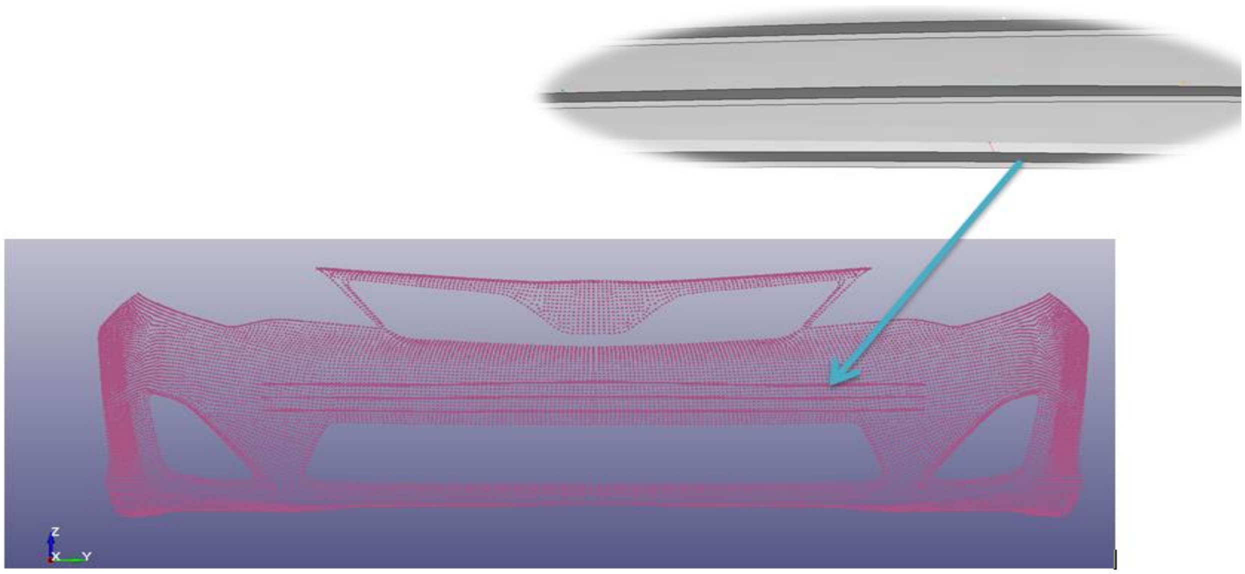

Figure 4.11 Corrugated bumper geometry

The added energy absorbing parts are designed in order to have a controlled deformation. This deformation is used to absorb the maximum kinetic energy during a crash. This deformation zones not only absorbed the kinetic energy of impactor, but also the kinetic energy of the whole vehicle (Ning et al., 2020).

4.4.2 Material for Bumper

The choice of bumper material has a decisive effect on the impact behavior of the vehicle and with the right choice; possible to achieve high fuel efficiency with minimal weight without sacrificing strength. “It is said that 75% of fuel consumption directly relates to vehicle weight. Lightweight composite materials provide opportunities for reducing vehicle weight, thus increasing fuel efficiency and reducing emission of harmful pollutants. On the condition of everything else remaining the same, 6%–8% increase in fuel economy can be realized for every 10% reduction in weight. Fiber-reinforced polymer composites possess several advantages over steel, the most salient of which are their high strength-to-weight ratio and excellent corrosion resistance. Carbon fiber composites can not only increase the strength of the structure but also decrease the weight of the structure" (Wang & Li, 2015).

The advantages of carbon polymeric composites compared to steels for automobiles are;

- Due to its extremely low density, it is 20-40% lighter
- Reduce tooling cost by 40%–60%
- Reduced installation costs and time
- Resistance to corrosion and scratches, reduced noise vibration harshness (NVH), and higher damping.
- Materials and process innovations capable of adding value while providing cost savings.
- Safer structures due to higher specific energy absorption.

Carbon polymeric composites are one of 21st century automotive materials. It has mostly known by its properties such as low density, high strength, high modulus, corrosion resistance, self-lubricating, high temperature resistance, low thermal expansion coefficient, and good conductivity/thermal performance. "However, the price of the carbon fiber composites too expensive to be widely used in the automobile manufacturing as compared to materials such as steel or aluminum. Since a lot of researches and efforts are on-going by researchers and research institutions to reduce the manufacturing cost of carbon fiber composites, the commercialization and use of carbon fiber polymeric composites with minimized cost for automobiles will come true in the near future" (Wang & Li, 2015). Therefore, carbon fiber polymeric composites bumper material is preferred and used instead of other material. With the given material property data obtained from literatures**,** the properties will be directly used as the physical parameters in LS-DYNA material cards. The type of the carbon fiber composite used is Polyamide-based Carbon fiber filled composite, which is manufactured by 3D printing technology through Selective Laser Sintering method, whose density is 1.10 g/cm^3, Poisson's ratio (y12 and y13) is 0.042 and y23 (0.23) and other mechanical properties are shown in Table 4.3:

Table 4.3 Material properties of carbon polyamide for LS-DYNA material cards

Material type	Material properties			
	Property		values	unit
Polyamide-based Carbon fiber polymeric composite	Mass density	ρ	1.16e-6	kg/mm^3
	Young's modulus	E_{11}	6.638	GPa
		E_{22}	2.661	GPa
	Poisson's ratio	μ_{12}	0.42	-
		μ_{23}	0.42	-
		μ_{13}	0.23	-
	Shear modulus	G_{12}	5.696	GPa
		G_{23}	5.696	GPa
		G_{31}	3.402	GPa
	Longitudinal strength	Compressive, XC	1.59	GPa
		Tensile, XT	2.56	GPa
	Transverse strength	Compressive, YC	0.185	GPa
		Tensile, YT	0.073	GPa
	Shear strength, SL		0.068	GPa
	Yield strength, YS		2.35	GPa

The material model or keyword used to define the material is * MAT_ENHANCED_COMPOSITE_DAMAGE or * MAT_054 or * MAT_055. "This material model is used to define a unidirectional thin shell. If the material is undamaged, the map assumes that the material is orthogonally anisotropy and linear elastic, and when damage occurs, non-linearity is introduced into the material" (Can, 2016).

The LSDYNA MAT54 material model is interesting for large-scale structural damage simulations because it is a relatively simple material model that requires only minimal input parameters.

This not only reduces the computational requirements of the simulation, but also reduces the difficulty and scope of the material test required to generate the input parameters. In addition to the composite properties listed in Table 4.3, other custom parameters for MAT 54/55 are listed below as shown in Table 4.4 below:

Table 4.4 MAT54 additional user input definitions from LSDYNA

Variable	Definition	Value	Unit	Description
SOFT	Crush front strength reducing parameter	1.00	[-]	Default value
YCFAC	Softening factor for fiber compressive strength after matrix failure	2	[-]	Default value
SOFT2	Optional transverse softening reduction factor	1.00	[-]	Default value
SLIMT1	Factor to determine the minimum stress limit after stress maximum (fiber tension)	0.01	[-]	Small but non-zero residual strength is assumed after tensile failure to avoid numerical instabilities
SLIMC1	Factor to determine the minimum stress limit after stress maximum (fiber compression)	0.35	[-]	Recommended
SLIMT2	Factor to determine the minimum stress limit after stress maximum (matrix tension)	0.10	[-]	Recommended
SLIMC2	Factor to determine the minimum stress limit after stress maximum (matrix compression tension)	1.00	[-]	Recommended

4.4.3 Bumper Thickness

Based on analyzing several references, it is concluded that materials of different thicknesses may exhibit different performances. Therefore, in this thesis, carbon polyamide composite bumpers of various thicknesses used to achieve the effect of thickness on the impact performance of the bumper.

The finite element model of the carbon polyamide composite bumper system was based on the original model of the steel bumper system. The cross-sectional dimensions and length of the bumper are the same as the conventional high-strength steel bumper. The wall thickness of the composite bumper should be designed bigger as the stiffness of the material is lower than high-strength steel given the same volume and the wall thickness of the composite set approximately twice that of the high strength steel bumper. Too much increasing the bumper thickness means, more kinetic energy transfer from impactor to vehicle and less plastic strain energy dissipates, this decrease the deformation after impact (Muhammad Nasiruddin et al., 2017). As the thickness of the composite changed, so does the mass and fiber orientation.

Unlike metals, the mechanical properties of composites depend on their fiber orientation. That is, different fiber orientations give different results. In other words, testing in different directions will give different results. This means that it is important to be aware of both the magnitude and direction of the load applied to the composite during the design phase. This is because the fibers have the best mechanical properties along the length, not the entire width. This increases the anisotropy of the composite.

The strength of a composite when measured in the direction of the fibers is referred to as the longitudinal strength. The stresses at which the fibers and the matrix fail determine the strength of a composite. The stresses in the unidirectional composite can be determined by taking an assumption. Thus are:

- ❖ The fibers are continuous
- ❖ The fibers are aligned in one direction only
- ❖ The load is applied normal to the direction of the fibers as shown in figure 4.12:

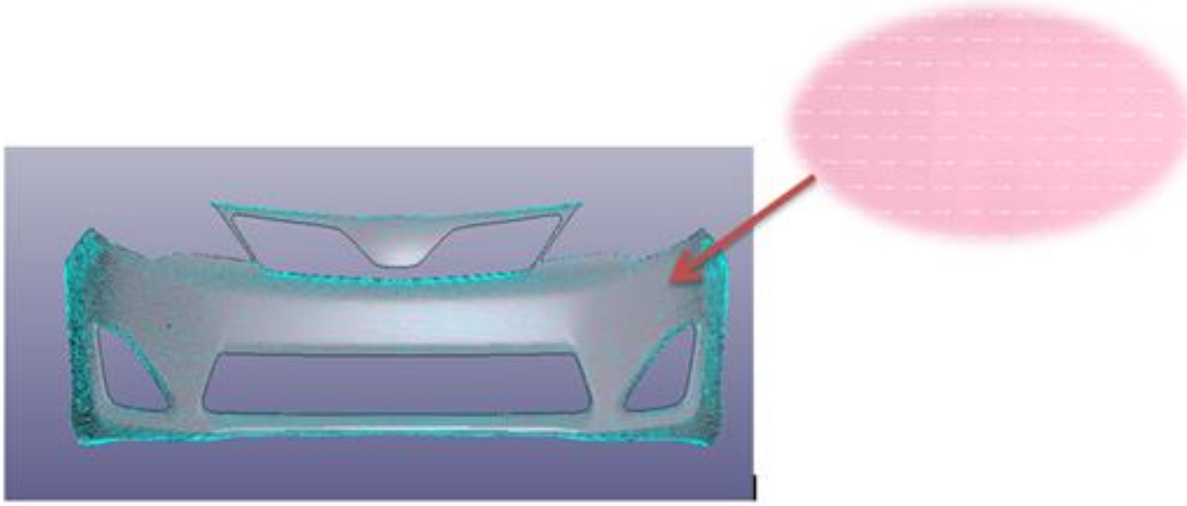

Figure 4.12 automobile bumper fiber orientations

Layup design is an important factor that contributes to the impact resistance of laminated composite structures at low speed impacts. Therefore, when designing a composite laminate, it is important to first consider the stacking order of the layers and define the proper symmetry and balance of the stacking. For this thesis, a bumper beam with 8 layers and fiber orientation of [0, ±30, ±60, and 90] are taken which is considered to be good (Tay, Papa, Koneru, Moradi, & Lankarani, 2015).

- Since the thickness of the bumper is very small as compared to its length, therefore a shell section is used to model and the ply angles (fiber orientation) were defined at each integration point in LS-DYNA using the input card:

*SECTION_SHELL/_TSHELL

- BOUNDARY CONDITIONS: The bumper is constrained at all degrees of freedom using BOUNDARY_SPC_SET, and the bumper and corrugated reinforcement are constrained together using the LSDYNA CONSTRAINT_NODAL_RIGID_BODY (CNRB) keyword in LS-DYNA as shown in fig 4.13-4.14 below:

Figure 4.13 Corrugated reinforcement CNRB (nodal rigid body)

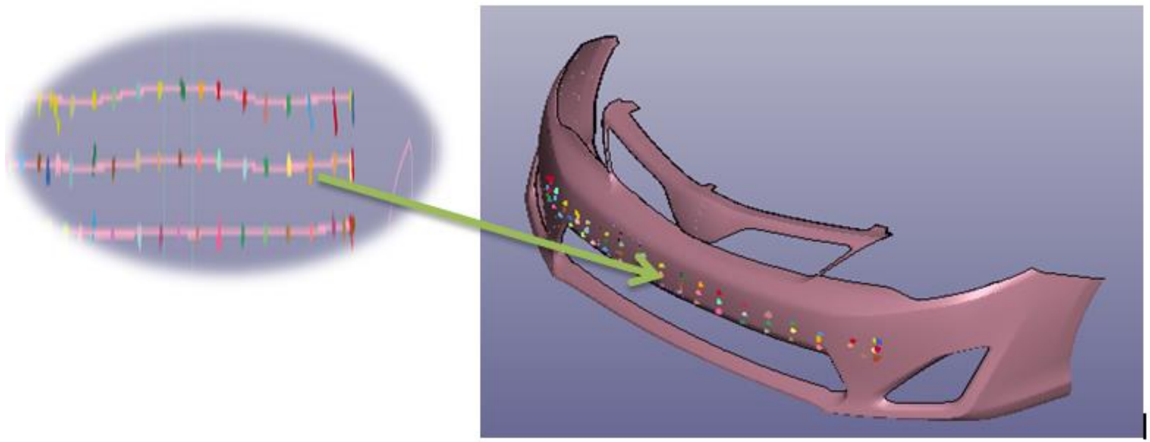

Figure 4.14 CNRB connects bumper with corrugated reinforcement

The different thickness and material limit settings for testing each bumper are displayed on the LSDYNA map as follows:

- INITIAL_VELOCITY_GENERATION was used to define the velocity of the moving components.
- CONTACT_AUTOMATIC_SINGLE_SURFACE_ID**,** used to define contact between the beam and support and CONTACT_AUTOMATIC_ SURFACE _SURFACE_ID between the bumper and the impactor (rigid pole).
- CONTROL_TERMINATION: is the run time of simulation and set as 300 ms.
- CONTROL_BULK_VISCOSITY: this may aid the stability in compressive mode of response and has default value of Q1=0, Q2=0, TYPE=-2**.**
- CONTROL_SHELL: Laminated shell theory corrects the false assumption of constant shear stress that is uniform throughout the shell thickness and has a default value of LAMSHT=1**.**
- CONTROL_HOURGLASS: a non-physical and zero energy mode of deformation. IHQ=4 (for shell element) and IHQ=5 (for solid element).
- DATABASE_EXTENT_BINARY: Used for post-treatment of fiber and base metal stress.

CHAPTER FIVE

5. RESULTS AND DISCUSSION

5.1 Introduction

In the previous chapter, steps and input parameters that are used in the analysis of the explicit dynamics are discussed briefly. In this chapter, a result of the analysis in relation to input parameters is discussed. The parameters that are specified in the previous chapter to give the result that change the bumper model analysis when it is exposed to these input parameters. In the analysis step, the effect of the velocity, thickness and material on the bumper model with different geometrical shapes.

The finite element model is generated in the LSDYNA software and deformation, impact force, structural response and energy absorption are obtained. The results are taken for both the hallow and corrugated geometry of the bumper model using carbon polyamide material. The effect of geometry, thickness, material and velocity are taken into consideration. The explicit dynamic analysis is mainly considered for analysis the bumper model. This will clearly explain the result of the bumper.

5.2 Result and discussion of existing model

1.2.1 Aluminum alloy 6061 bumper

1. The result of maximum resultant deformation and equivalent (von-Misses) stress distributions of Al 6061 alloy bumper model with a velocity of 4KMPH along with the direction of the impact with a rigid pole in hallow geometrical shapes.

As it is indicated on the counter plot 5.1, the maximum resultant deformation and von-Misses stress for the existing bumper geometry is 15.61mm and 483.5MPa respectively.

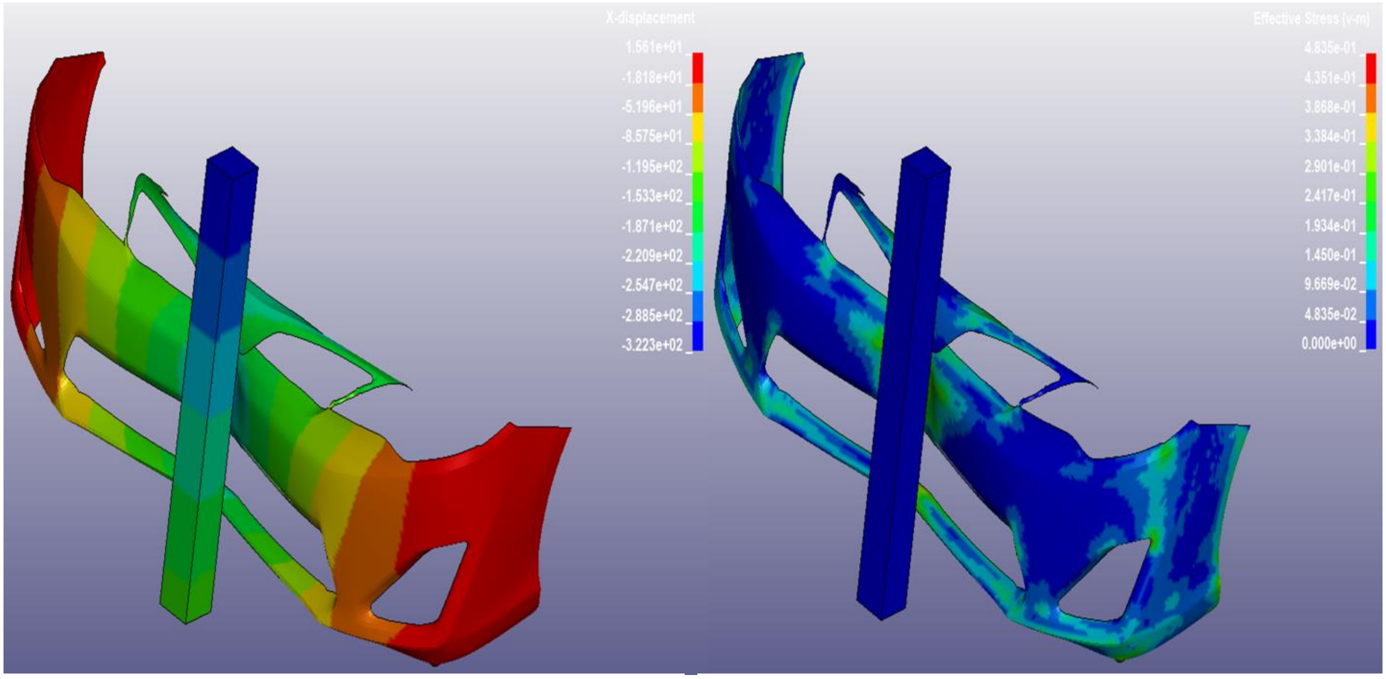

Max. Resultant deformation = 15.61 mm | Max equivalent (von-misses) stress = 483.5 MPa

Figure 5.1 Result Analysis of Al 6061 alloy bumper model with a velocity of 4KMPH

2. Energy balance

According to the law of conservation of energy, energy cannot be produced or destroyed, but it can be converted from one form of energy to another. Applying the same principle to collision analysis, the amount of kinetic energy lost during impact must be converted to other forms of energy such as internal energy, sliding energy, and hourglass energy. From Figure 5.2, the total energy consumed is constant throughout the simulation, and the total energy is the sum of the kinetic energy and potential energy of the entire system.

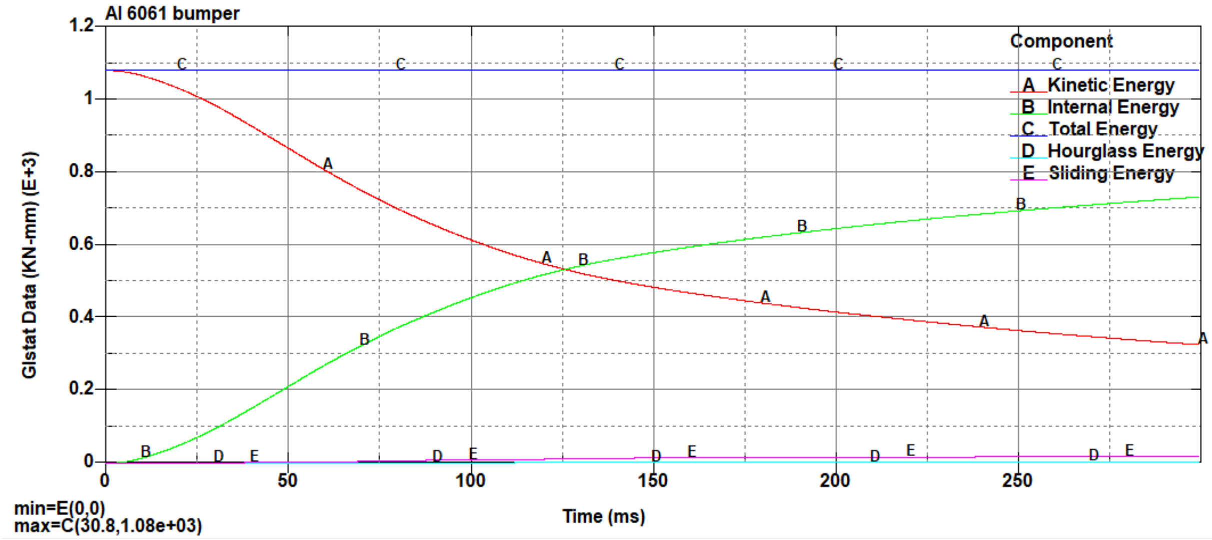

Figure 5.2 Energy balance curve

3. Energy absorption

Initially the high kinetic energy which is high at the beginning of the impact is equal to the total energy with value equal to 1080 J and as the crush event starts to take place the kinetic energy of the system starts to slowly getting decayed and converted to other forms of energy and then finally reaches to 327 J of energy. From this difference, it can be observed that 753 J of energy is absorbed and converted to internal energy, sliding energy and hour glass energy. Among this 735 J or 68.05% of energy is converted in the form of internal energy as shown in Figure 5.3-5.4 and the remaining 31.95% energy is dissipated in the form of sliding, hourglass energy.

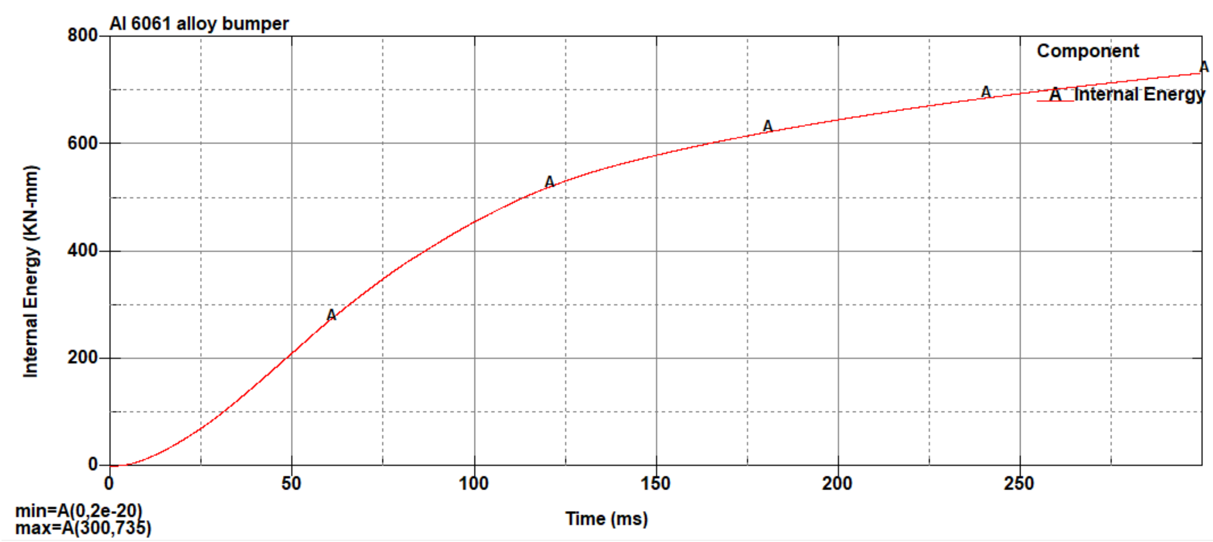

Figure 5.3 Total internal energy

Internal energy is one of the main criteria to determine the crash worthiness of the vehicle. It gives information about how much of energy (kinetic energy for this case) is absorbed by deformation of the vehicle. This helps in decreasing the impact energy which is likely to be transferred and cause problem to the components of the vehicle.

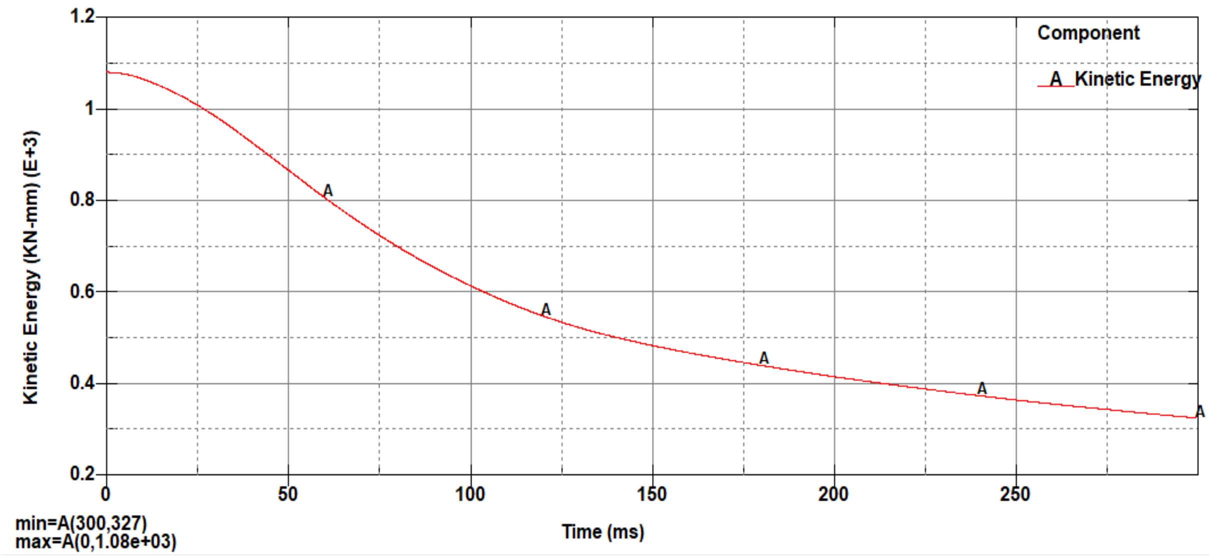

Figure 5.4 Kinetic energy

The kinetic energy of the system is decreasing and internal energy is increasing. Ideally the sum of kinetic energy and internal energy should be equal to total energy.

4. Deformation

In LS DYNA displacement is obtained by measuring the relative distance between two nodes So to measure the change in displacement of the bumper, two nodes (node id 2176465 relative to node2181714), as Shown on Figure 5.5. From this it is know that the maximum displacement on node 2176465 relative to node 2181714 in X direction is about 24.5 mm. Then finally by measuring the relative distance between two similar nodes of different materials after collision we can easily know the total deformation of the bumper.

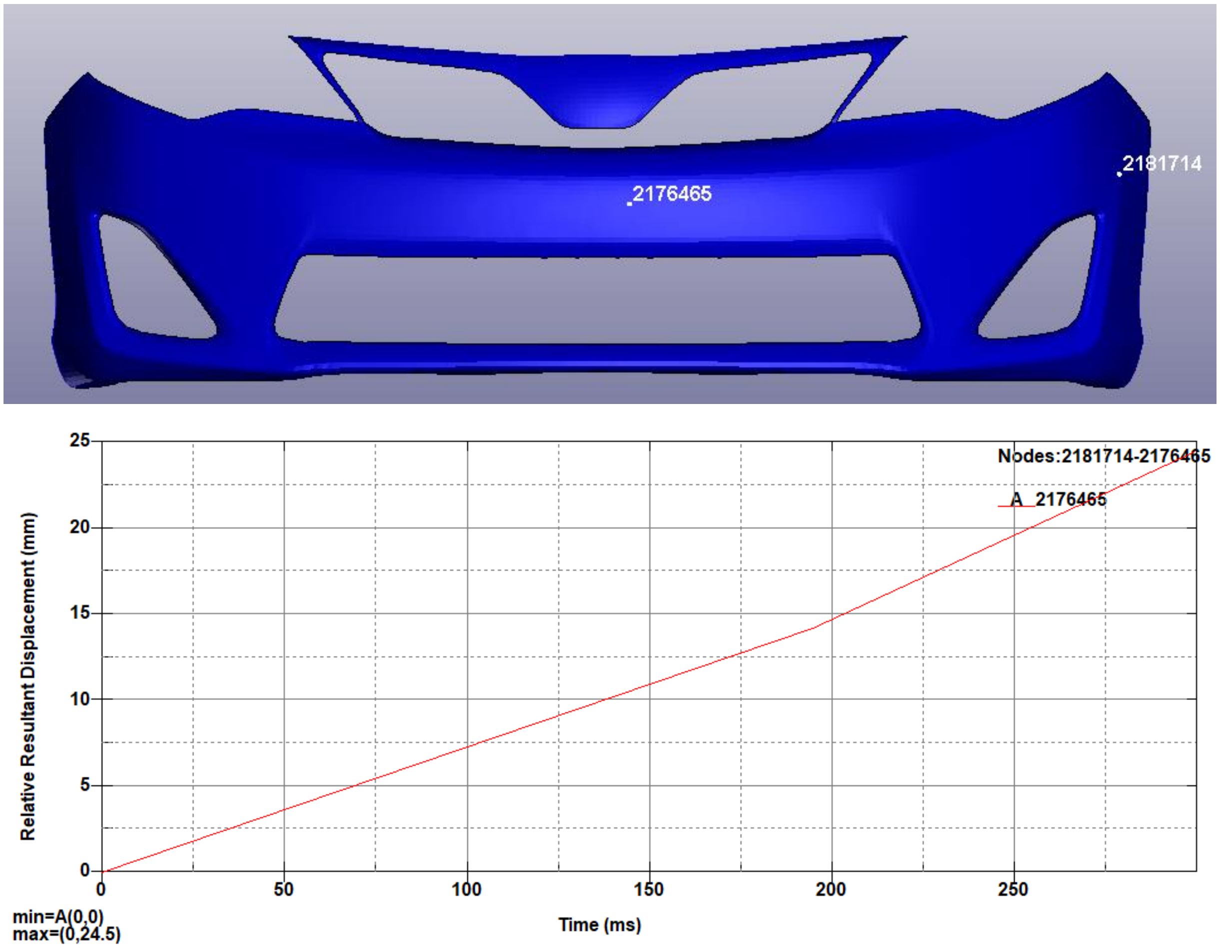

Figure 5.5 Relative X-displacement vs time

5. Impact force

The impact force between the rigid pole and the bumper in the x-axis direction. Initially, the contact force is almost zero until the time reaches 0.55ms. From this point on, the force begins to increase, showing some fluctuations. Fluctuations are due to temporary (time-dependent) movements of the simulation, as the forces exerted on the elements are not always constant. Maximum force occurs at a value of 4.10KN in 7ms when the pole in full direct contact with the bumper. At this point, the bumper and the entire vehicle are severely damaged. Therefore, the rigid pole and bumper have the same net contact force impulse, but in opposite directions as shown in figure 5.6-5.7:

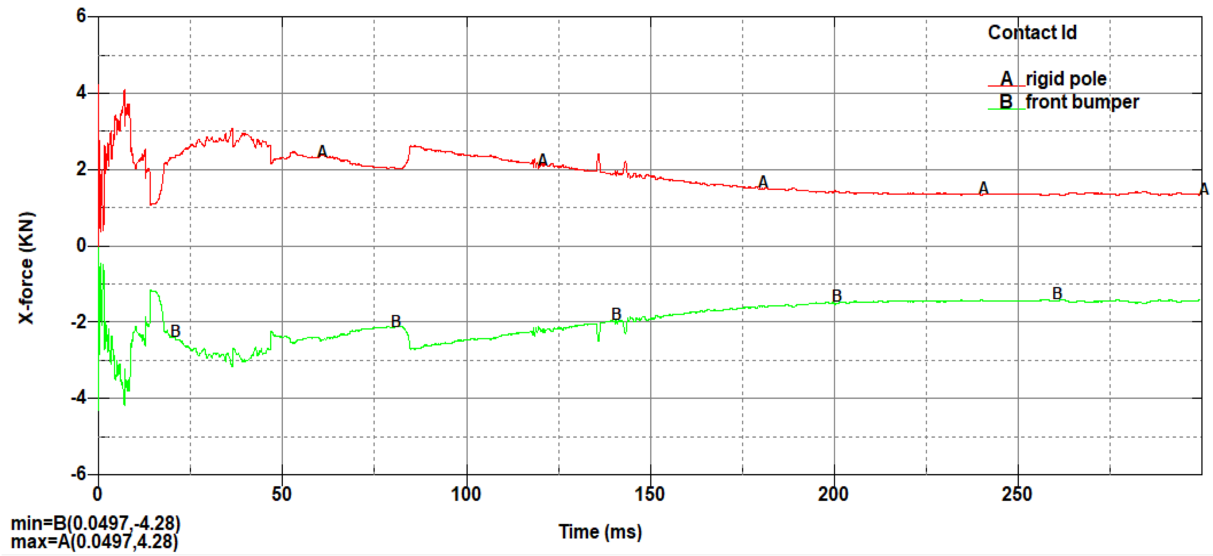

Figure 5.6 X-impact force

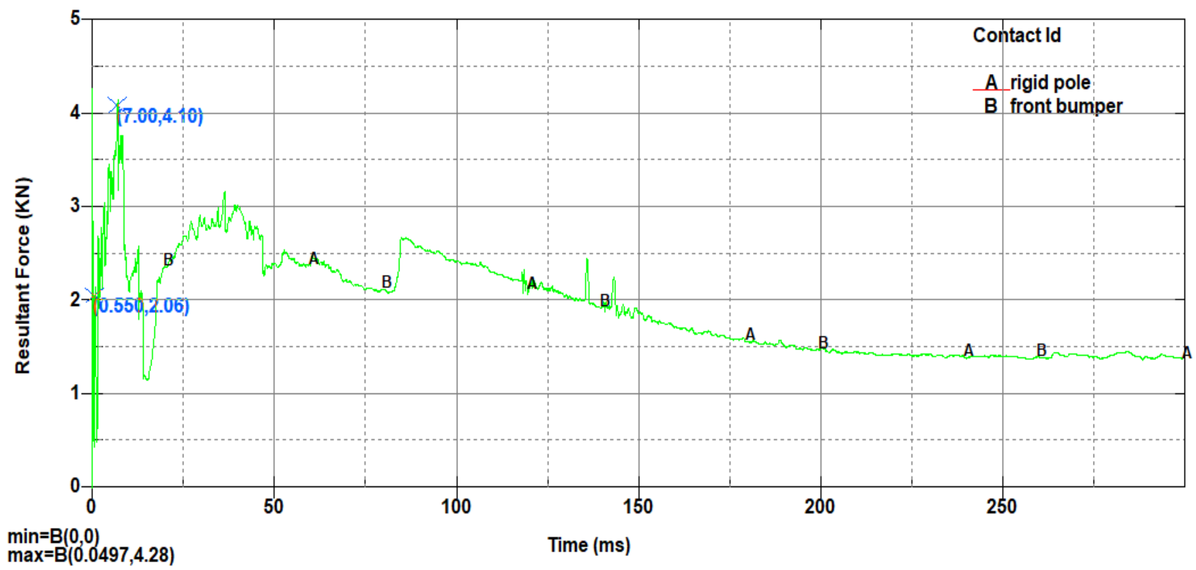

Figure 5.7 Resultant impact force

6. Relative Velocity

To analyze the speed changes of the various bumper sections, we use three nodes, two nodes on the two opposite edges, and one node on the central spread of the bumper and then by measuring the relative speed of each node at different time interval we can determine the relative speed of the bumper.

The resulting speed is shown in the following figure 5.8. Initially, the vehicle's speed is minus 1.11 mm /ms, and when the collision begins, the resulting speed slows down to the final value of minus 1.246 mm /ms. This indicates that the bumper has undergone plastic deformation due to its low coefficient of restitution.

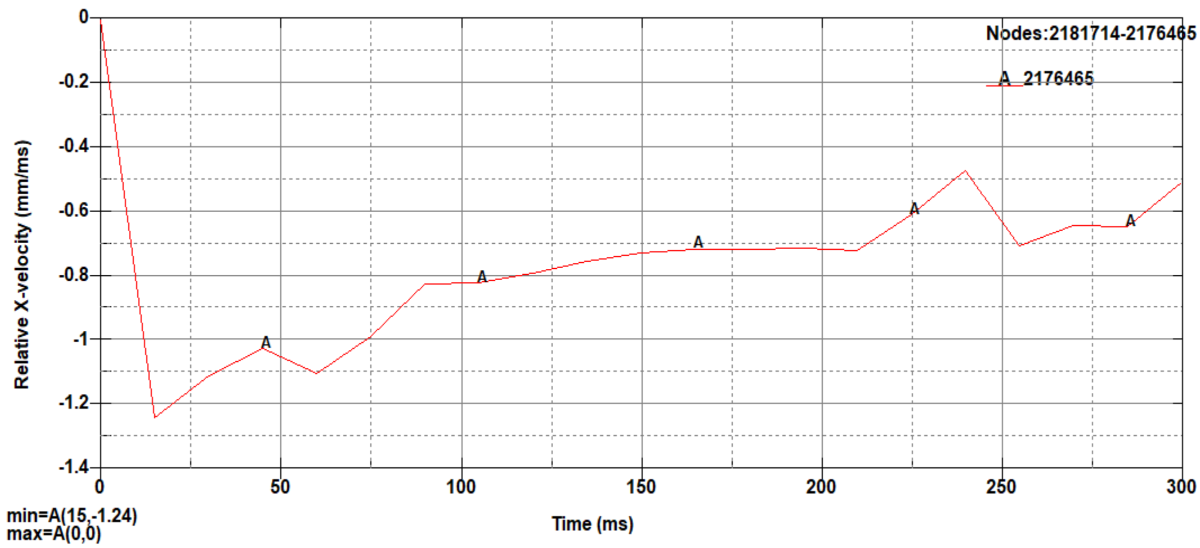

Figure 5.8 Relative velocity

7. Verification

Energy ratio

The energy balance curve shows that the system energy is not fully conserved and this is due to zero energy form of some elements. So it may be noted that, all the processes in this universe are irreversible and some losses are always included which deviates energy ratio slightly from one. This can be observed in the energy ratio graph.

The energy ratio value should be 1.00 +/- 0.07. As shown in the figure 5.9, the simulation produces an energy ratio with a maximum value of 1.004, which is approximately 1, with an error of 0.0004%, which is acceptable.

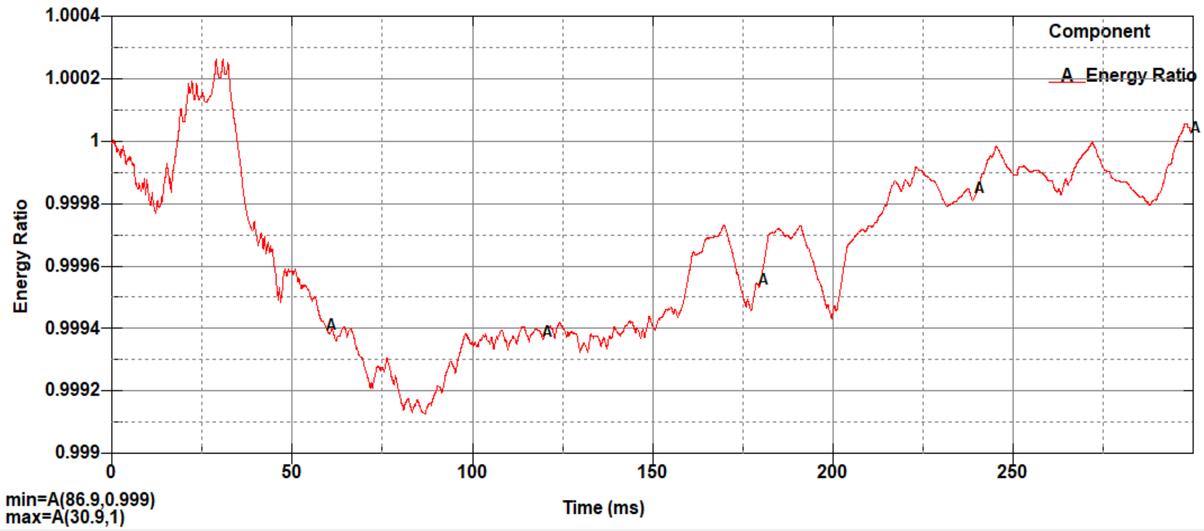

Figure 5.9 Energy ratio

Ratio of TE/HE

By analyzing the energy curve, the validity of the finite element model can also be judged from the relationship between total energy and hourglass energy. The energy of the hourglass can trigger a zero energy model. If the energy of the hourglass is less than 5% of the total energy, the finite element model is reliable. As it can be seen in the figure 5.10-5.11, the peak of the hourglass is equal to 0.00374 kJ, the total energy is equal to 1.08 kJ, and the HE / TE ratio is 0.346%, which is acceptable.

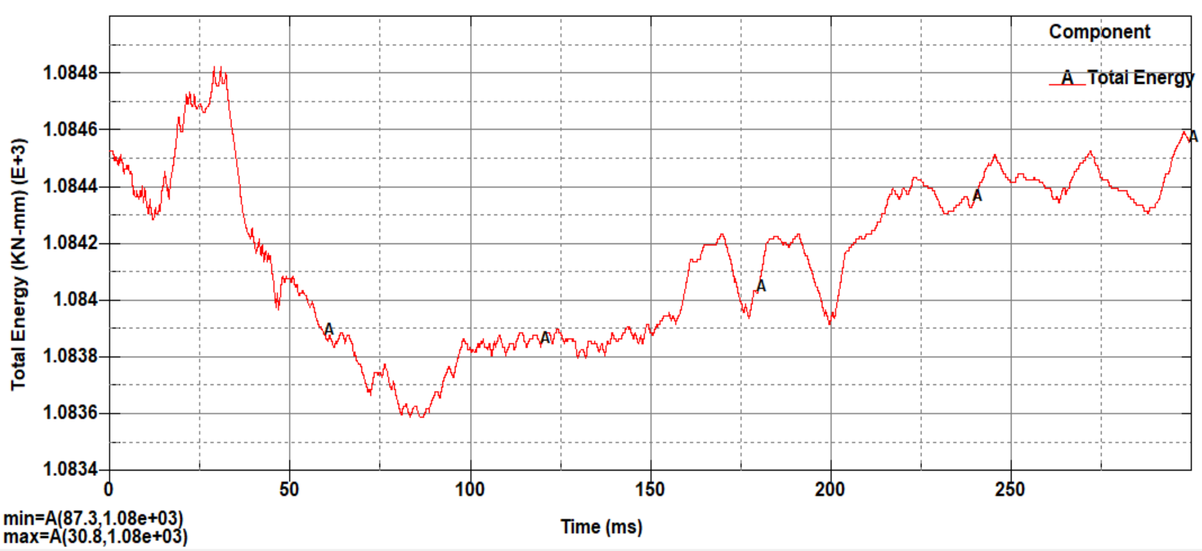

Figure 5.10 Total energy

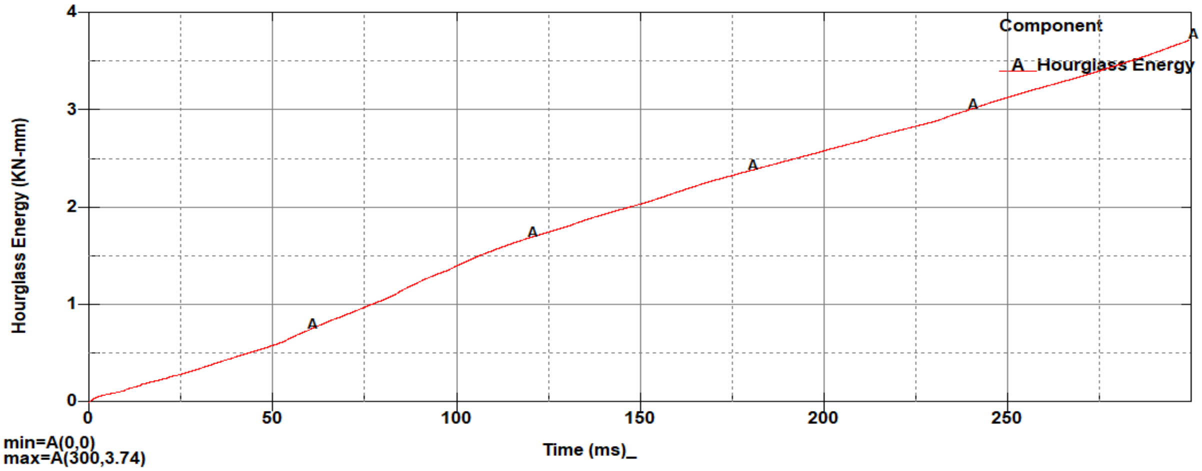

Figure 5.11 Hourglass energy

1.2.2 Aluminum alloy 7075 bumper

1. The result of maximum resultant deformation and equivalent (von-Misses) stress distributions of Al 7075 alloy bumper model with a velocity of 4KMPH along with the direction of the impact with a rigid pole in hallow geometrical shapes.

As it is indicated on the counter plot 5.12, the maximum resultant deformation and von-Misses stress for the existing bumper geometry is 14.5 mm and 569.7 MPa respectively.

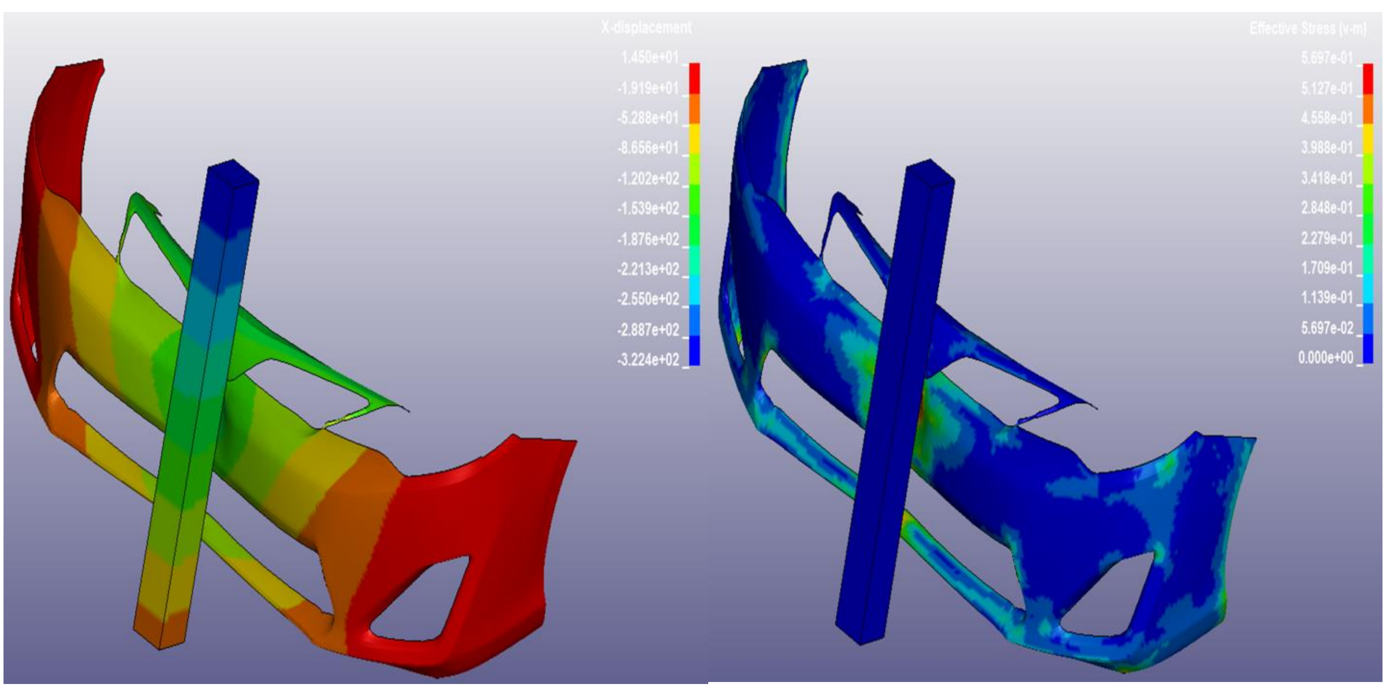

Max. Resultant deformation = 14.5 mm Max equivalent (von-misses) stress = 569.7 MPa

Figure 5.12 Result Analysis of Al 7075 alloy bumper model with a velocity of 4KMPH

2. **Energy balance**

According to the law of conservation of energy, energy cannot be produced or destroyed, but it can be converted from one form of energy to another. Applying the same principle to collision analysis, the amount of kinetic energy lost during impact must be converted to other forms of energy such as internal energy, sliding energy, and hourglass energy. From Figure 5.13, we can see that the total energy consumed is constant throughout the simulation, and the total energy is the sum of the kinetic energy and potential energy of the entire system.

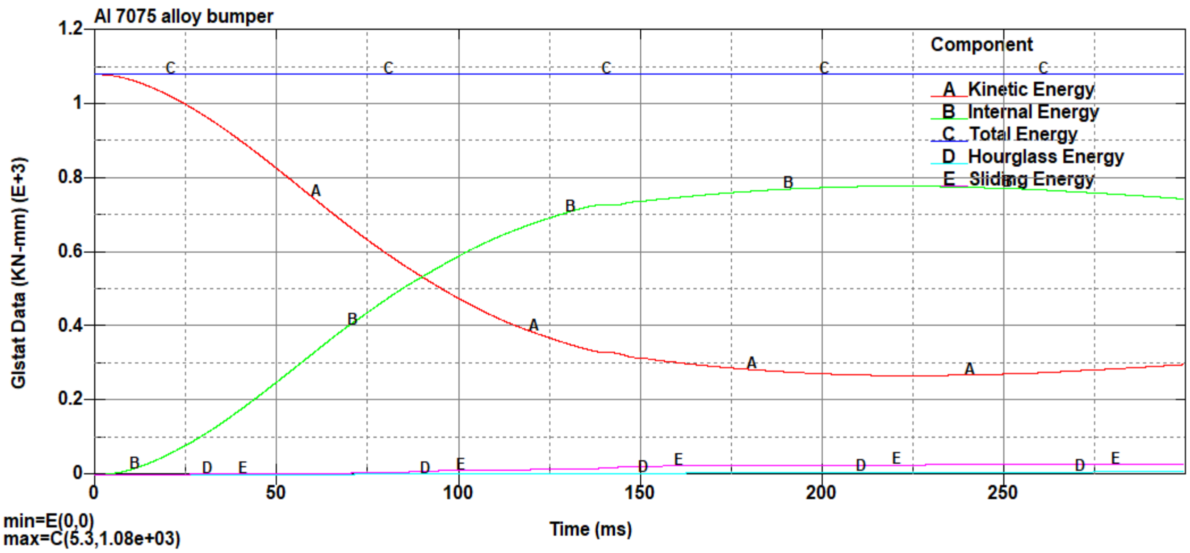

Figure 5.13 Energy balance curve

3. **Energy absorption**

Initially, the high kinetic energy at the beginning of the impact is equal to the total energy with a value of 1080 J, and when the crushing event begins, the system's kinetic energy begins to decay slowly and eventually reaching an energy of 269J. From this difference, we can see that the energy of 811 J is absorbed and converted into internal energy, sliding energy and hourglass energy. Of these 782J or 72.4% of the energy is dissipated in the form of internal energy, and the remaining 27.59% of the energy is dissipated in the form of an hourglass-energy that slides , as shown in the figure 5.14-5.15.

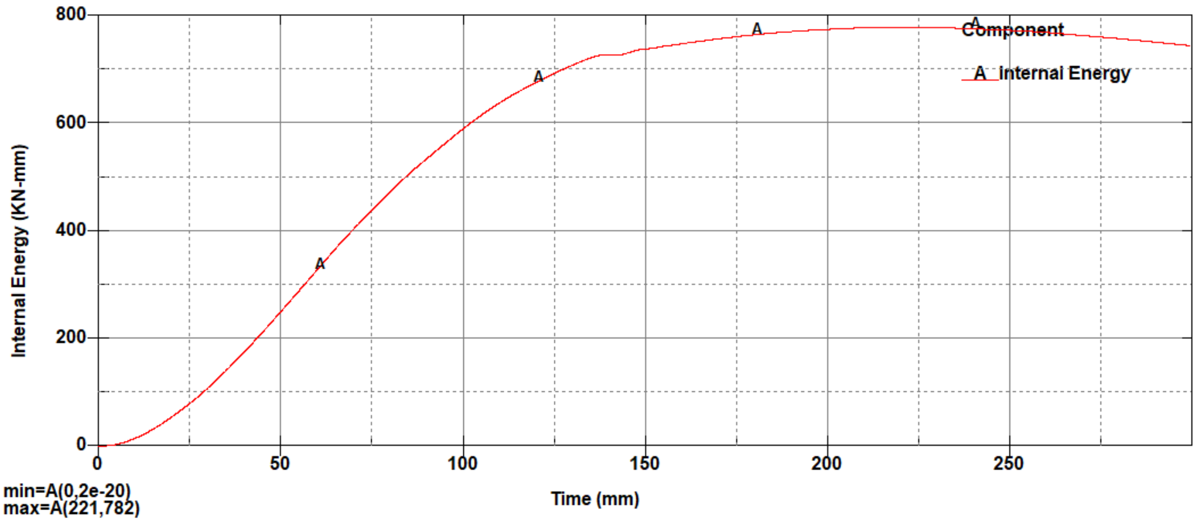

Figure 5.14 Internal energy graph

Internal energy provides information about the energy absorbed by the deformation of the vehicle. This reduces the impact energy that is likely to be transmitted and can cause problems for vehicle components.

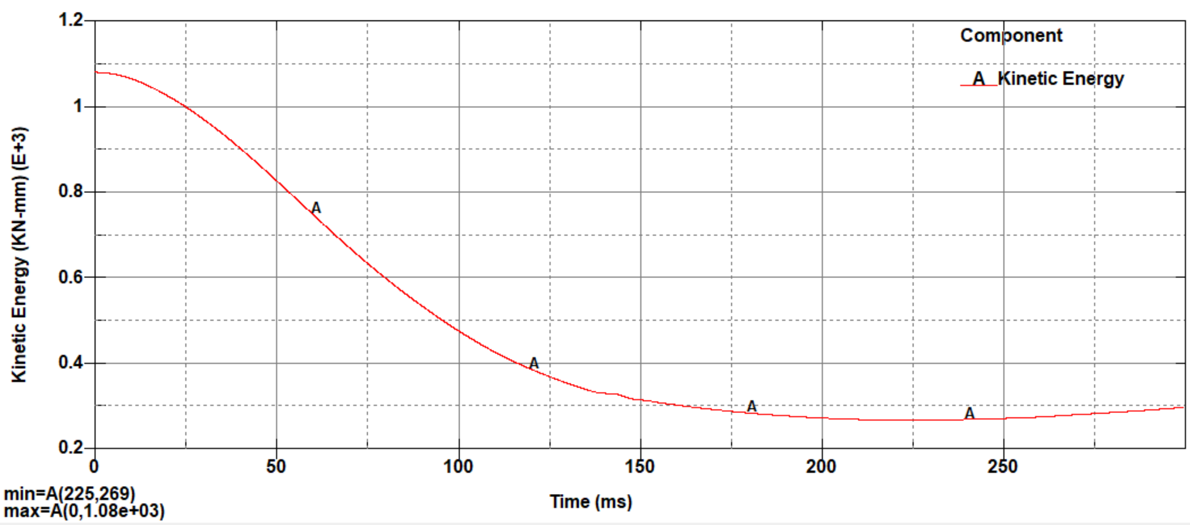

Figure 5.15 Kinetic energy graph

The kinetic energy of the system is decreasing and internal energy is increasing and the sum of the two energies is ideally equivalent to the total energy of the system.

4. Deformation

Displacement is detected by measuring the relative distance between two nodes. Therefore, to measure the change in bumper displacement, we will use two nodes (node ID 2176465 for node 2181714), as shown in the figure 5.16. From this, we can see that the maximum displacement of node 2176465 with respect to node 2181714 in the X direction is about 19.6 mm.

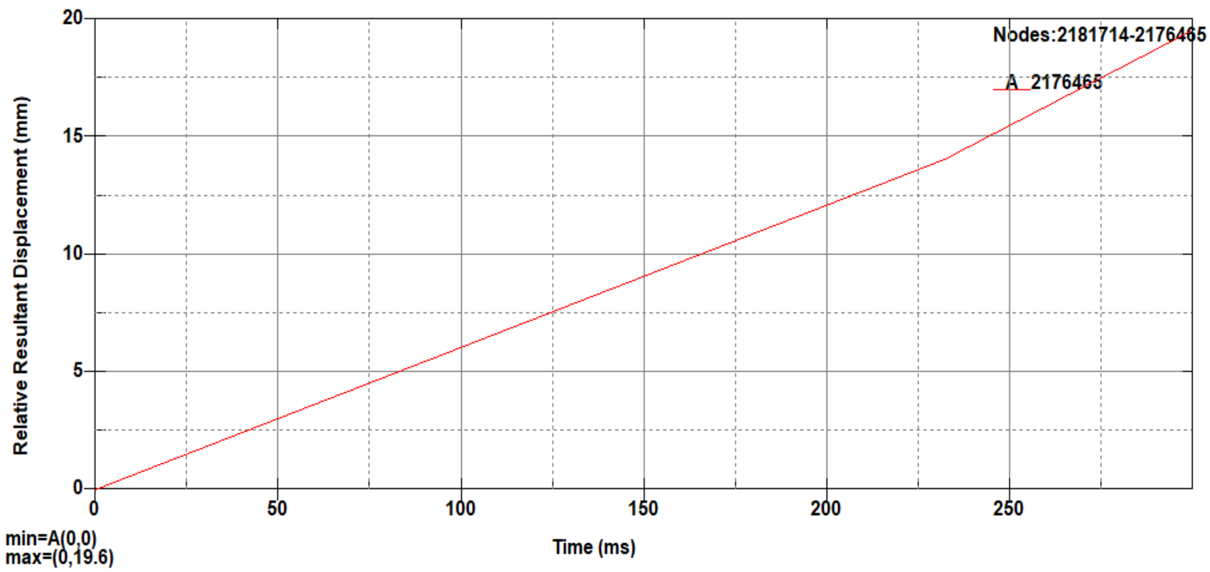

Figure 5.16 Relative X-displacement vs time graph

5. Impact force

The contact force between the rigid pole and the bumper is almost zero until the time reaches 3.10ms. From this point on, the force begins to increase, showing some fluctuations. Fluctuations are due to temporary (time-dependent) movements of the simulation, as the forces exerted on the elements are not always constant. Maximum force occurs in 52.2ms at a value of 4.87kN when the rod is in full direct contact with the bumper. At this point, the bumper and the entire vehicle are severely damaged as shown in figure 5.17-5.18:

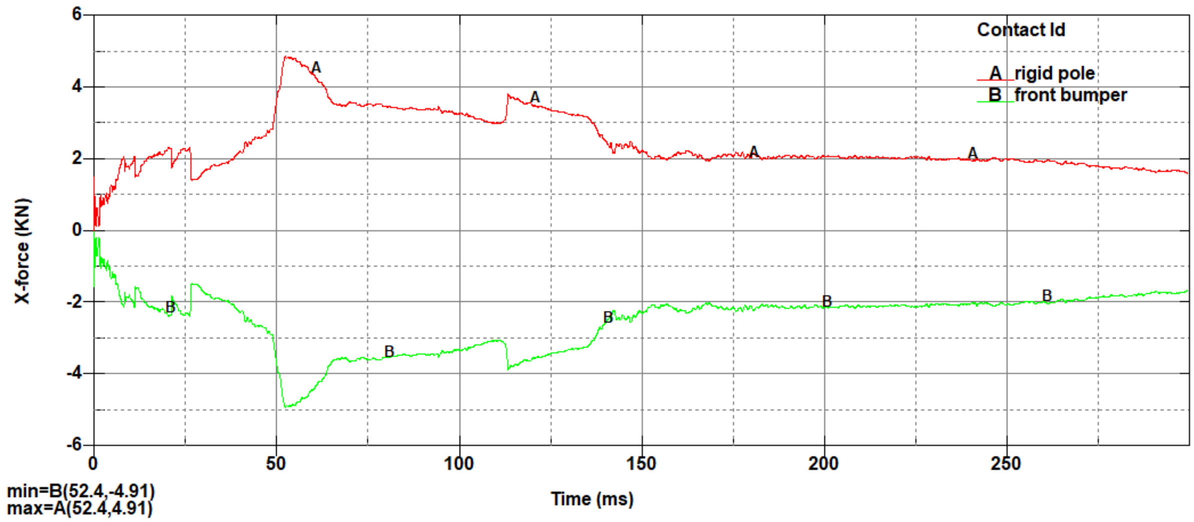

Figure 5.17 X-impact force graph

As shown in figure above the rigid pole and bumper have the same net contact force impulse, but in opposite directions.

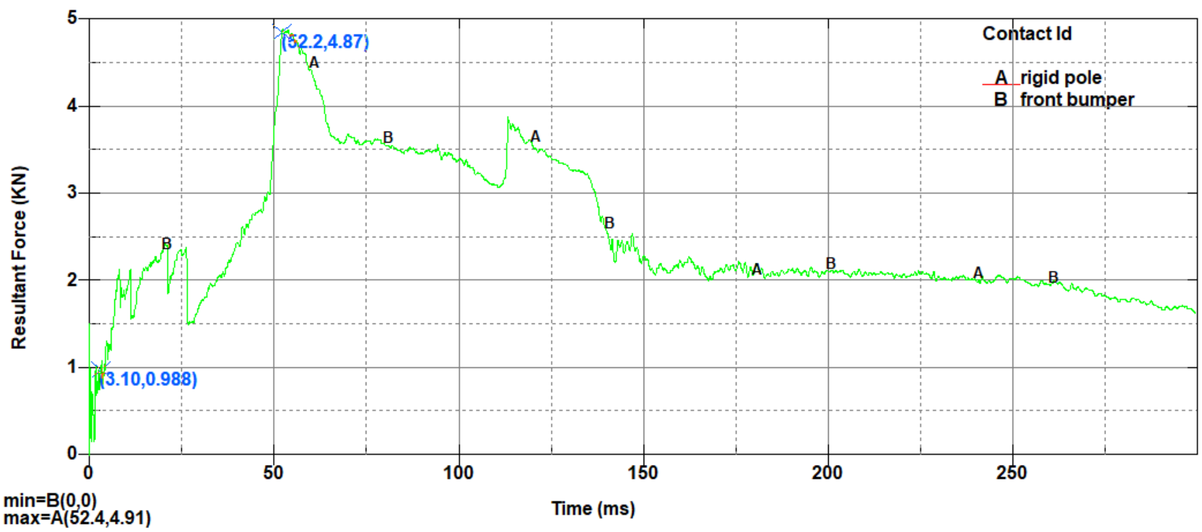

Figure 5.18 Resultant impact force graph

6. Relative Velocity

The resulting speed is shown in the following figure 5.19 below. Initially, the vehicle's speed is minus 1.11mm/ms, and when the collision begins, the resulting speed slows down to the final value of minus 1.19mm/ms. This indicates that the bumper has undergone a plastic deformation.

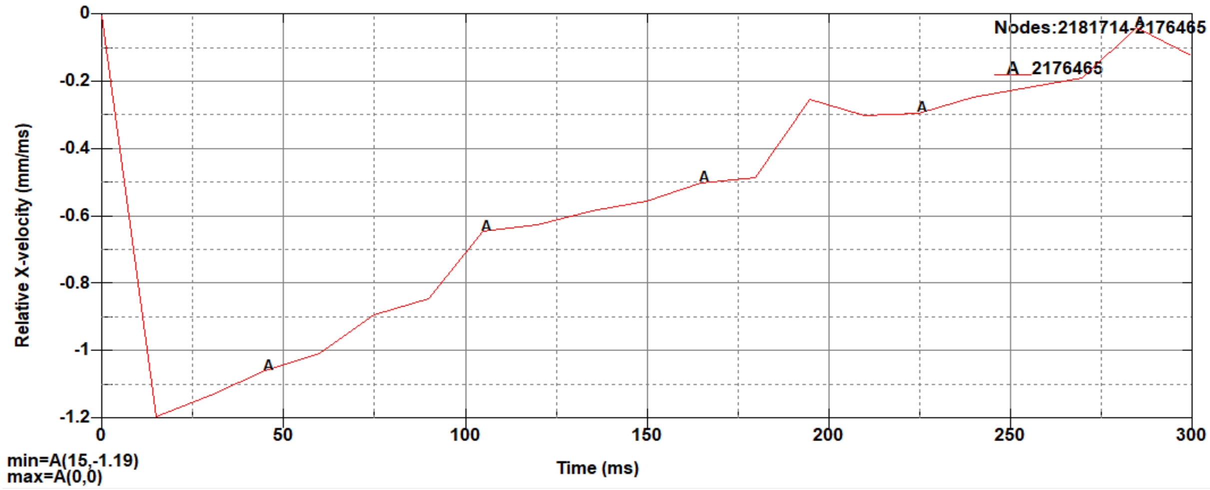

Figure 5.19 Relative velocity graph

7. Verification

Energy ratio

The energy ratio value should be 1.00 +/- 0.07. As it is seen from figure 5.20, the simulation produces an energy ratio with a maximum value of 1.0002. This value is close to 1 with an error of 0.0002%, which is an acceptable margin of error.

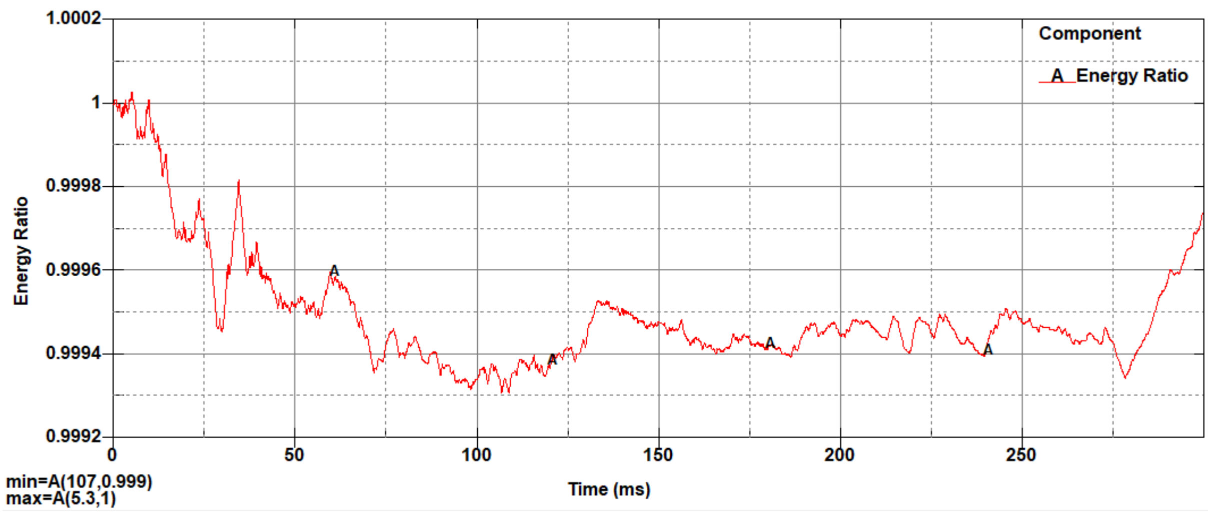

Figure 5.20 Energy ratio graph

Ratio of TE/HE

By analyzing the energy curve, the validity of the finite element model can also be judged from the relationship between total energy and hourglass energy. The energy of the hourglass can trigger a zero energy model. If the energy of the hourglass is less than 5% of the total energy, the finite element model is reliable. As shown in the figure 5.21-5.22. The peak of the hourglass is equal to 0.00844kJ, the total energy is equal to 1.08kJ and the HE/TE ratio is 0.78%, which is acceptable.

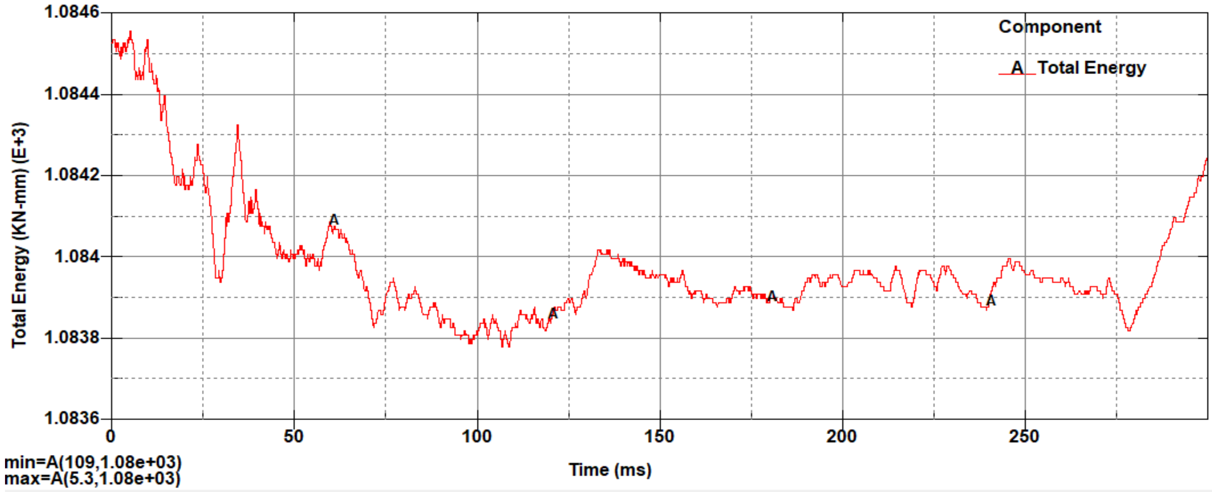

Figure 5.21Total energy graph

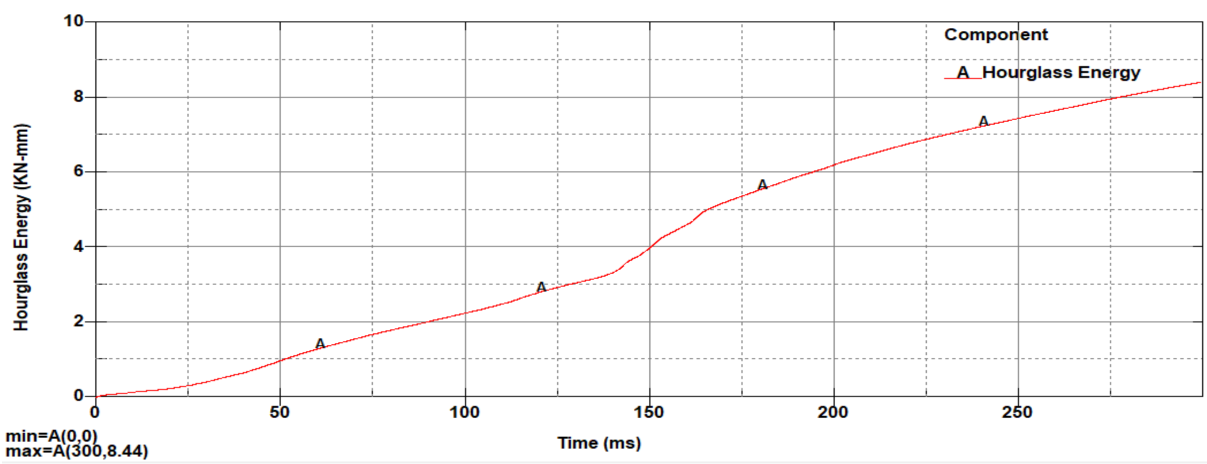

Figure 5.22 Hourglass energy graph

1.2.3 Steel bumper

1. The result of maximum resultant deformation and equivalent (von-Misses) stress distributions of Steel bumper model with a velocity of 4KMPH along with the direction of the impact with a rigid pole in hallow geometrical shapes.

As it is indicated in the figure 5.23, the maximum resultant deformation and von-Misses stress for the existing bumper geometry is 15.05mm and 363.7MPa respectively.

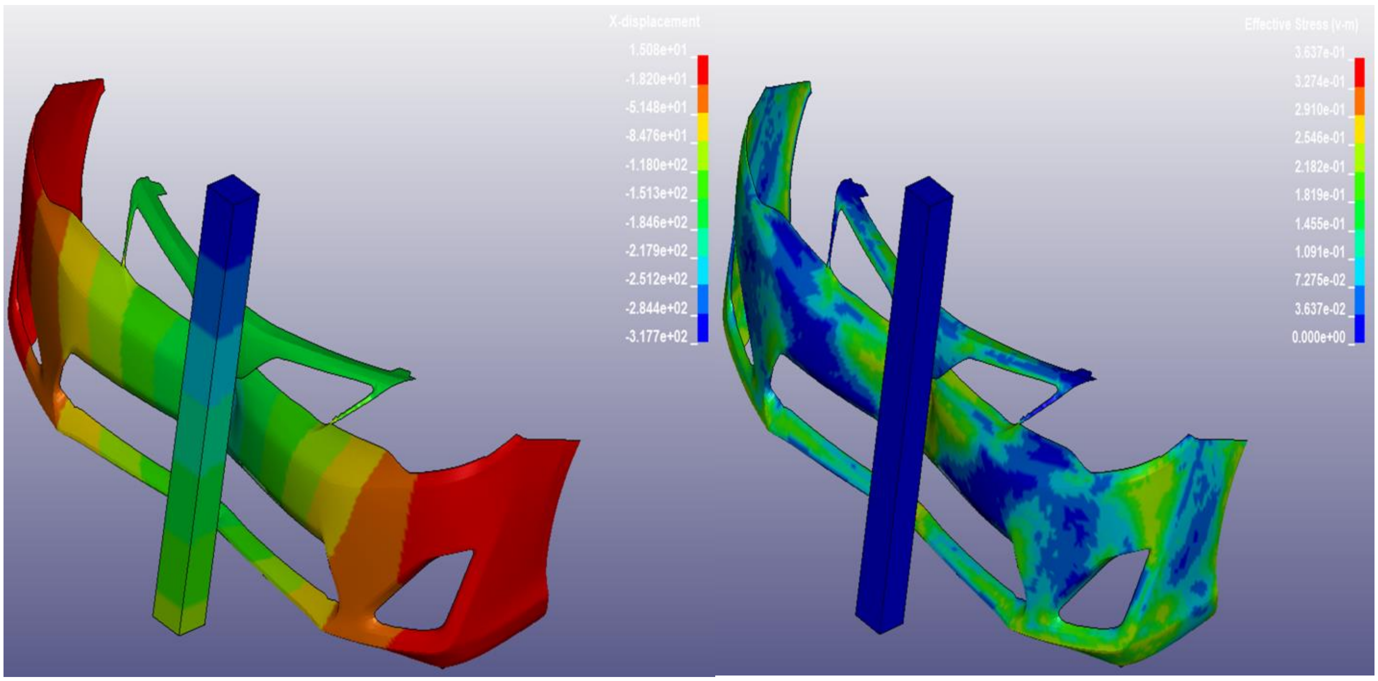

Max. Resultant deformation = 15.05 mm   Max equivalent (von-misses) stress = 363.7 MPa

Figure 5.23 Result Analysis of steel bumper model with a velocity of 4kmph

2. Energy balance

From Figure 5.24 below, we can see that the kinetic energy is initially high, with a value of 1080 J at the start of the impact, and a slight difference between the values of 1090 J of the total energy at the start of the crushing event. When generated, the kinetic energy of the system slowly begins to degrade and is converted into other forms of energy, eventually reaching 267 J of energy. The total energy consumed is constant throughout the simulation.

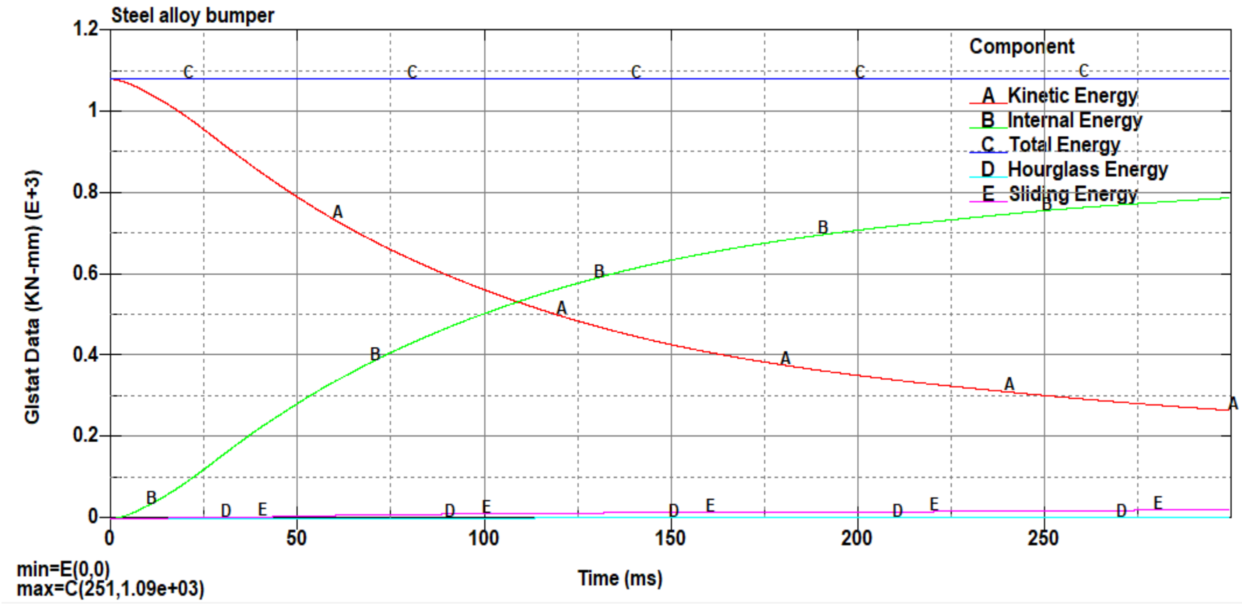

Figure 5.24 Energy balance

2 Energy absorption

Initially, there is a high kinetic energy at a value of 1080 J at the beginning of the impact, and when the crushing event begins; the system's kinetic energy slowly begins to dissipate, being converted to other forms of energy and finally reaching 267J of energy. From this difference, we can see that the energy of 813 J is absorbed and converted into internal energy, sliding energy and hourglass energy. Of this, 791 J, or 73.24% of the energy, is dissipated in the form of internal energy, and the remaining 26.76% is dissipated in the form of sliding and hourglass energy as shown in figure 5.25-5.26 below:

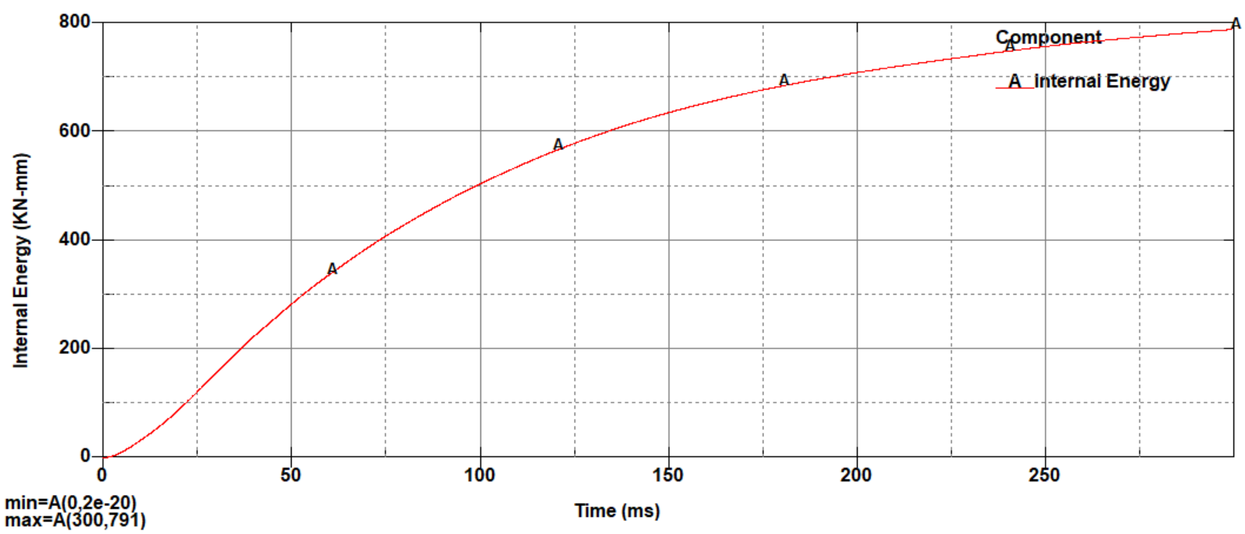

Figure 5.25 Internal energy

Internal energy provides information about the energy absorbed by the deformation of the vehicle. This reduces the transmitted impact energy that can cause problems for vehicle components.

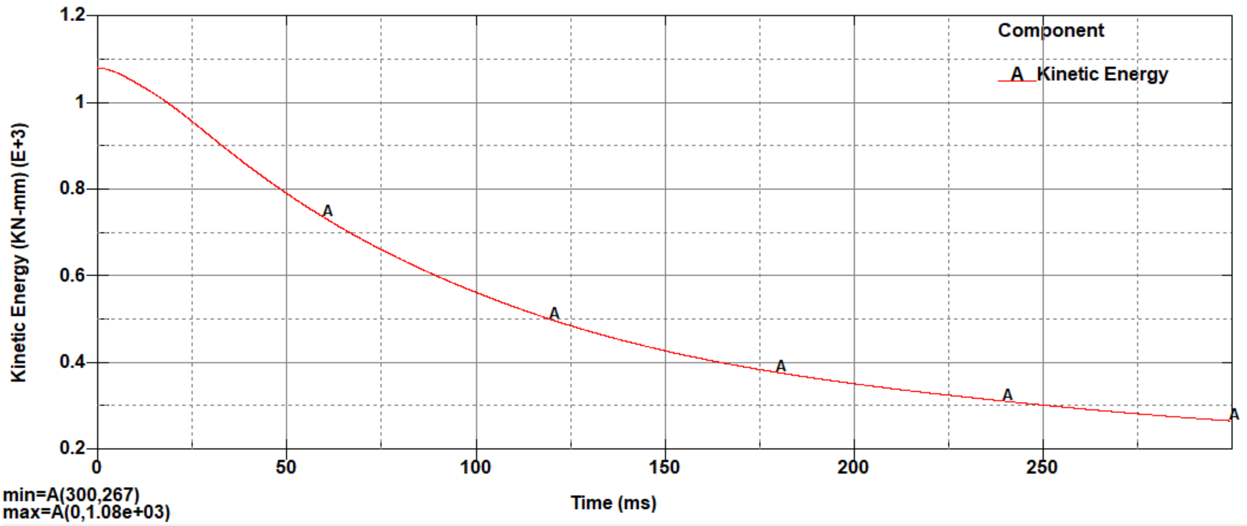

Figure 5.26 Kinetic energy

The kinetic energy of the system decreases, the internal energy increases, and the sum of the two energies is ideally equal to the total energy of the system.

3 Deformation

To measure the change in bumper displacement, we will use two nodes (node ID 2176465 for node 2181714), as shown in the figure 5.27. From this, we can see that the maximum displacement of node 2176465 with respect to node 2181714 in the X direction is about 20.2 mm.

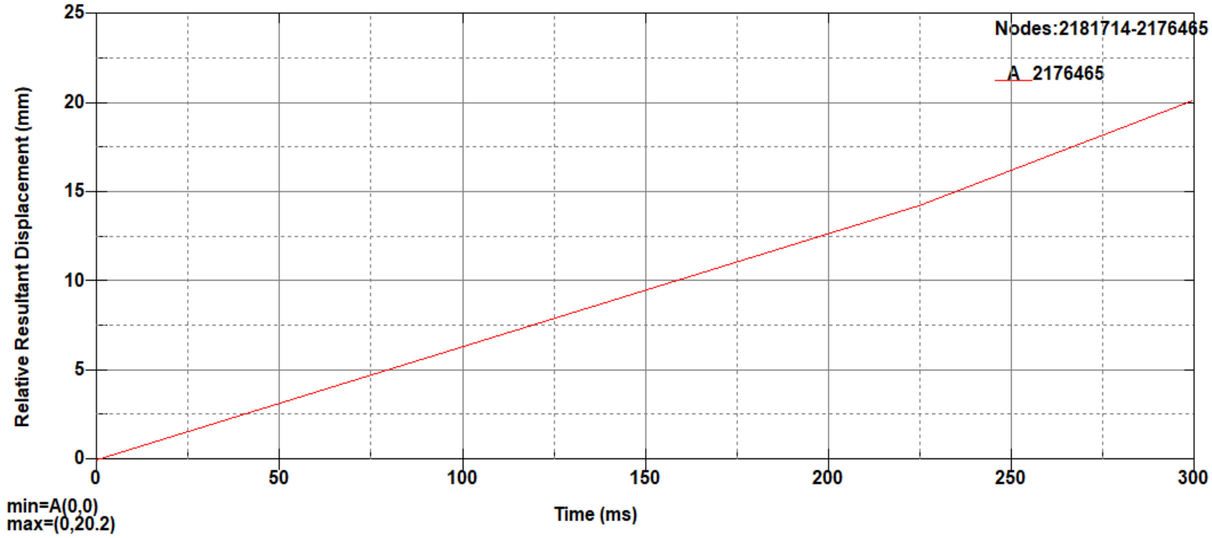

Figure 5.27 Deformation

4 Impact force

As shown figure 5.28-5.29 below, the contact force between the rigid pole and the front bumper is almost zero at first until the time reaches 4.55ms. From this point on, the force begins to increase, showing some fluctuations due to time-dependent movements of the simulation, as the forces exerted on the elements are not always constant. Maximum force of 9.78KN occurs at 64.7ms when the rigid pole is in full direct contact with the bumper.

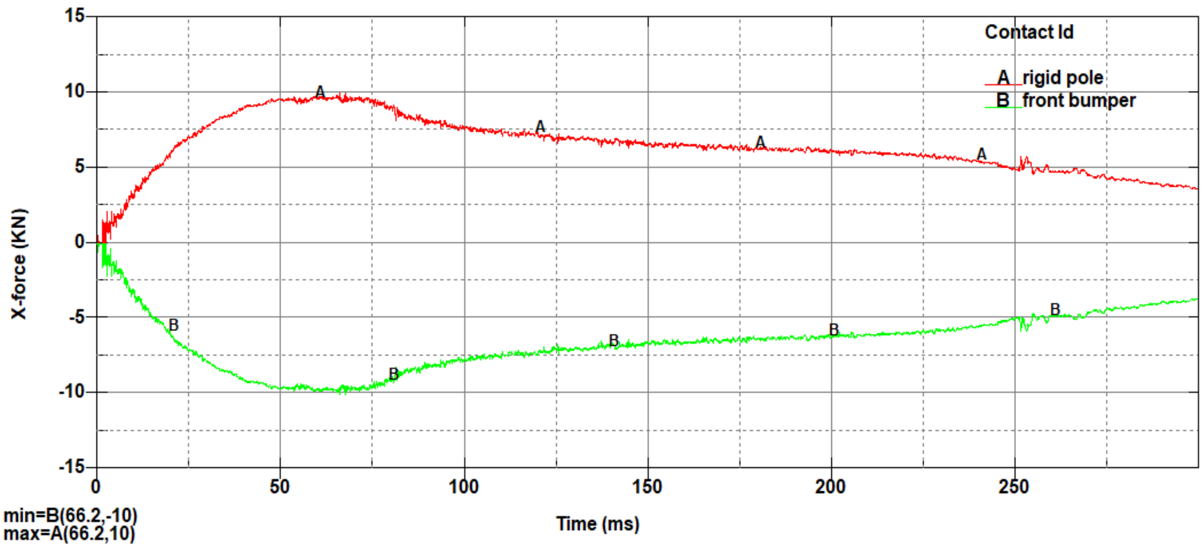

Figure 5.28 X-impact force

The rigid rods and bumpers have the same net contact force impulses, but in opposite directions.

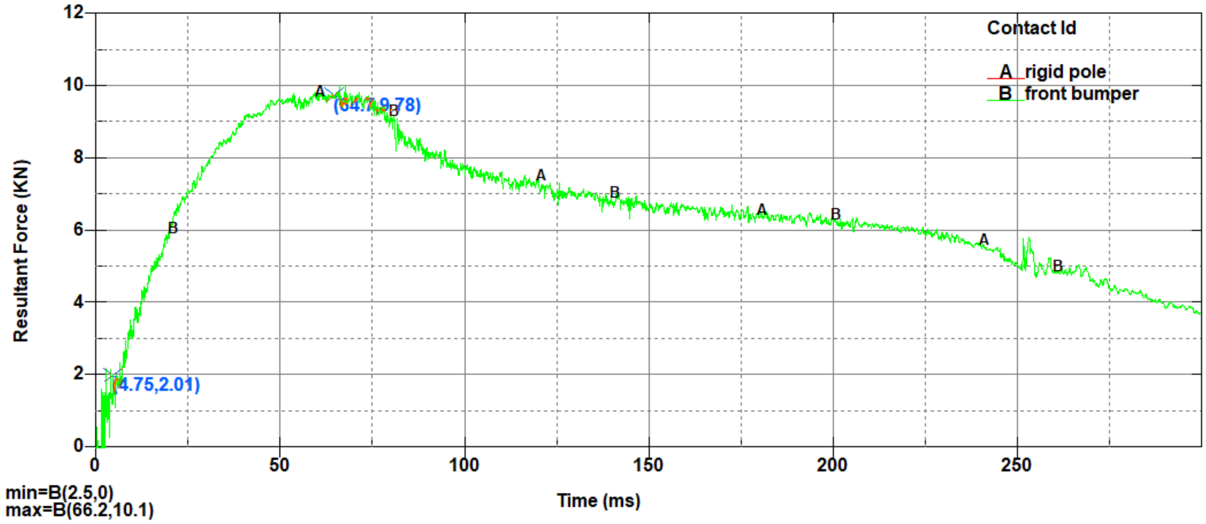

Figure 5.29 Resultant impact forcegraph

5 Resultant Velocity

The resulting speed is shown in the following figure 5.30. Initially, the vehicle's speed is minus 1.11mm/ms, and when the collision begins, the resulting speed slows down to the final value of minus 1.19mm / ms. This indicates that the bumper has undergone plastic deformation.

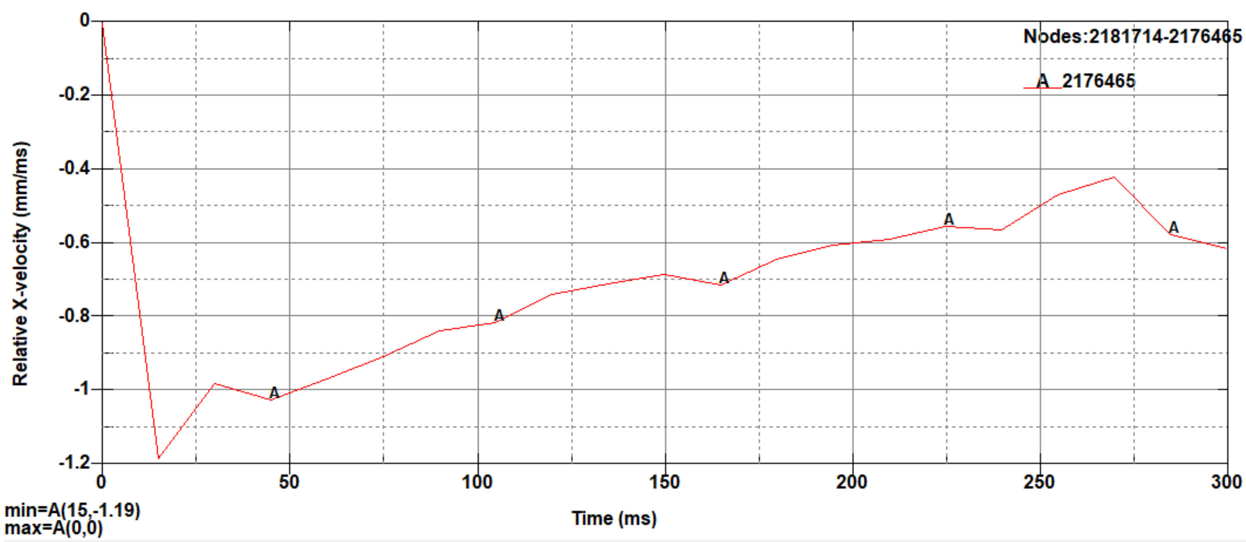

Figure 5.30 Relative velocity

6 Verification

Energy ratio

The energy ratio value should be 1.00 +/- 0.07. As shown in figure 5.31 below, the simulation produces an energy ratio with a maximum value of 1.001. This value is close to 1 with an error of 0.001%, which is an acceptable margin of error.

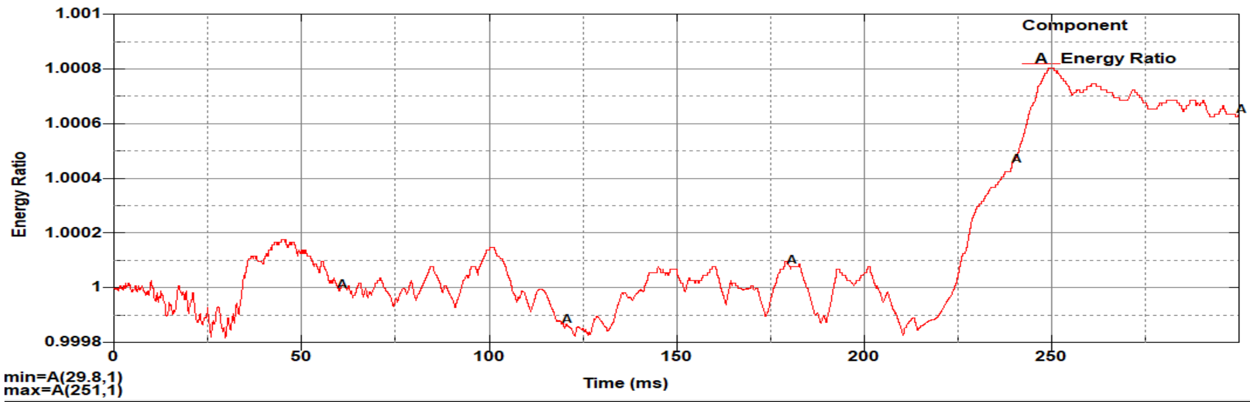

Figure 5.31 Energy ratio

Ratio of TE/HE

By analyzing the energy curve, the validity of the finite element model can also be judged from the relationship between total energy and hourglass energy. If the energy of the hourglass is less than 5% of the total energy, the finite element model is reliable. As shown in the figure 5.32-5.33. The peak of the hourglass is equal to 0.00326kJ, the total energy is equal to 1.09kJ, and the HE/TE ratio is 0.299%, which is acceptable.

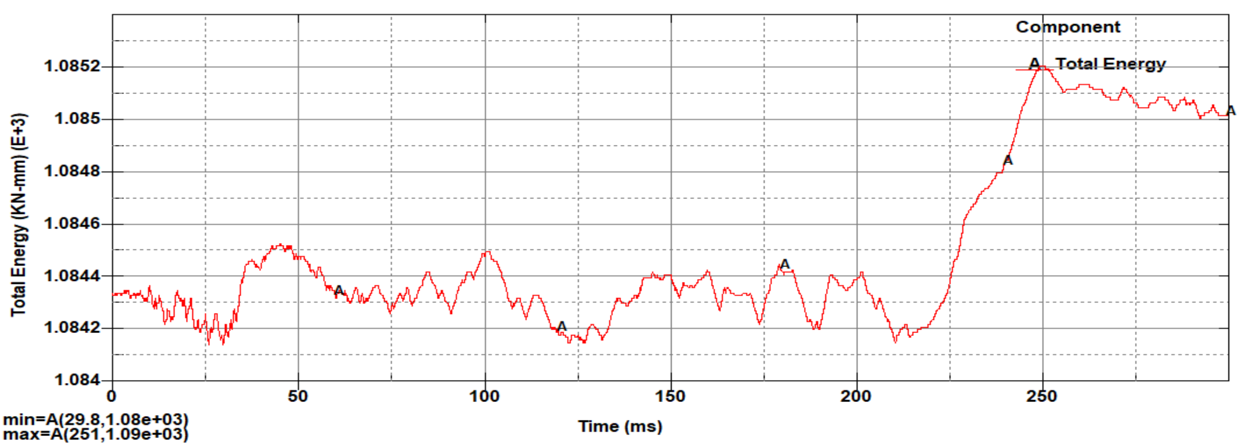

Figure 5.32 Total energy

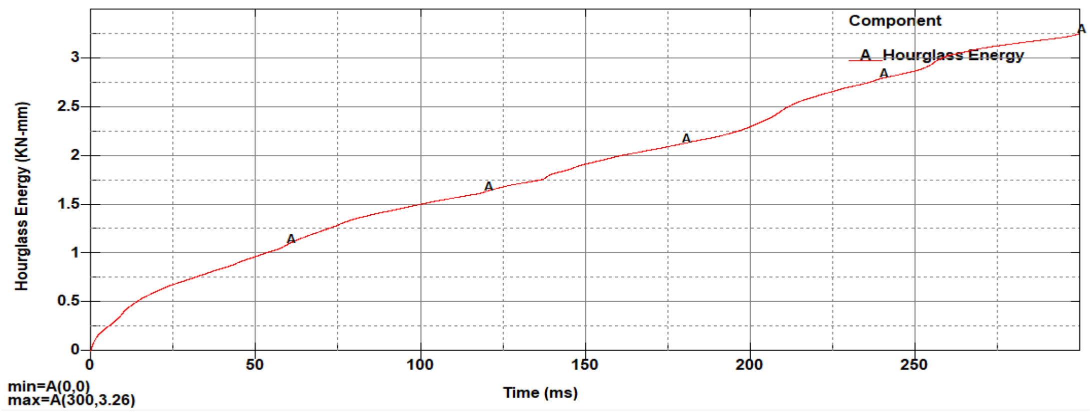

Figure 5.33 Hourglass energy

5.3 Result and discussion of Modified model

5.3.1 Carbon polyamide composite bumper

1. The result of maximum resultant deformation and equivalent (von-Misses) stress distributions of carbon polyamide bumper model with a velocity of 4KMPH along with the direction of the impact with a rigid pole in hallow geometrical shapes.

As it is indicated on the figure 5.34, the maximum resultant deformation and von-Misses stress for the existing bumper geometry is 12.88mm and 1480MPa respectively.

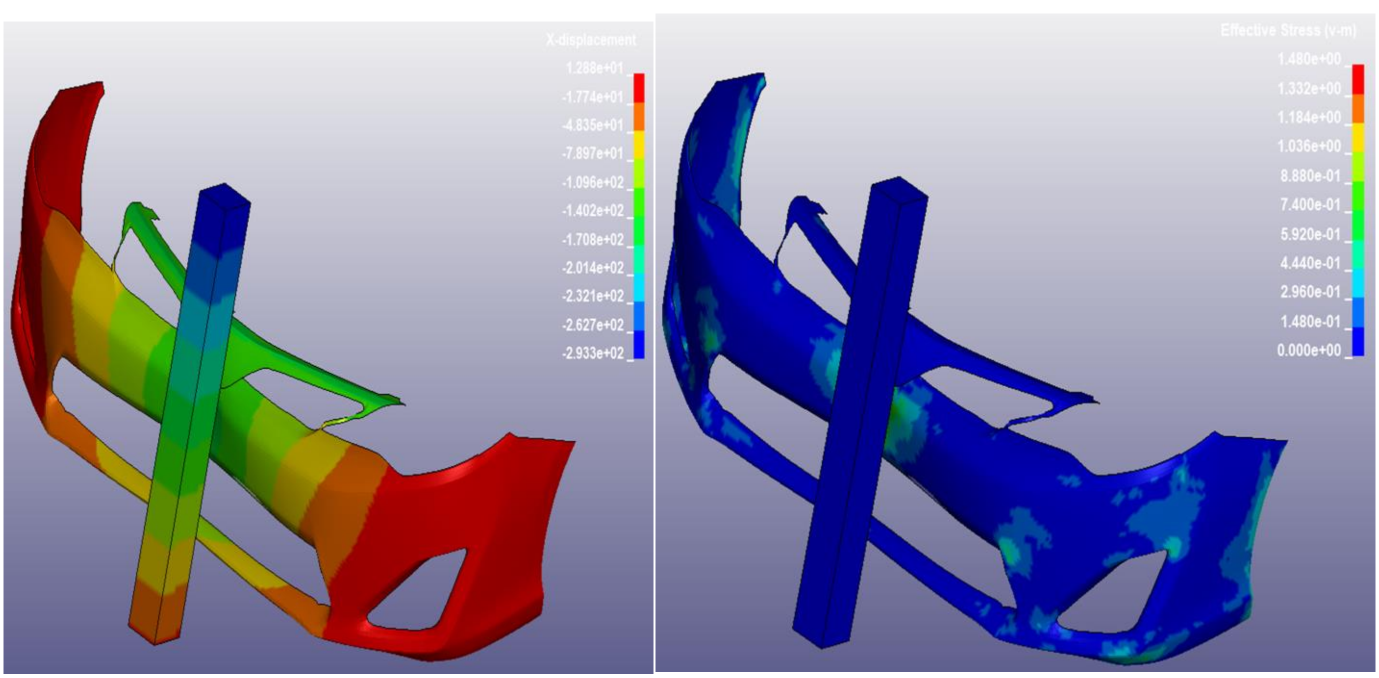

Max. Resultant deformation = 12.88 mm

Max equivalent (von-misses) stress = 1480 MPa

Figure 5.34 Result Analysis of CPA bumper model with a velocity of 4kmph

2. Energy balance

According to the law of conservation of energy, energy cannot be produced or destroyed, but it can be converted from one form of energy to another. Applying the same principle to collision analysis, the amount of kinetic energy lost during impact must be converted to other forms of energy such as internal energy, sliding energy, and hourglass energy. From Figure 5.35 below, we can see that the total energy consumed is constant throughout and the total energy is the sum of the kinetic energy and potential energy of the entire system.

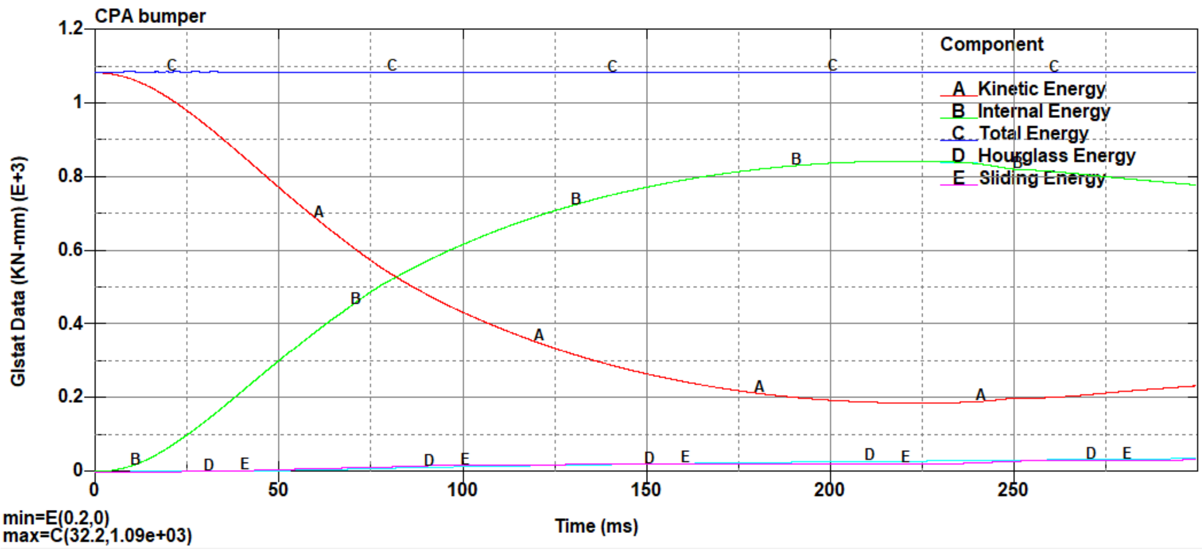

Figure 5.35 Energy balance

3. Energy absorption

Initially, the high kinetic energy at the start of the impact is equal to the total energy with a value of 1090 J, and when the crushing event begins, the system's kinetic energy begins to decay slowly and is transformed to Other form energy, eventually reaching an energy of 188J. From this difference, we can see that the energy of 902 J is absorbed and converted into internal energy, sliding energy and hourglass energy. Of these, as shown in the figure 5.36-5.37, 847 J, or 77.7% of the energy, is dissipated in the form of internal energy, and the remaining 22.3% of the energy is dissipated in the form of sliding and hourglass energy.

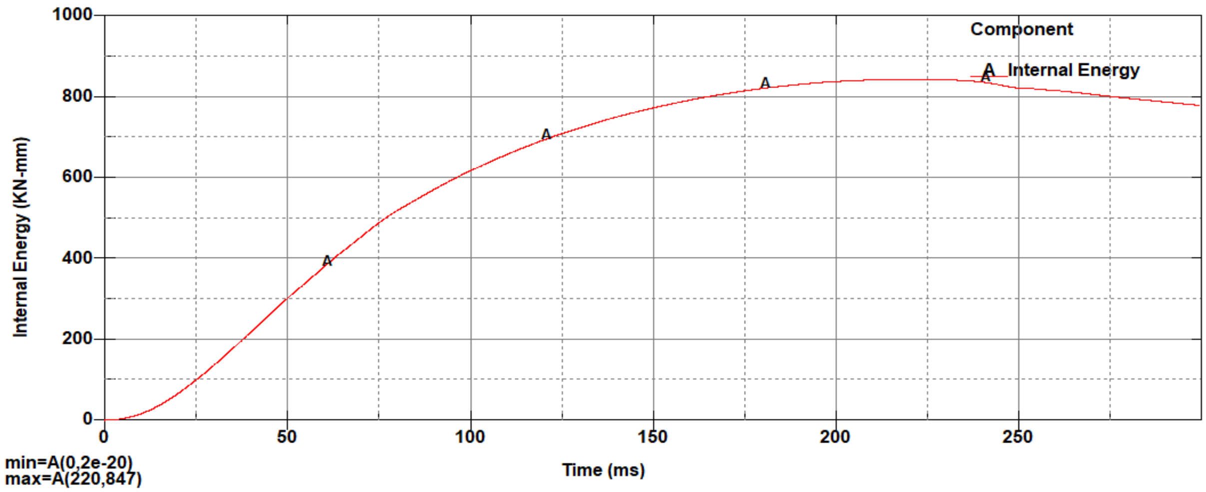

Figure 5.36 Internal energy

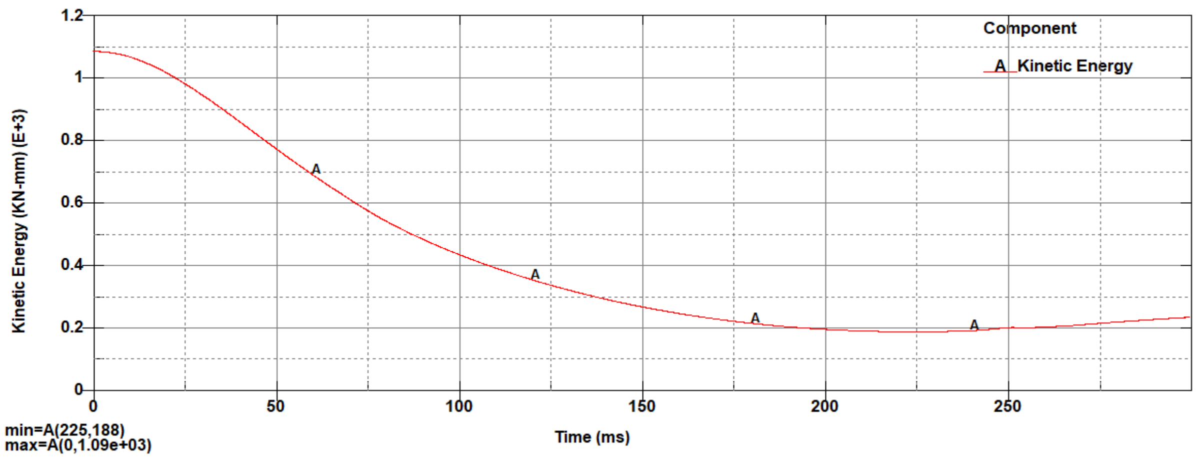

Figure 5.37 Kinetic energy

The kinetic energy of the system decreases, the internal energy increases, and Internal energy provides information about the energy absorbed by the deformation of the bumper.

4. Deformation

In LS DYNA, displacement is detected by measuring the relative distance between two nodes. Therefore, to measure the change in bumper displacement, we will use two nodes (node ID 2176465 for node 2181714, by measuring the relative distance between the two nodes after a collision, it is easy to find the overall deformation of the bumper. From this, we can see that the maximum displacement of node 2176465 with respect to node 2181714 in the X direction is about 15.8 mm as shown in figure 5.38:

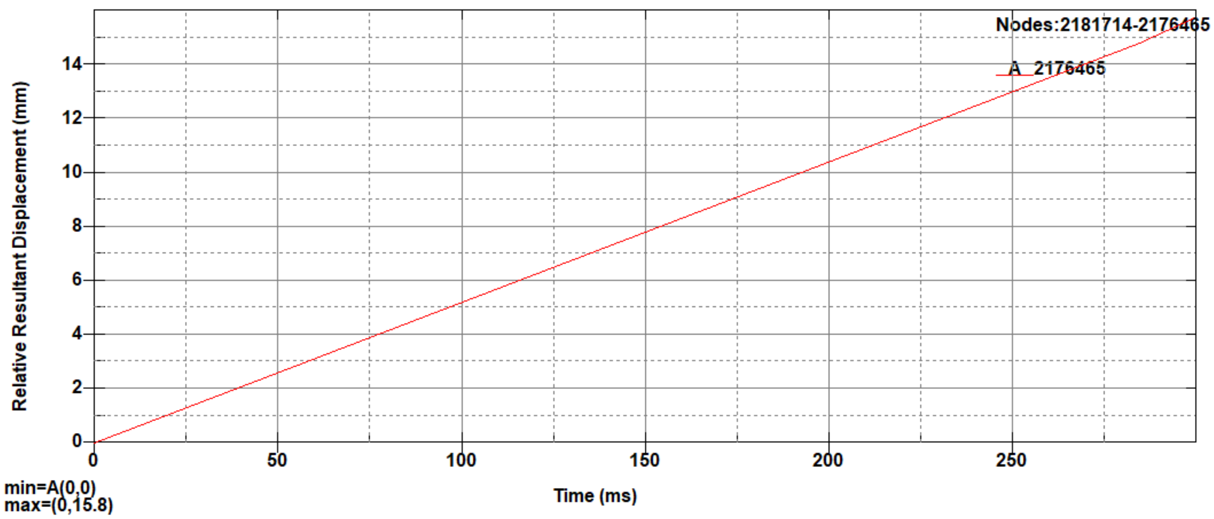

Figure 5.38 deformation

5. Impact force

The figure 5.39-5.40 shows the contact force between the rigid rod and the bumper in the x-axis direction. Initially, the impact force between the rigid pole and front bumper is almost zero until the time reaches 4.55 ms. after this point, the force begins to increase to its maximum in 48.1ms with the force value of 3.21kN and there is almost no fluctuation.

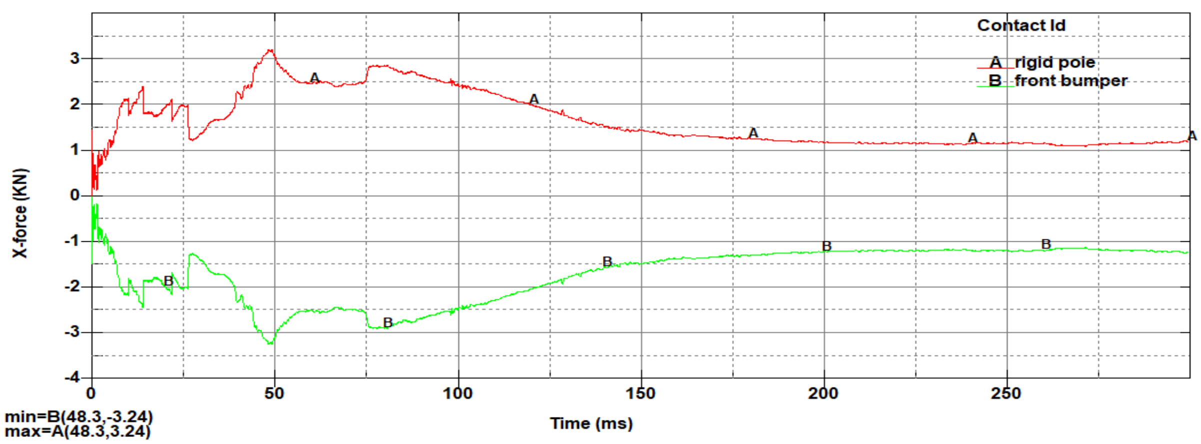

Figure 5.39 X-impact force

The rigid pole and front bumper have equal resultant contact force pulse but acted in opposite direction.

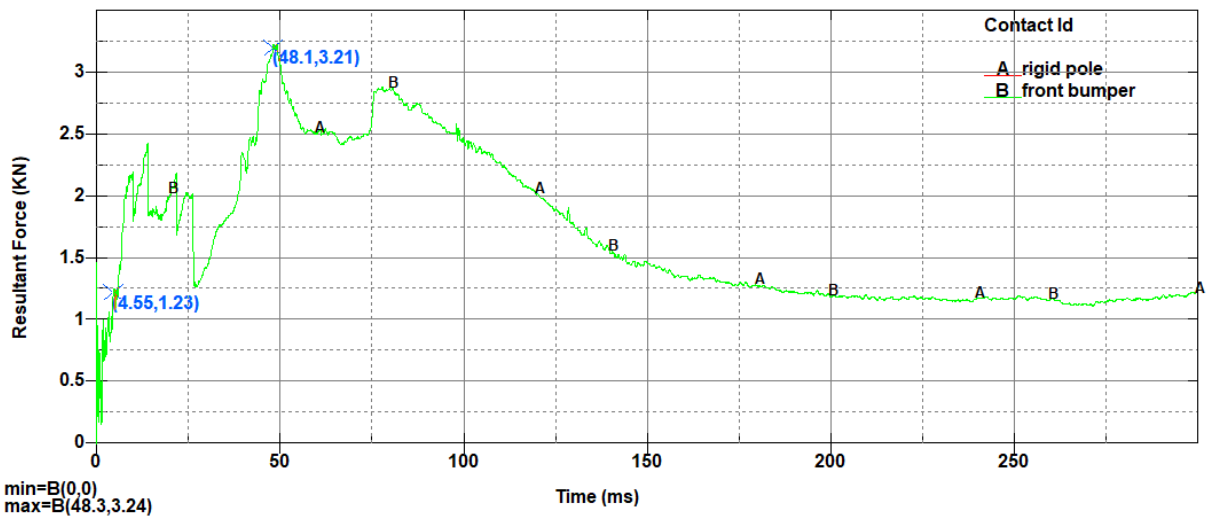

Figure 5.40 Resultant impact force

Because the force applied to the element is not always constant. Maximum force is generated when the bar is in full direct contact with the bumper.

6. Resultant Velocity

The resulting speed is shown in Figure 5.41. Initially, the vehicle's speed is minus 1.11mm/ms, and when the collision begins, the resulting speed slows down to a final value of minus 1.14mm/ms. This indicates that the bumper has undergone plastic deformation due to its low coefficient of restitution.

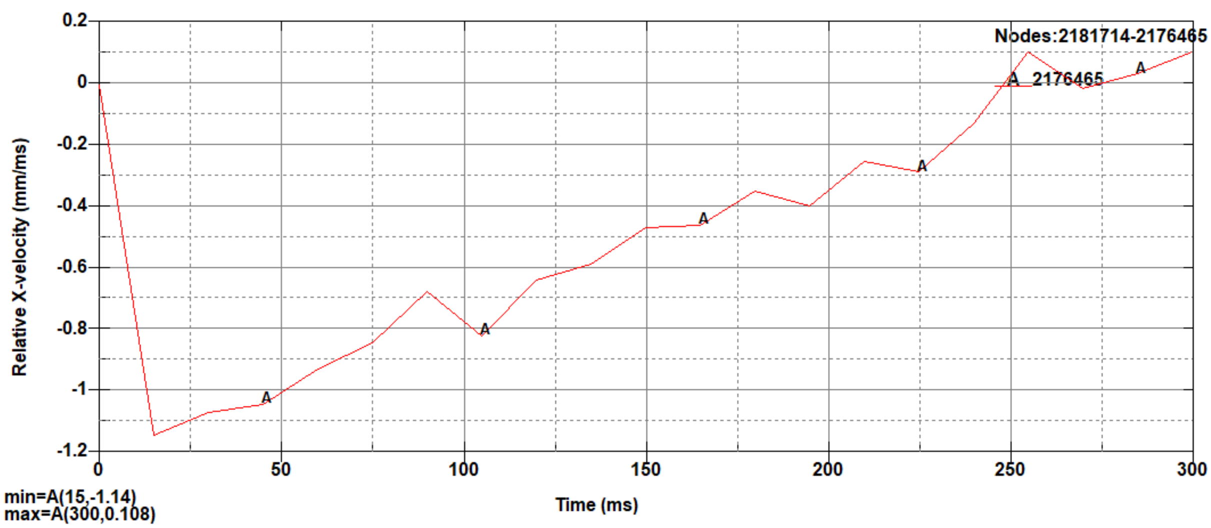

Figure 5.41 Relative velocity

7. Verification

Energy ratio

From the energy balance curve it has been seen that the system energy is not fully conserved and this is due to zero energy form of some elements. So it may be noted that, all the processes in this universe are irreversible and some losses are always included which deviates energy ratio slightly from one. This can be observed in the energy ratio graph.

The energy ratio value should be 1.00 +/- 0.07. As it can be seen in Figure 5.42, the simulation produce maximum value of 1.001 energy ratios and this value is approximately one with an error of 0.001% which is acceptable.

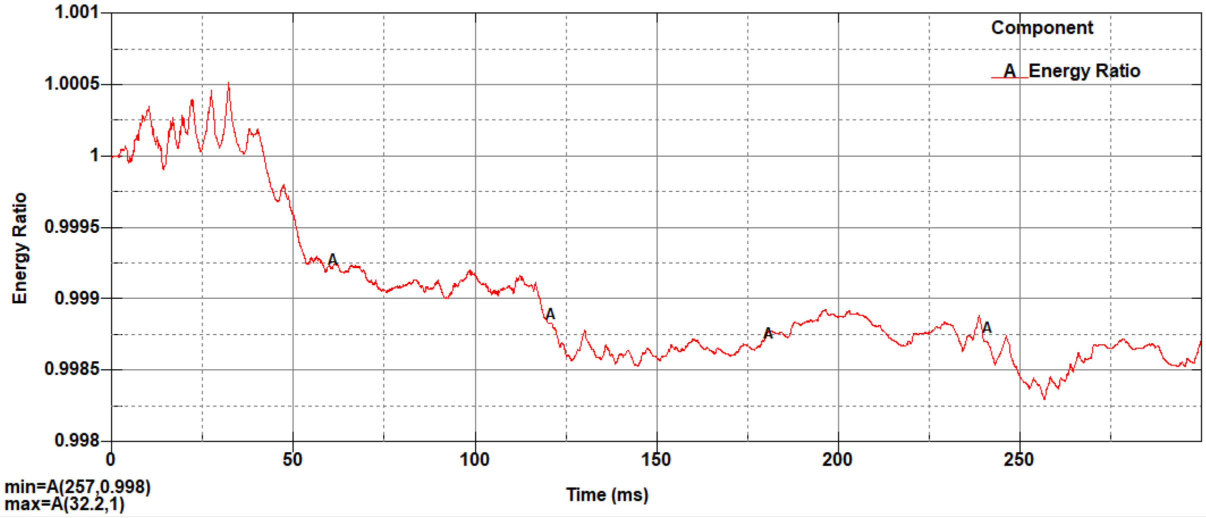

Figure 5.42 Energy ratio graph

Ratio of TE/HE

By analyzing the energy curve, the validity of the finite element model can also be judged from the relationship between total energy and hourglass energy. The energy of the hourglass can trigger a zero energy model. If the energy of the hourglass is less than 5% of the total energy, the finite element model is reliable. As shown in figure 5.43-5.44, the maximum value of the hourglass energy is 0.0377kJ, the total energy is 1.09kJ, and the HE/TE ratio is 3.46%, which is acceptable.

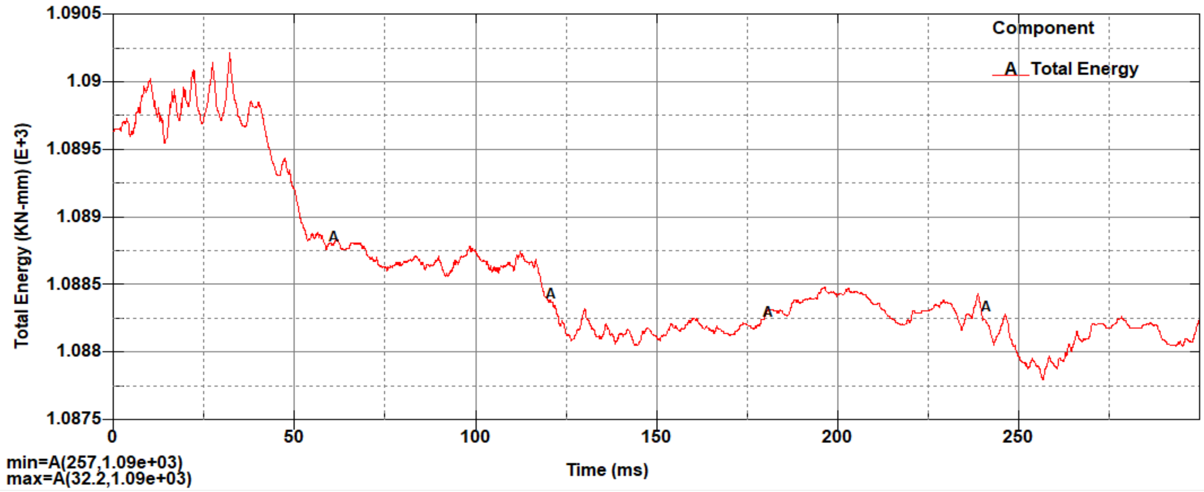

Figure 5.43 Total energy

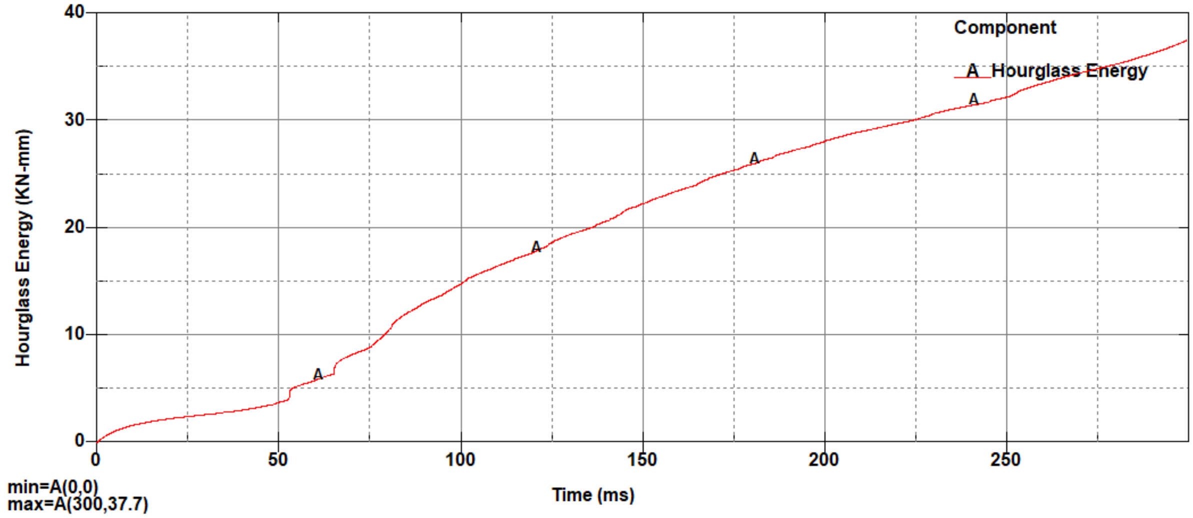

Figure 5.44 Hourglass energy

5.3.2 Comparison between the existing and modified bumper material

- ❖ **Displacement (Deformation)**

As shown on Figure 5.45, maximum deformation occur for the existing Al 6061 alloy and steel bumper with a value of 24.5mm and 20.2mm respectively but the modified model deformed with less value equal to 15.8mm. This indicates that the modified model provide better survival space and protection for the main front components of vehicle at event of front crash.

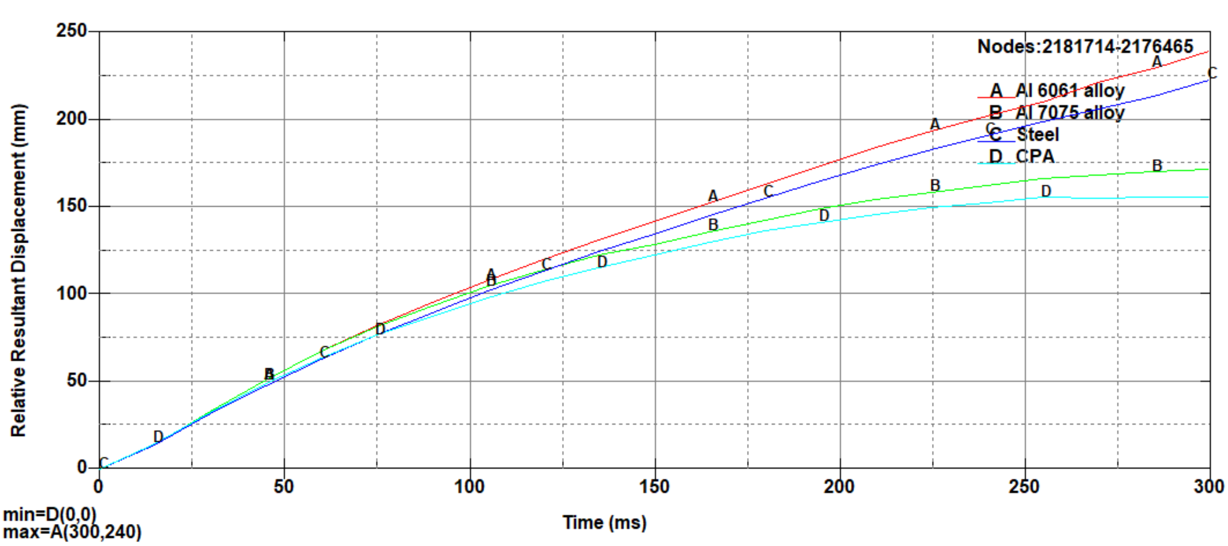

Figure 5.45 Comparison of deformation for different materials

❖ Energy absorption

The energy absorption value is obtained by measuring the amount of internal energy absorbed relative to the total kinetic energy loss. A graph of the energy absorption (internal energy) values of various bumper materials from this measurement is shown in figure 5.46. Maximum energy absorption was achieved with CPA bumpers with a value of 847 J, while bumper values for steel and Al 6061 alloys are 791 J and 735 J, respectively.

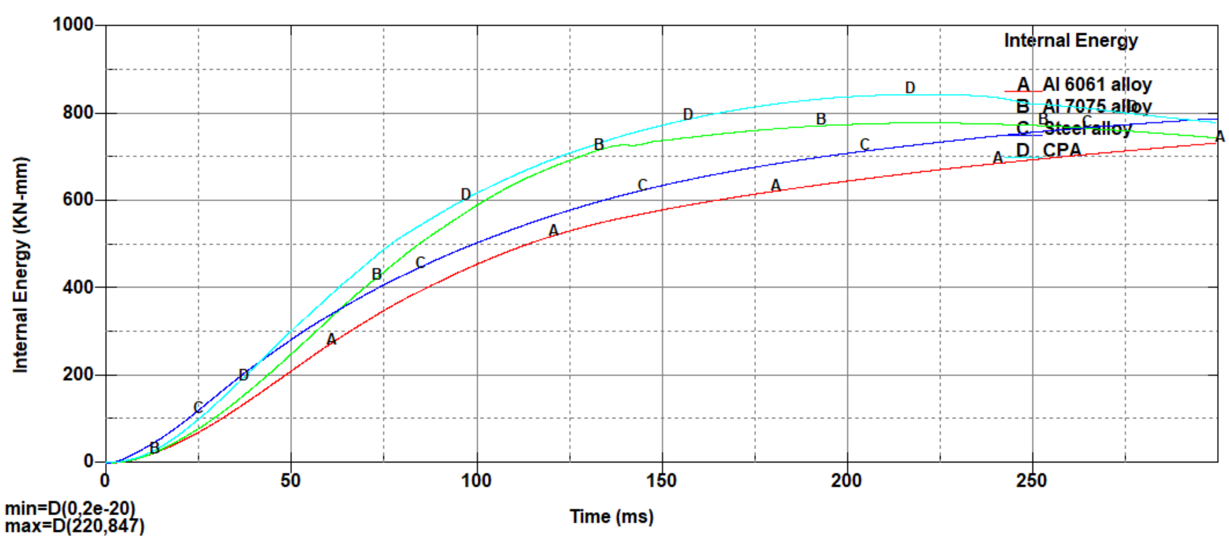

Figure 5.46 Comparison of energy absorption for different materials

❖ **Impact force**

The contact force between the front bumper and the rigid pole is shown in Figure 5.47. As shown in the graph below, maximum impact forces occur at 9.78kN, 4.87KN, and 4.10KN values in existing steel, Al7075 alloy, and Al6061 alloy models respectively. But in the modified model, the force applied is 3.21KN. If the force difference is too large, it will gain momentum and can further damage the components of the vehicle.

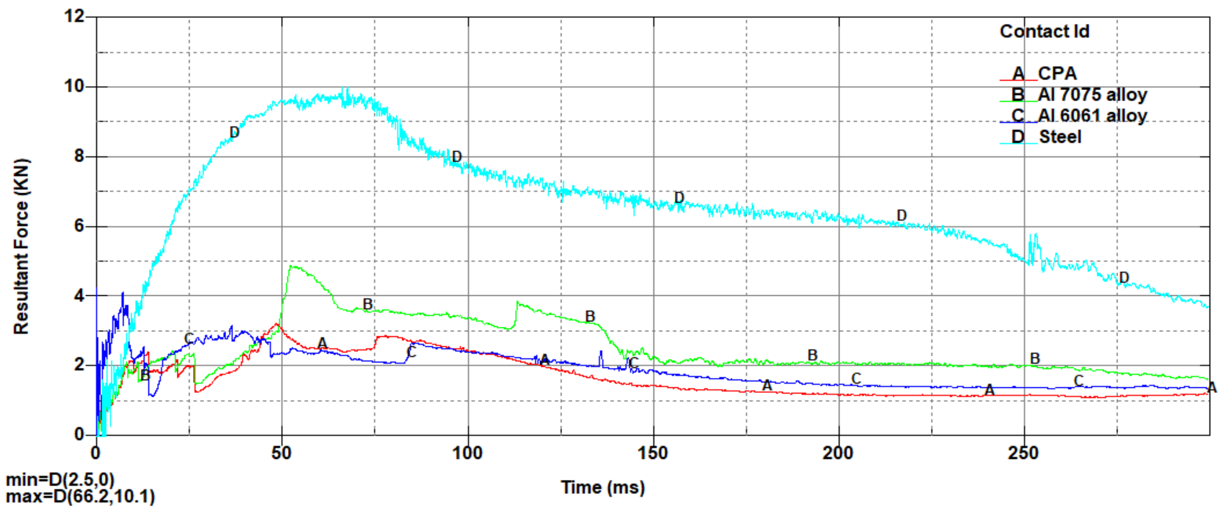

Figure 5.47 comparison of impact forces

❖ **Relative velocity**

To analyze the change of speed of varying bumper material, we take three nodes on front part section, two nodes at the opposite edges and one node at the middle (node 2190868, node 2176465and node 2181714 respectively). In all of the four bumper materials initially the velocity of the bumper is given negative initial velocity of 1.11 mm/ms in horizontal X-direction, the speed on node 2176465 (middle part) falls down most quickly because it is the point where the first impact contact occur, and reach maximum negative velocity of 0.06mm/ms at time of 15ms, it has come down and then up which shows the rebounding of the bumper. Once after the crash is happened, CPA material reduces the speed faster than the other materials as shown in figure 5.48, this shows that comparatively CPA has less intrusion and less/no damage occur to the front most parts.

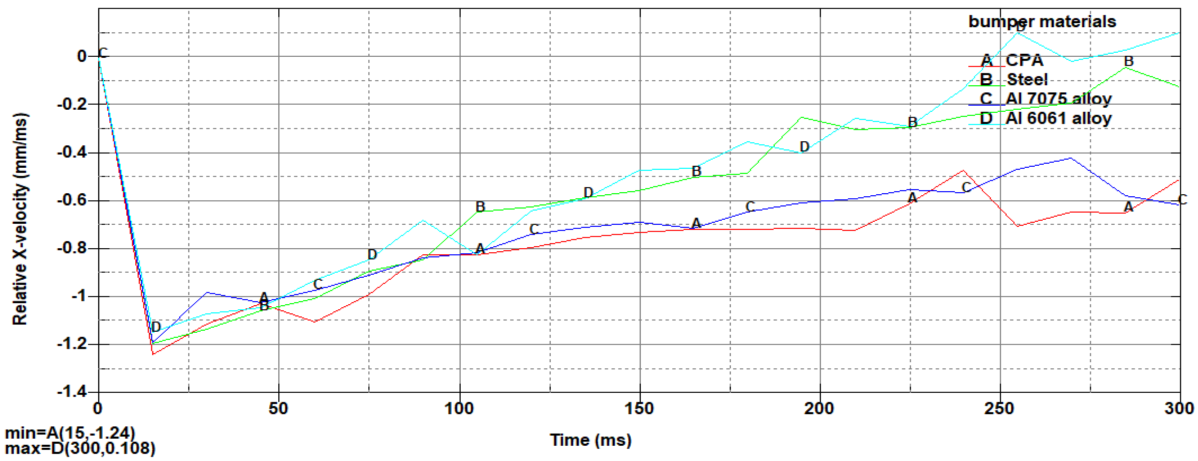

Figure 5.48 Comparison of relative velocity

5.3.3 Modified bumper geometry

1. The result of maximum resultant deformation and equivalent (von-Misses) stress distributions of CPA bumper model with a velocity of 4kmph along with the direction of the impact with a rigid pole in corrugated geometrical shapes.

As it is indicated in the figure 5.49, the maximum resultant deformation and von-Misses stress for the existing bumper geometry is 17.75 mm and 1364 MPa respectively.

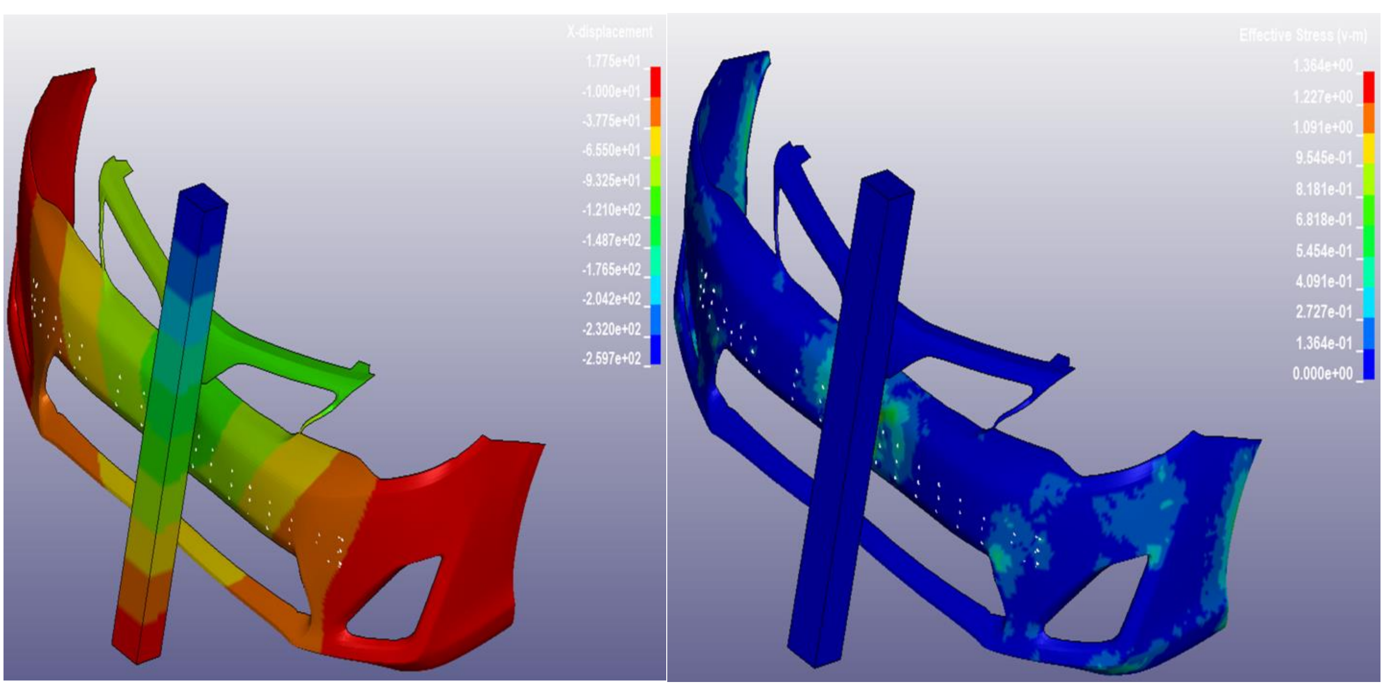

Max. Resultant deformation = 17.75 mm Max equivalent (von-misses) stress = 1364 MPa

Figure 5.49 Result Analysis of CPA corrugated bumper model with a velocity of 4kmph

2. Energy balance

According to the law of conservation of energy, energy cannot be produced or destroyed, but it can be converted from one form of energy to another. Applying the same principle to collision analysis, the amount of kinetic energy lost during impact must be converted to other forms of energy such as internal energy, sliding energy, and hourglass energy. From Figure 5.50, we can see that the kinetic energy is high at the beginning, with a value of 1080 J at the start of the impact, and slowly decreased and converted into other forms of energy, eventually reaching energy of 146 J.

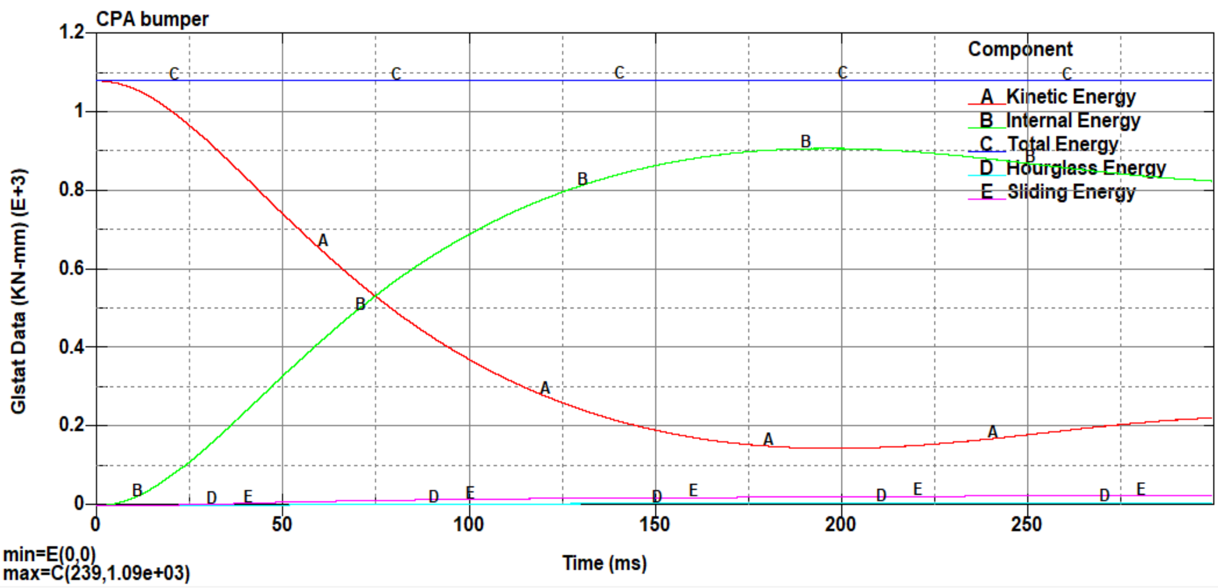

Figure 5.50 Energy balance

3. Energy absorption

Initially, the kinetic energy is high at a value of 1080J at the beginning of the impact, and when the crushing event begins, the kinetic energy of the system begins to decrease slowly. It is then converted into other forms of energy, eventually reaching energy of 146J. From this difference, we can see that the energy of 934 J is absorbed and converted into internal energy, sliding energy and hourglass energy. Of this, 84.35% or 911J of energy is dissipated in the form of internal energy, as shown in the figure 5.51-5.52, and the remaining 15.65% of the energy is dissipated in the form of sliding and hourglass energy.

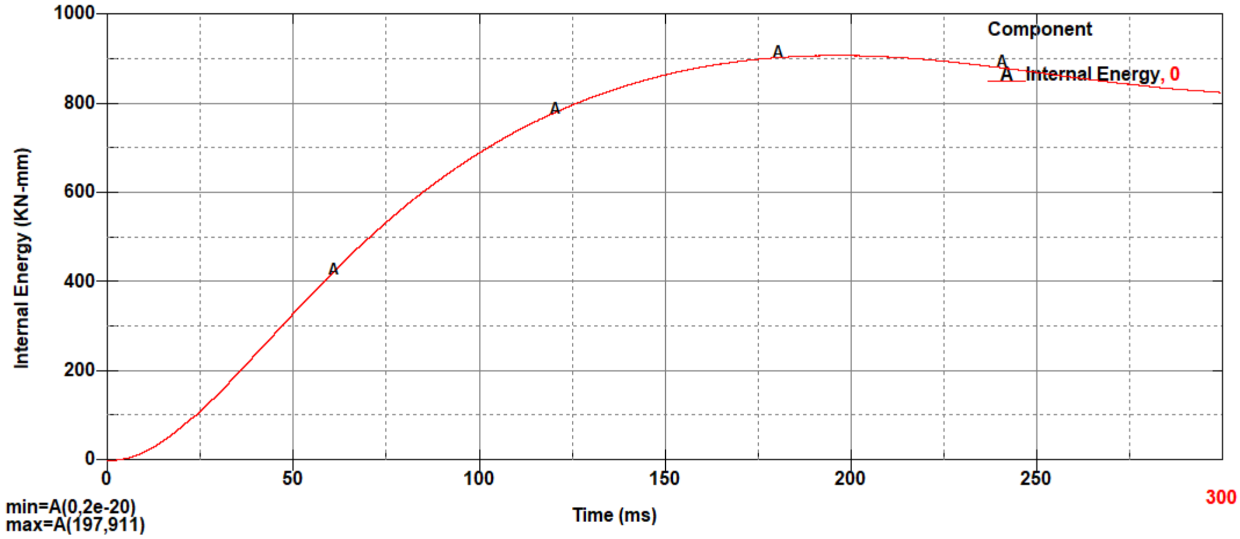

Figure 5.51 Internal energy

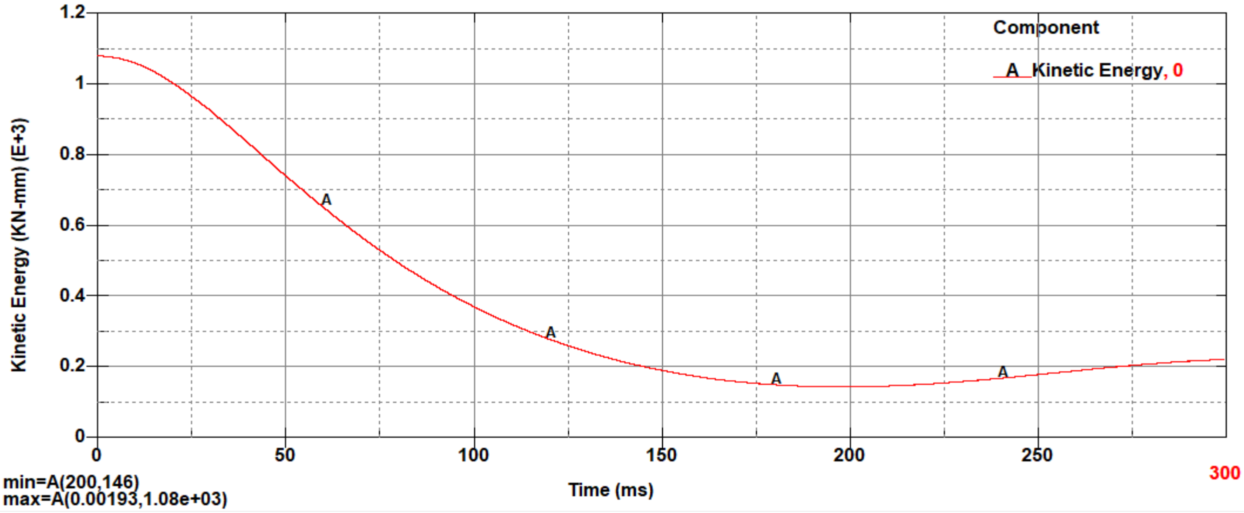

Figure 5.52 Kinetic energy

4. Deformation

Using two nodes of a corrugated bumper (node ID 2176465 for node 2181714), as shown in figure 5.53. From this, we can see that the maximum displacement of node 2176465 with respect to node 2181714 in the X direction is about 13.5 mm. Finally, the total deformation of the bumper can be easily found by measuring the relative distance between the two nodes after a collision.

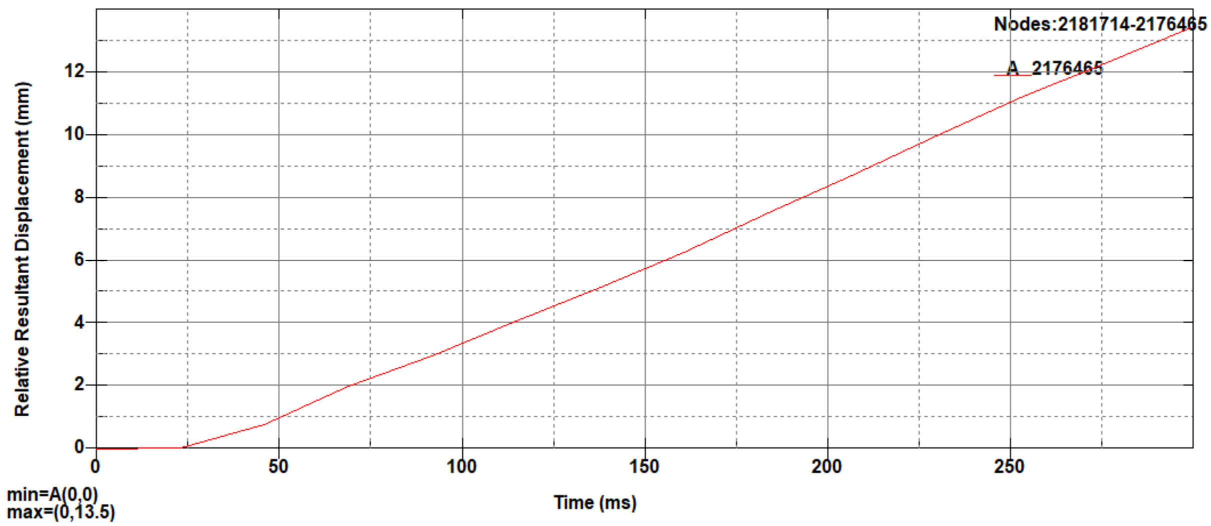

Figure 5.53 Resultant x- displacement

5. Impact force

The contact force between the rigid pole and the bumper along x-axis is shown in the Figure 5.54-5.55 below. Initially the contact force is almost zero until the time reaches 0.00027ms. After this point the force starts to increase to its maximum at 0.016ms with force value of 1.49kN and shows some fluctuations. The maximum force occurs when the pole is directly in full contact with the bumper. At this point, the bumper and the entire vehicle are severely damaged.

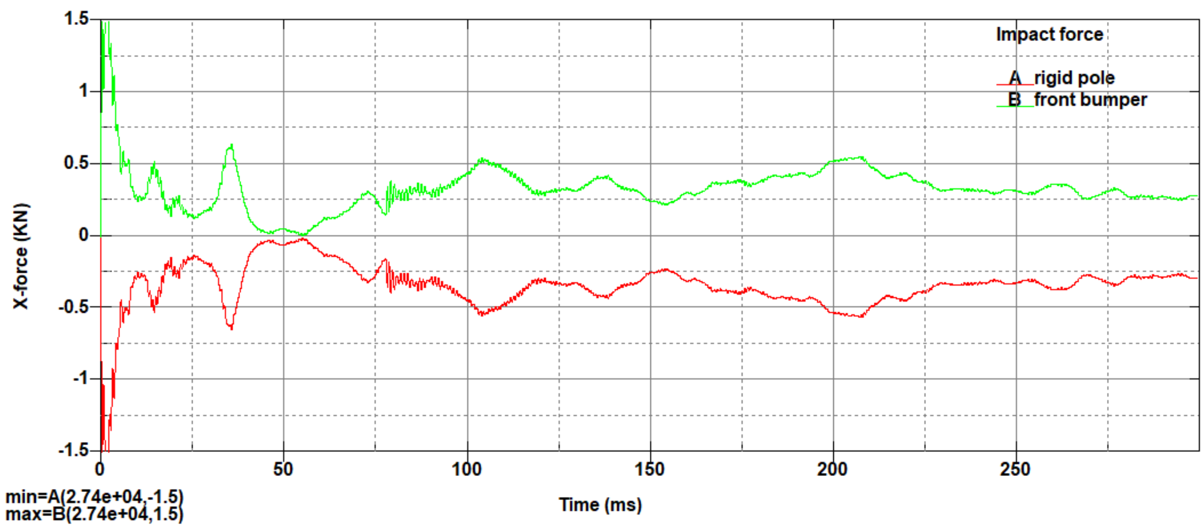

Figure 5.54 X- Impact force

The momentum of the net contact force of the rigid pole and the bumper is the same, but in the opposite direction.

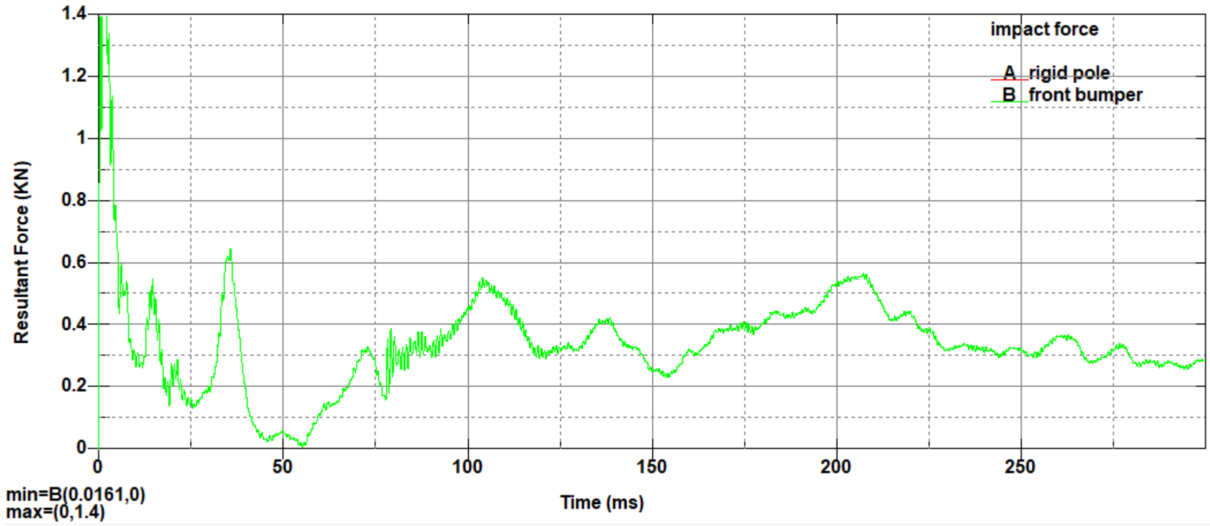

Figure 5.55 Resultant impact force

6. Resultant Velocity

The resulting speed is shown in Figure 5.56. Initially, the speed of the vehicle is minus 1.11mm /ms, and when the collision begins, the resulting speed slows down to the final value of minus 1.23 mm/ms. This indicates that the bumper has undergone plastic deformation due to its low coefficient of restitution.

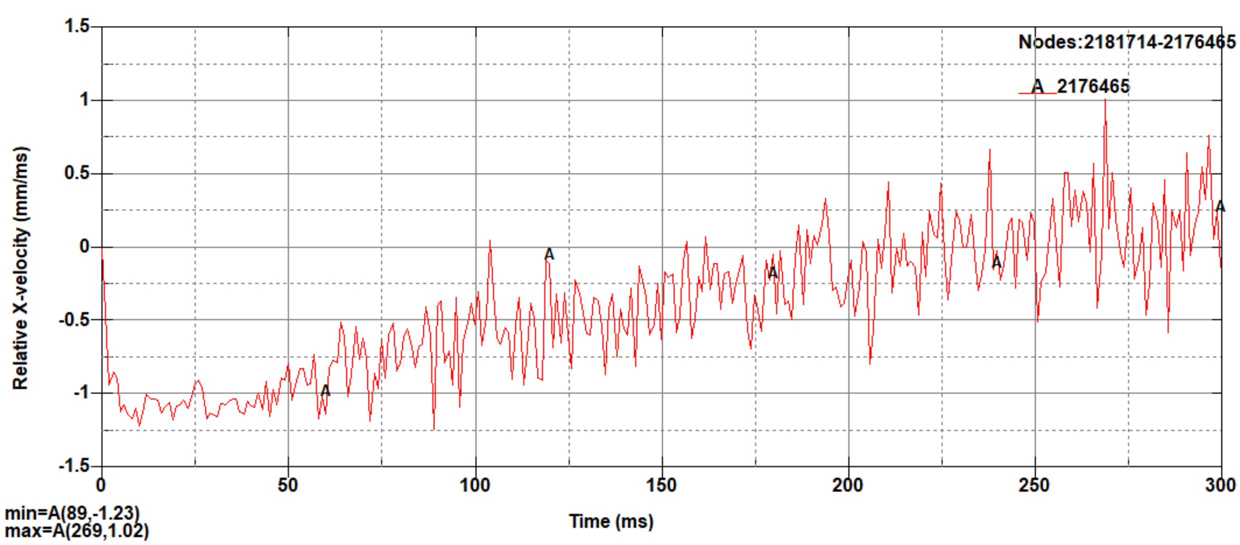

Figure 5.56 Relative velocity vs time

7. Verification

Energy ratio

The energy balance curve shows that the system energy is not completely conserved. This is due to the zero energy form of some elements. Therefore, note that all processes in this universe are irreversible and always contain some loss, so the energy ratio is slightly different from 1. This can be seen in the energy ratio diagram.

The energy ratio value should be 1.00 +/- 0.07. As shown in the figure 5.57, the simulation produces an energy ratio with a maximum value of 1.0015, which is approximately 1, with an error of 0.0015%, which is acceptable.

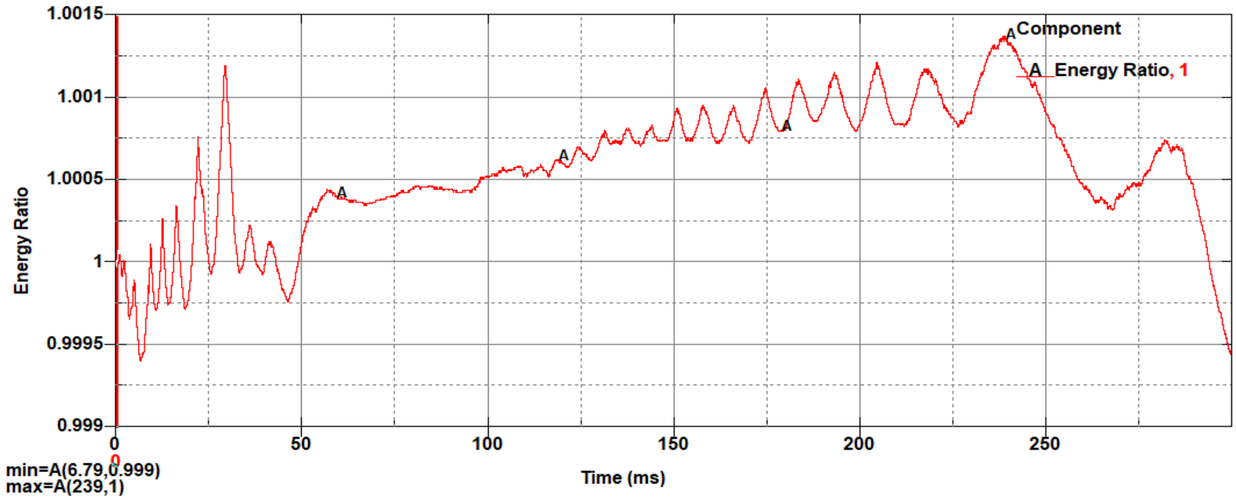

Figure 5.57 Energy ratio

Ratio of TE/HE

By analyzing the energy curve, the validity of the finite element model can also be judged from the relationship between total energy and hourglass energy. If the energy of the hourglass is less than 5% of the total energy, the finite element model is reliable. As shown in figure 5.58-5.59, the maximum value of the hourglass is 0.00721 kJ, the total energy is 1.09 kJ, and the ratio of HE / TE is 0.66%, which is acceptable.

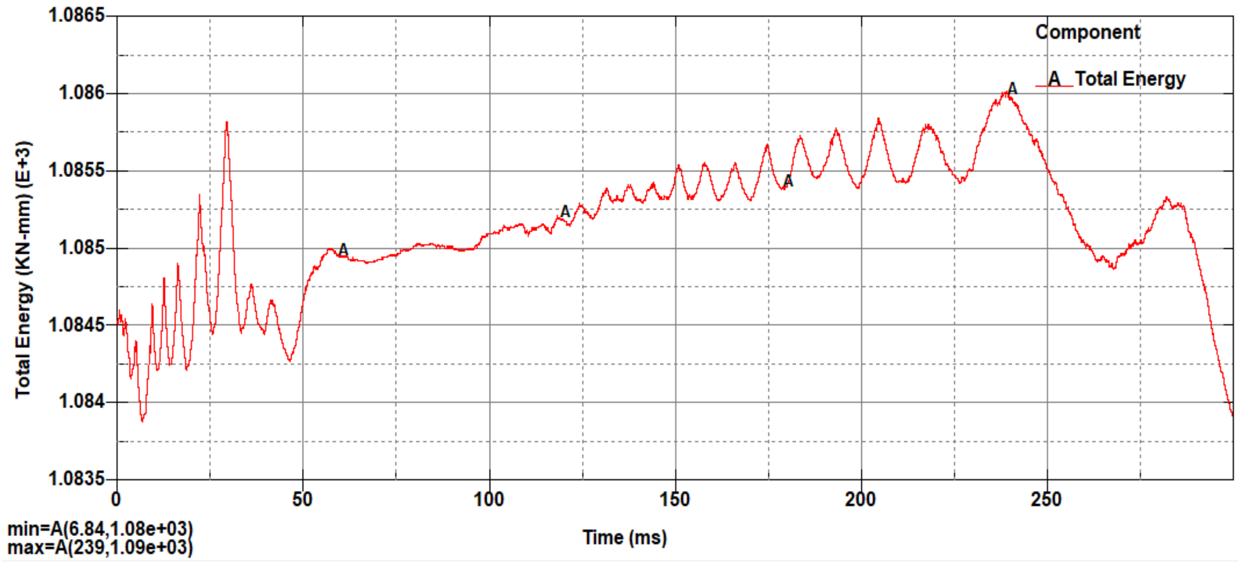

Figure 5.58 Total energy

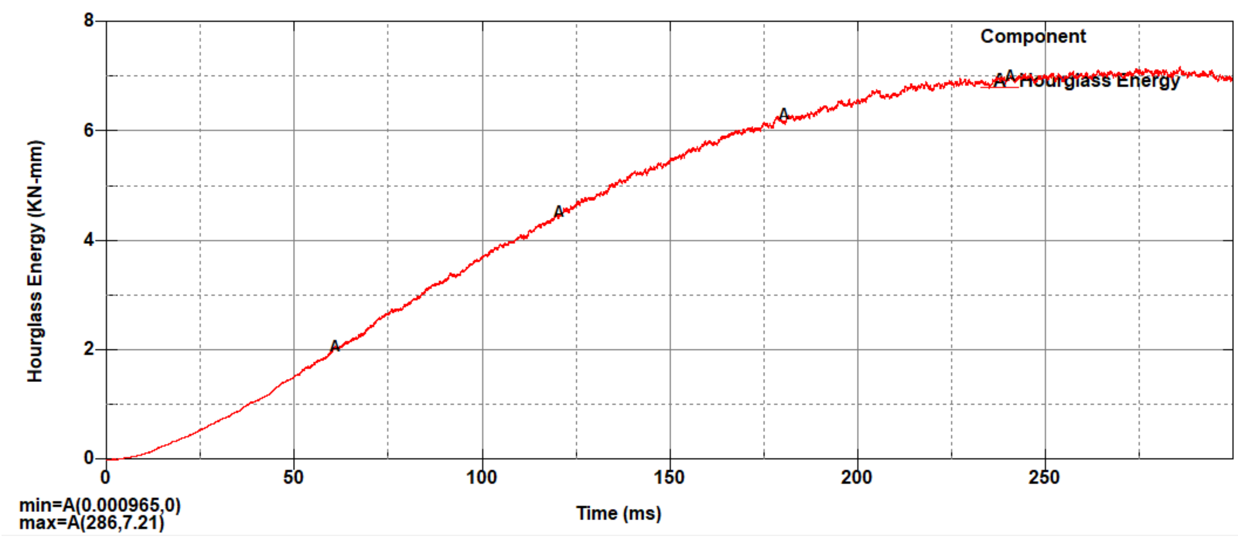

Figure 5.59 Hourglass energy

5.3.4 Thickness optimization for Modified bumper geometry

The results for different bumper thicknesses are plotted at regular time intervals as shown in figure 5.60. It is necessary to observe and judge the results of impact analysis such as energy absorption, displacement (deformation), and impact force.

1. Deformation

Deformation values are obtained by measuring the relative displacement of two nodes, one at the right or left edge of the bumper and the other at the center of the bumper. From this measurement, the values of the deformation diagram for various thicknesses of the bumper are shown below.

The bumper thickness is 2.5, 3.0, 3.5 and 4.0 mm as shown in Figure 5.60 below. As we can see, as the thickness of the bumper increases from 2.5 mm to 4 mm, the maximum deformation of the bumper decreases and the rate of decrease becomes also less with the increase of thickness. This does not mean that a bumper with less thickness is always better because more deformation means that there is probability of intrusion to the vehicle main compartments.

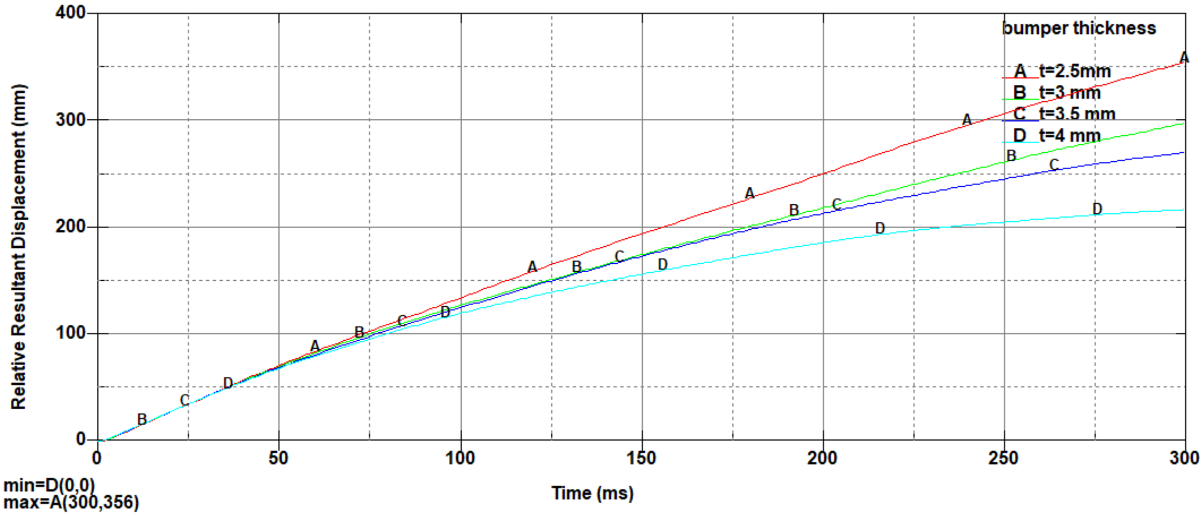

Figure 5.60 Comparison of deformation for different thickness

2. Energy absorption

On the other hand, as shown in Figure 5.61, the greater the deformation of the beam, the greater the energy absorption of the composite bumper. The maximum amount of energy that the bumper absorbs decreases with increasing thickness.

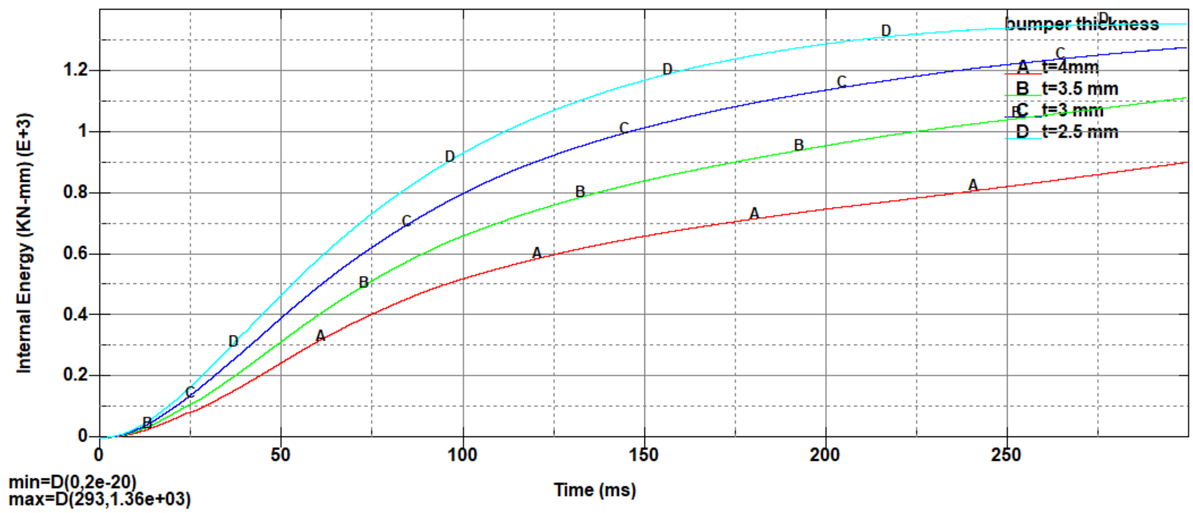

Figure 5.61 Comparison of internal energy graph for different thickness

3. Impact force

The Impact force between rigid pole and bumper increases with the increase of thickness as shown in figure 5.62, because as with increase in thickness the mass of the bumper increases as a result, high impact force is produced. But that does not mean that bumper with smaller thickness is better because the stress on the on the bumper increases with the use of less thickness. Therefore, from the above results it can be concluded that neither a bumper with less thickness nor with higher thickness is better; rather it depends on the application it is required for. The main purpose of this investigation is to select a lightweight front bumper without sacrificing the impact behavior. From the viewpoint of impact performance, among the listed thickness taking the optimum value provides improved performance relative of others for the front most parts of the vehicles. Therefore, the bumper with 3mm thickness is better.

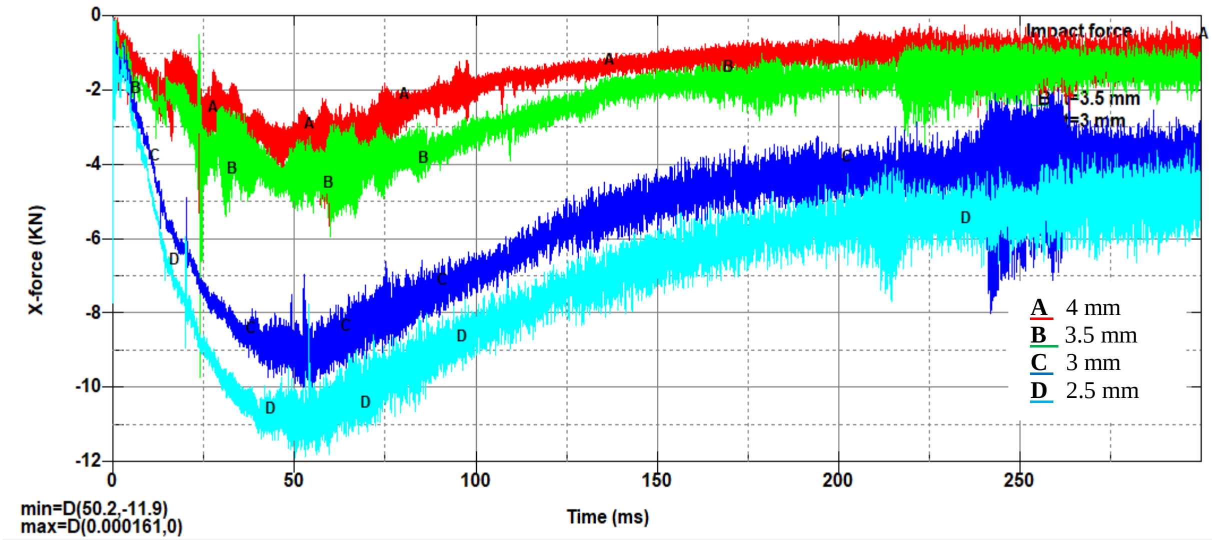

Figure 5.62 Comparison of impact forces for different thickness

4. Relative Velocity

To analyze the change of speed of varying bumper material, we take three nodes on front part section, two nodes at the opposite edges and one node at the middle (node 2190868, node 2176465and node 2181714 respectively). As shown in Figure 5.63, in all of the four bumper thicknesses initially the velocity of the bumper is given negative initial velocity of 1.11 mm/ms in horizontal X- direction, the speed on node 2176465 (middle part) falls down most quickly because it is the point where the first impact contact occur, and reach maximum negative velocity of 0.06 mm/ms at time of 15 ms, it has come down and then up which shows the rebounding of the bumper. Once after the crash is happened, a bumper with higher thickness reduces the speed faster than a less bumper thickness, comparatively a bumper with higher thickness has less intrusion and less/no damage occur to the front most parts. This does not mean that a bumper with higher thickness is always better because less deformation means less energy absorbed and the bumper got easily broken.

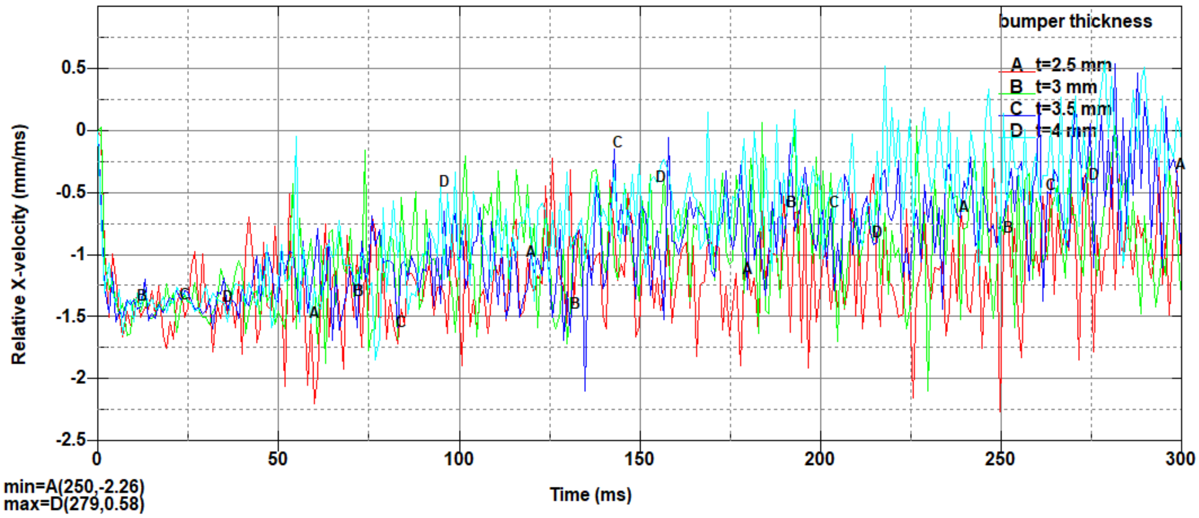

Figure 5.63 Comparison of relative velocity

5.4 Comparison between the existing and optimized bumper model

Under this section the crash worthiness ability of the existing and modified bumper model will be compared with the following parameters:

- **Displacement (Deformation)**

As shown on Figure 5.64 below, Maximum deformation occur at the existing bumper with 20.2 mm but the modified model deformed with less value equal to 13.5 mm this indicate that the modified model provide better survival space and protection for the main front components od vehicle at event of front crush.

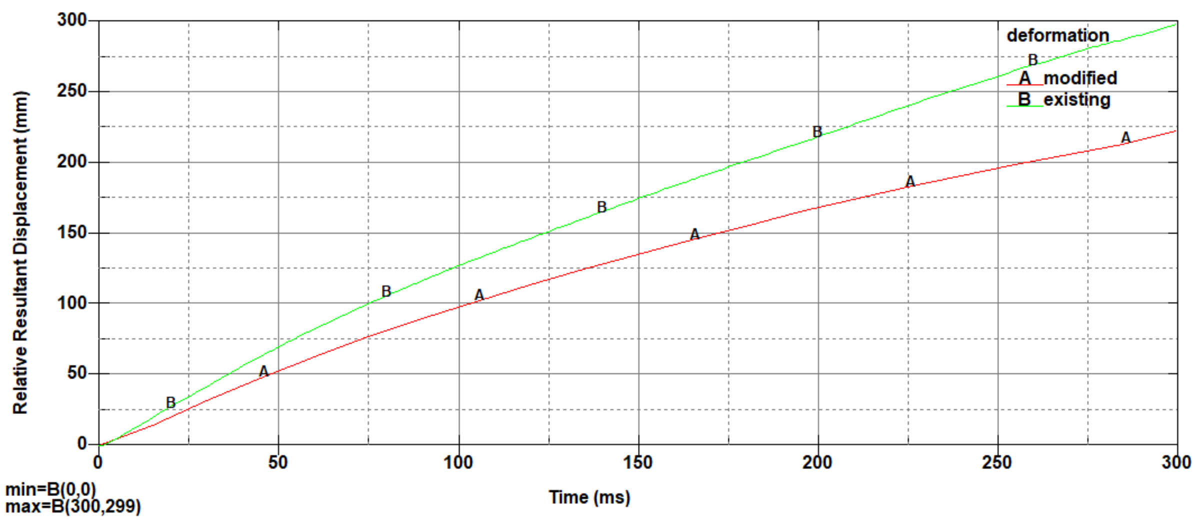

Figure 5.64 Comparison of deformation for existing and optimized model

- ❖ **Energy absorption**

The absorption ability of the modified and existing model is shown on Figure 5.65 below. Since the same conditions are applied in simulation of both models so that their energy absorption capacity of the models are determined by using the total internal energy graph. As it is indicated on the graph below among them maximum amount of kinetic energy is absorbed in case of modified model with value equal to 911 J of internal energy, but the existing model remain with 791 J. This shows that the modified model can absorb more kinetic energy with less deformation under the same conditions. This helps in reducing the energy transferred to the front most important components.

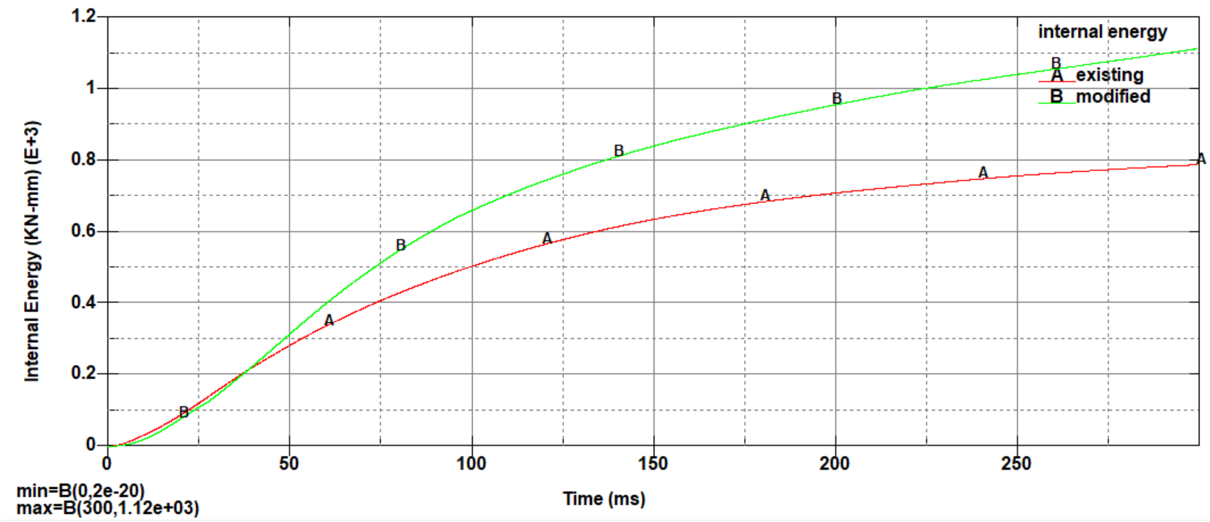

Figure 5.65 Comparison of internal energy for existing and optimized model

- ❖ **Impact force**

The contact force between the front bumper and the rigid pole is shown in the Figure 5.66 below. As it is shown on the graph below the maximum impact force occur at the existing model with value 9.78kN. The force on the modified model is equal to 1.38KN and their difference equals 8.40kN. This much difference in force can create more momentum to the vehicle as a result the vehicle is highly damaged. Higher force of impact causes more damaged to the components of the vehicle.

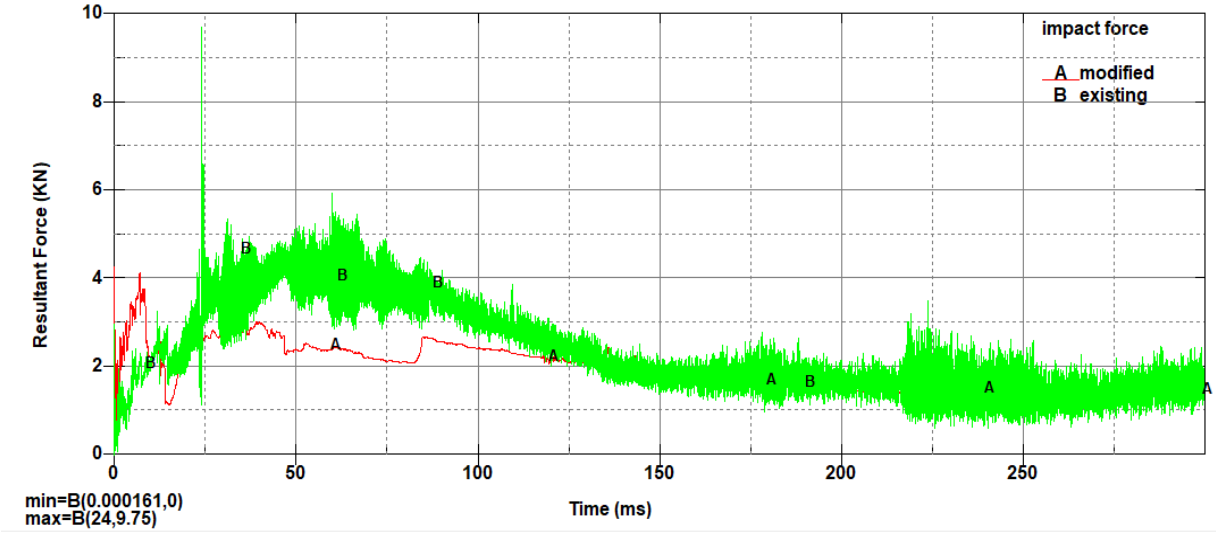

Figure 5.66 Comparison of impact forces between existing and modified model

5.5 Modified Vehicle Model

Under this section the crash worthiness ability of the optimized bumper model incorporated with the corresponding whole vehicle (overall structure) will be assessed with the following parameters:

- ❖ **Structural response**

As it is indicated in the figure 5.67, the maximum resultant deformation and resultant velocity for the optimized bumper with whole vehicle structure are 24.89mm and 4mm/ms respectively.

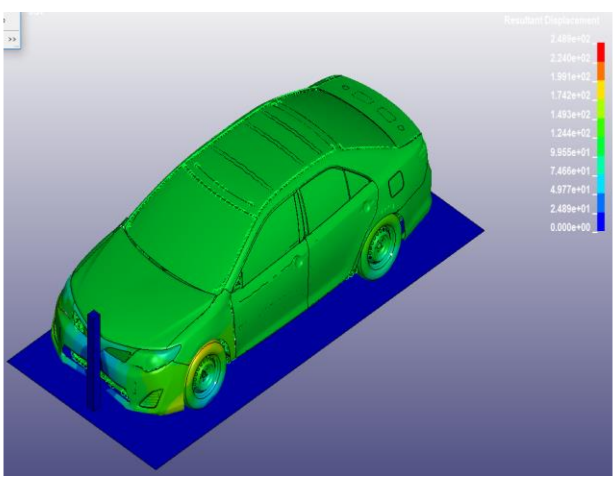
(a)
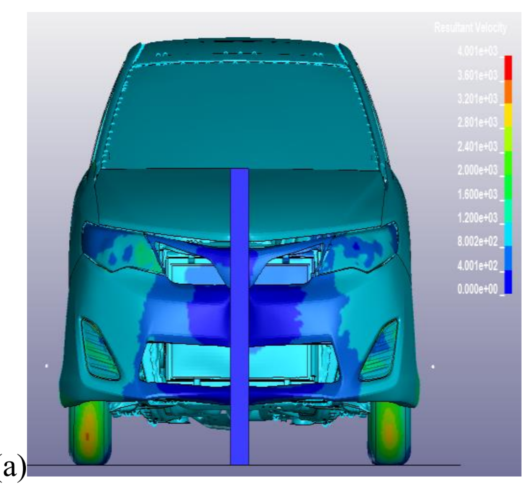
(b)

Figure 5.67 Result Analysis of optimized vehicle model with a velocity of 10kmph

- ❖ **Energy balance**

According to the law of conservation of energy, no energy can be produced or it is destroyed, but it can be converted from one form of energy to another. Apply the same principle to a set of collision analysis and kinetics, the energy lost by the impact needs to be converted into other forms of energy, such as: As internal energy, sliding energy, hourglass energy. From Figure 5.68, the total energy consumed is approximately constant throughout and Total energy is the sum of kinetic energy and potential energy.

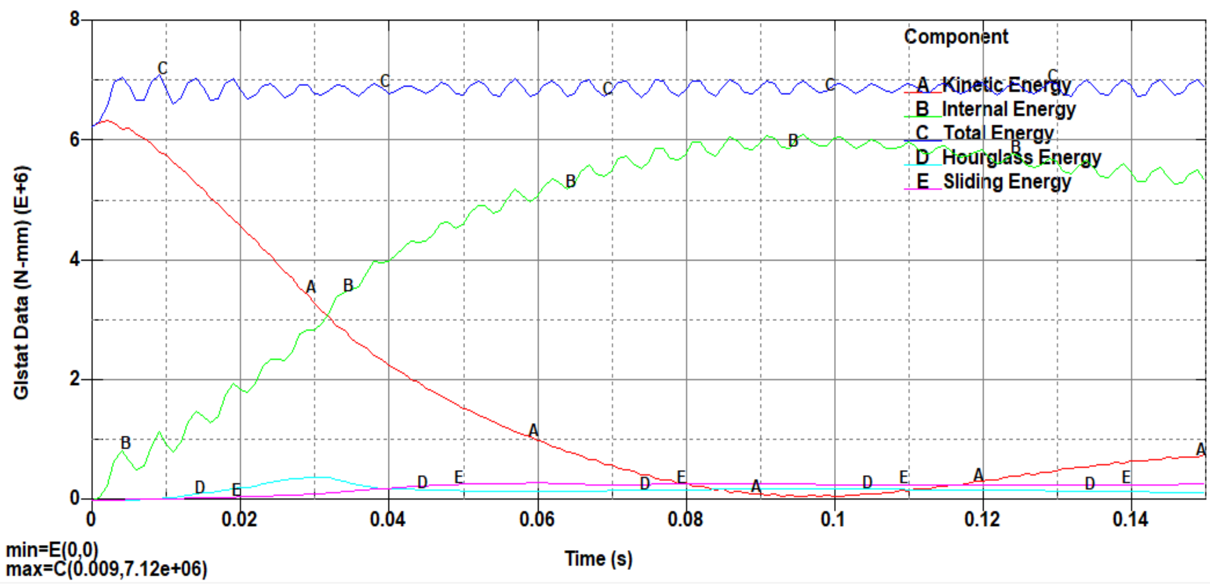

Figure 5.68 Energy balance cure for whole vehicle structure

- ❖ **Energy absorption**

First, there is a high kinetic energy of 7120 J at the beginning of the impact and when the crushing event begins; the kinetic energy of the system slowly begins to dissipate and is converted into other forms of energy, eventually reaching energy of 55.8 J. From this difference, we can see that the energy of 7064.2 J is absorbed and converted into internal energy, sliding energy, and hourglass energy. Of this, 6130 J or 86.77% energy is dissipated in the form of internal energy as shown in figure 5.69-5.70, and the remaining 13.23% is dissipated in the form of sliding and hourglass energy.

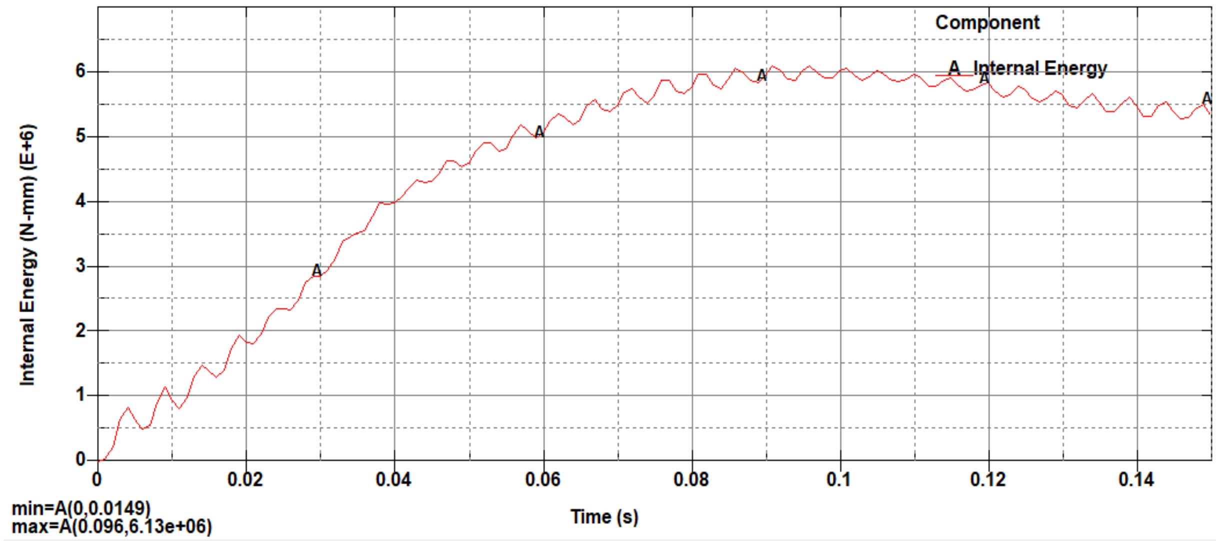

Figure 5.69 Internal energy

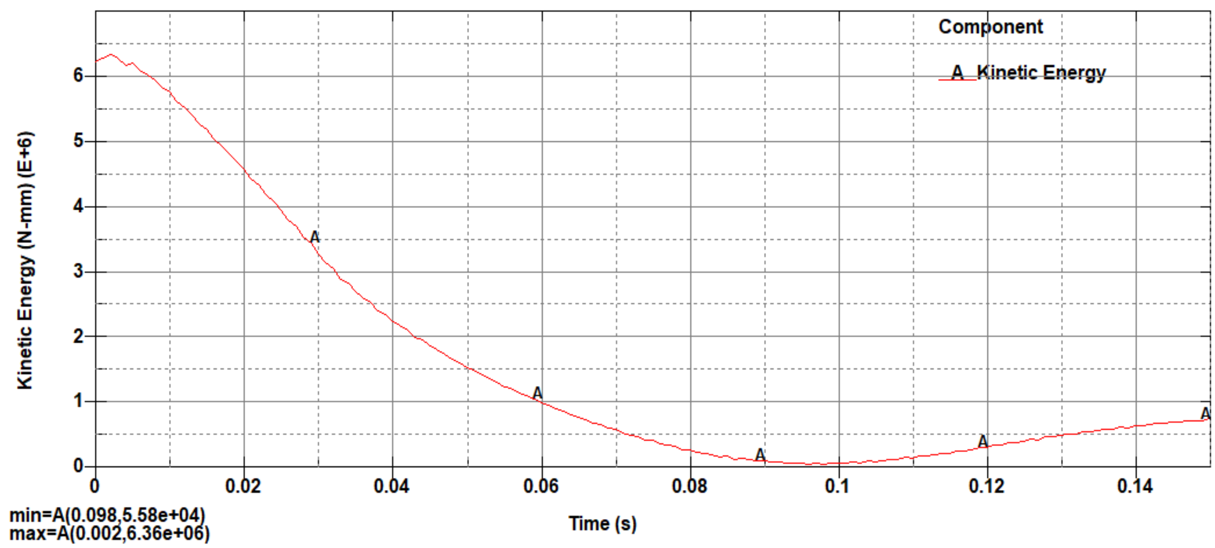

Figure 5.70 Kinetic energy

❖ **Impact force**

The contact force between the rigid pole and the whole vehicle structure is almost zero until the time reaches 2.10ms. From this point on, the force begins to increase, showing some fluctuations. Fluctuations are due to temporary (time-dependent) movements of the simulation, as the forces exerted on the elements are not always constant. Maximum force occurs in 32.2ms at a value of 619.76kN when the pole is in full direct contact with the vehicle. At this point, the bumper and the entire vehicle are severely damaged as shown in figure 5.71-5.72.

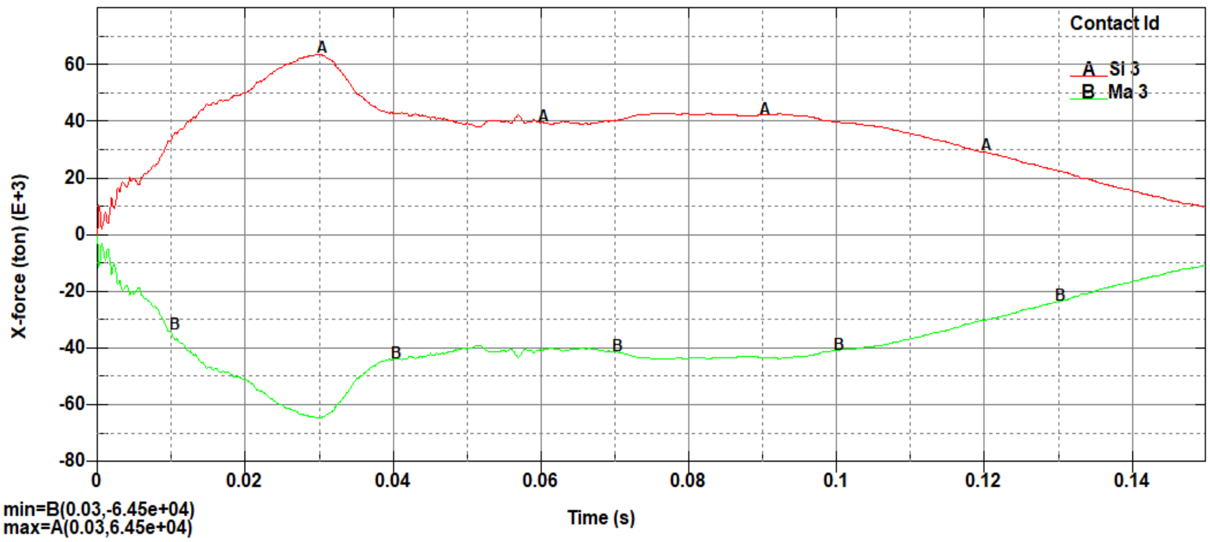

Figure 5.71 X impact force

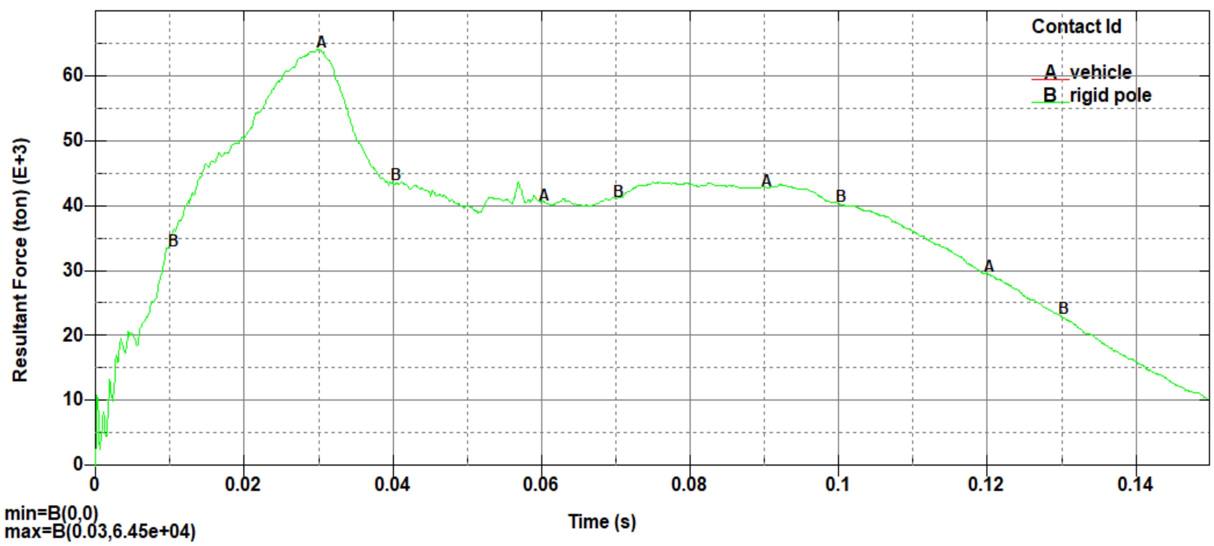

Figure 5.72 Resultant impact force

- **Verification**

Energy ratio

All processes in this universe are irreversible and always contain some loss, so the energy ratio is slightly different from 1. This can be seen in the energy ratio diagram.

The energy ratio value should be 1.00 +/- 0.07. As shown in the figure 5.73, the simulation produces an energy ratio with a maximum value of 1.01, which is approximately 1, with an error of 0.1%, which is acceptable.

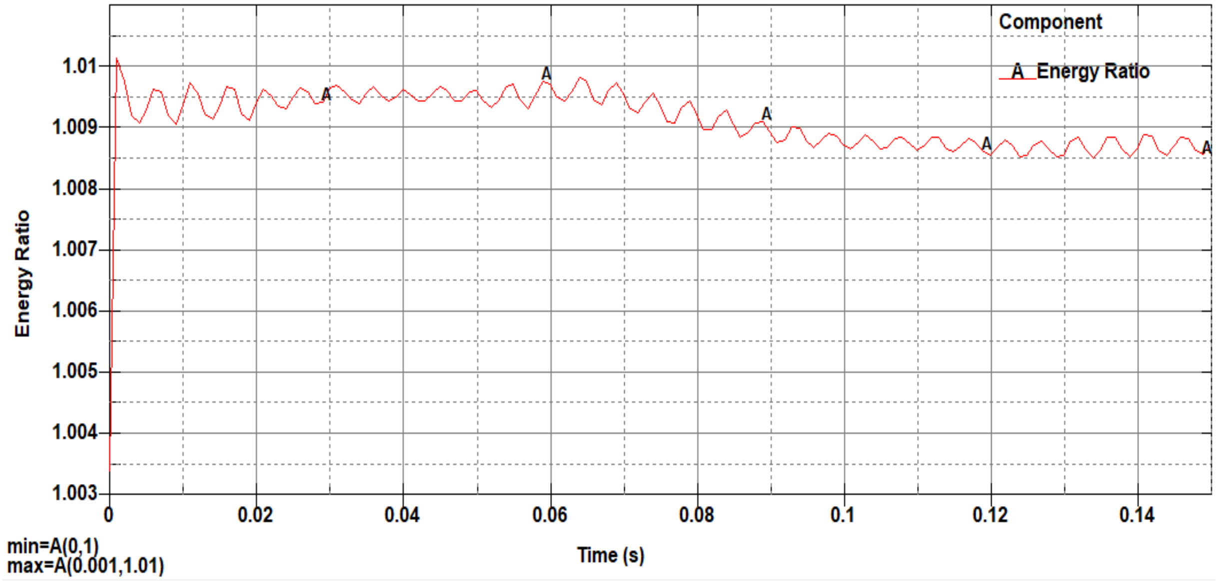

Figure 5.73 Energy ratio gr

Ratio of TE/HE

By analyzing the energy curve, the validity of the finite element model can also be judged from the relationship between total energy and hourglass energy. If the energy of the hourglass is less than 5% of the total energy, the finite element model is reliable. As shown in the figure 5.74-5.75. The peak of the hourglass is equal to 3.92kJ, the total energy is equal to 7.12kJ, and the HE/TE ratio is 0.55%, which is acceptable.

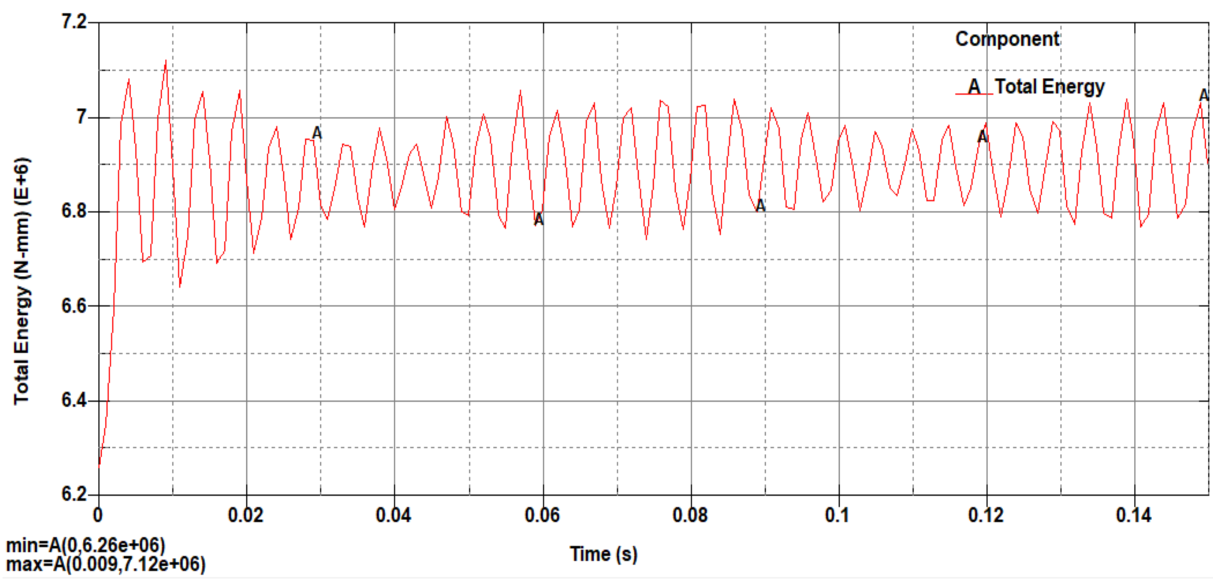

Figure 5.74 Total energy

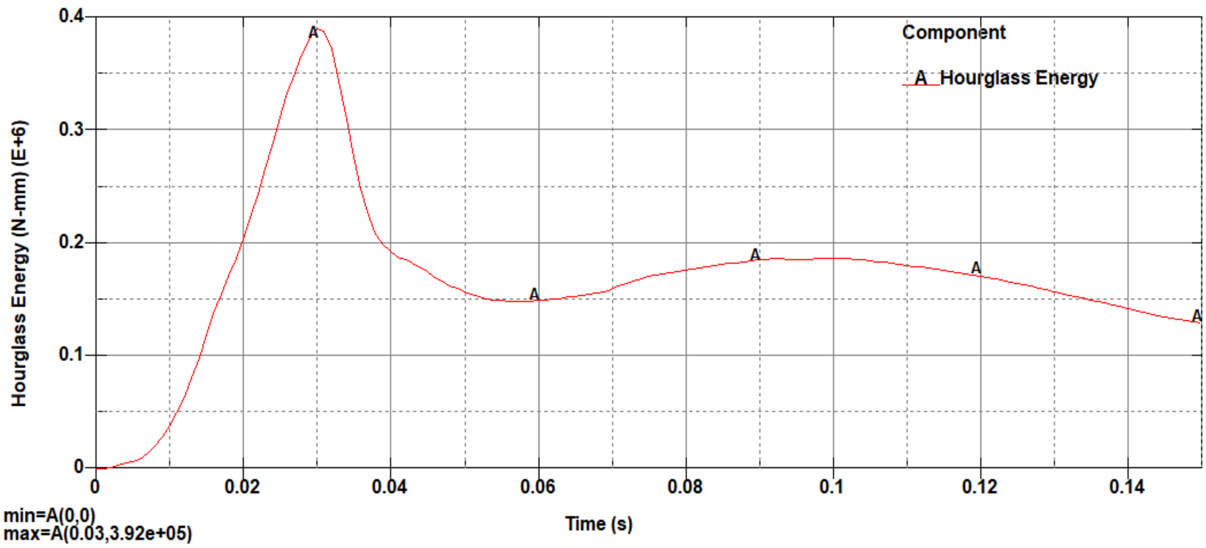

Figure 5.75 Hour glass energy

In general, a comparison of the existing (steel) model with the optimized bumper model is summarized in Table below. Vehicles with good collision protection structures absorb more energy with less deformation and impact force. As can be seen from table 5.1 the crashworthiness performance of a bumper is mainly depends up on the material used to produce, as compared from the existing bumper materials carbon-PA material bumpers provides better impact protection, Table 5.2 shows, the modified model deformation, impact force, and energy absorption results are better and from table 5.3, when the impact velocity increases deformation, energy absorption and impact forces are increased, but too much increasing causes the bumper fail to withstand the impact loads and violating the standards. Table 5.4 shows that as the thickness of the bumper increases the mass do so and causes for more inertia and too much decreasing the thickness means deformation increases highly and reaches to the interior vehicle parts, therefore as per the results we obtained the optimal thickness chosen is 3mm, table 5.5-5.6-5.7 describes the comparison between the existing and optimized model of automobile bumper crashworthiness parameters at different speed scenario and table 5.8 briefs the basic crashworthiness parameter result analysis for the two geometries of hallow and corrugated bumper, in this the corrugated geometry has good CFE and energy absorption with less crash stroke. Similarly as shown in table 5.9 the CFE is high for thickness of 3mm, even though the energy absorption capacity is increased with thickness but the rate is very small.

From this it can be concluded that the modified model has better crash safety performance in each crash scenario compared to the existing model.

Table 5.1Simulation results on different materials of bumper with a hollow geometry at velocity of 4KMPH

Criteria	The different materials of bumper			
	Al 6061 alloy	Al 7075 alloy	steel	CPA
Max. Deformation (mm)	24.5	19.6	20.2	15.8
Max. Energy absorption (J)	735	782	791	847
Max. Impact force (kN)	4.1O	4.87	9.78	3.21
Mass of bumper (kg)	6.56	6.63	18.5	8.3
.Resultant displacement (mm)	15.61	14.5	15.05	12.88
Von Misses stress (MPa)	483M	569	363.7	1480

Table 5.2 Tabular representation of analysis result of hollow and corrugated bumper geometry using CPA material at a velocity of 4KMPH

Criteria	Bumper geometry	
	hollow	corrugated
Maximum Deformation (mm)	15.8	13.5
Maximum Impact force (kN)	3.21	1.4
Maximum Energy absorption (J)	847	911
Max. Resultant displacement (mm)	12.88	17.75
Von Misses stress (MPa)	1480	1364

Table 5.3 Comparison of hollow and corrugated bumper model with CPA material at a velocity of 4KMPH, 5KMPH and 6KMPH

	4KMPH			**5KMPH**			**6KMPH**		
Criteria	hollow	corrugated	Percentage for corrugated	Hollow	corrugated	Percentage for corrugated	hollow	corrugated	Percentage for corrugated
Maximum Deformation (mm)	15.8	13.5	-17.03%	24.1	20.6	-16.99%	29.83	25.5	-16.98%
Maximum Energy absorption (J)	847	911	+7.02%	1269	1360	+6.69%	1690	1860	+9.14%
Von misses stress (MPa)	1480	1364	-8.53%	1578	1456	-8.38%	1606	1482	-8.36%

Table 5.4 Simulation results of different thicknesses of the CPA bumper with a corrugated geometry at a velocity of 4KMPH

Criteria	Thickness of bumper			
	4mm	3.5mm	3mm	2.5mm
Maximum Deformation (mm)	13.5	16.7	18.52	22.04
Maximum Impact force (kN)	1.49	1.41	1.38	1.5
Maximum Energy absorption (J)	911	908.2	906.7	905
Max. Resultant displacement (mm)	17.75	15.98	15.73	15.27
Von Misses stress (MPa)	1364	1391	1421	1447
Mass of bumper (kg)	8.82	7.13	6.12	5.51

Table 5.5 Tabular representation of analysis result between the existing (steel) and optimized model at a velocity of 4KMPH

Criteria	Existing model	Optimized model
Maximum Deformation (mm)	20.2	18.52
Maximum Impact force (kN)	9.78	1.38
Maximum Energy absorption (J)	791	906.7

Table 5.6 Tabular representation of analysis result between the existing (steel) and optimized model at a velocity of 5KMPH.

Criteria	Existing model	Optimized model
Maximum Deformation (mm)	29.7	24.2
Maximum Impact force (kN)	10.2	1.44
Maximum Energy absorption (J)	1060	1015.04

Table 5.7 Tabular representation of analysis result between the existing (steel) and optimized model at a velocity of 6KMPH

Criteria	Existing model	Optimized model
Maximum Deformation (mm)	36.77	29.3
Maximum Impact force (kN)	11.08	1.56
Maximum Energy absorption (J)	1270	1216

Table 5.8 Crashworthiness parameter result analysis of hollow and corrugated bumper geometry using CPA material at a velocity of 4KMPH

Criteria	Bumper geometry	
	hollow	corrugated
Crush stroke (mm)	15.8	13.5
Maximum Impact force (kN)	3.21	1.4
Total Energy absorption (TEA) (J)	847	911
Mass (kg)	8.3	8.82
F_{mean} (kN)	53.6	67.48
F_{max} (kN)	81.42	86.52
CFE (%)	65.83	77.99
SEA (J/kg)	102.04	103.28

Table 5.9 Crashworthiness parameter result analysis of different thicknesses of the CPA bumper with a corrugated geometry at a velocity of 4KMPH

Criteria	Thickness of bumper			
	4mm	3.5mm	3mm	2.5mm
Crush stroke (mm)	13.5	16.7	18.52	22.04
Maximum Impact force (kN)	1.49	1.41	1.38	1.5
Total Energy absorption (TEA) (J)	911	908.2	906.7	905
Mass of bumper	8.82	7.13	6.12	5.51
F_{mean} (kN)	67.48	54.38	48.95	41.06
F_{max} (kN)	86.52	69.94	60.04	54.05
CFE (%)	77.99	77.75	81.52	75.96
SEA (J/kg)	103.28	127.37	148.15	164.24

CHAPTER SIX

6. CONCLUSION AND RECOMMENDATION

6.1 Conclusions

This research focuses on the design optimization and FE analysis of automobile bumper with different material, geometrical shapes and thickness for Toyota Camry vehicles. The energy absorption is the most important thing to be considered in the design optimization process. The Toyota Camry automobile bumper and the whole vehicle is modeled and analyzed by LSDYNA software. Since the bumper model is subjected to an impact velocity of different magnitude and geometry, a rigid pole modeling is used for the analysis. The model is then analyzed by an explicit dynamic method using LSDYNA software. Among the two models (hallow and corrugated shapes) used for the explicit dynamic analysis, corrugated geometrical bumper model possesses slightly lower Von Misses stress value and the lower deformation compared to hallow geometry, which means that the corrugated geometry is the better bumper model. During the impact analysis maximum internal energy absorption is obtained in the corrugated geometry than the hallow one, corrugated geometry also shows the lowest deformation and the highest internal energy absorption during the explicit dynamic analysis in comparison with hallow geometry.

In the model analysis, the corrugated geometry shows the higher energy absorption than the hallow model. Therefor the result shows that corrugated bumper model has high energy absorption and least deformation as compared to hallow bumper model. During explicit dynamic analysis, the corrugated geometry gives the lower von misses stress value and deformation, due to the geometry of the model and the material that used in the analysis. From the previous analysis, we can conclude that corrugated geometry meets most of the requirements of high strength, higher energy absorption and stiffness than the hallow one. The corrugated geometry bumper model is used as the best and suitable models for minimization of injuries on the automobiles component as well as humans during an accident than hallow geometry.

The main findings are:

- ✓ The structure of the corrugated model created more living space than the hollow model by only deforming 13.5mm, while the hollow model deformed by 15.8 mm. This shows that the corrugated model provides 17.03% more protection for sensitive parts of the vehicle.
- ✓ When comparing the corrugated with the hollow model the energy absorption at 4 km/hr, 5 km/hr and 6 km/hr is increased by 64J, 91J and 170J respectively.
- ✓ The energy absorption capability of carbon polyamide bumper is improved from the existing steel and aluminum alloy bumper by 11.15% and 16.3% respectively and with this modification, the impact force is reduced from the existing steel bumper, which has 9.78kN and aluminum alloy bumper, which has 4.10kN to 1.86kN.
- ✓ the crashworthiness parameter result analysis showed that the corrugated bumper geometry had a structural energy absorption (SEA), total energy absorption (TEA) and crush force efficiency (CFE) of 103.28J/kg, 911J and 77.99%, which is higher than the hallow bumper geometry of 102.4 J/kg,847J and 65.83% respectively.
- ✓ As the thickness of carbon polyamide bumper reduced from 4mm to 3.5mm, 3mm and 2.5mm, correspondingly the weight reduced from 8.81kg to 7.71kg, 6.62 kg and 5.5kg respectively. With this reduction in thickness; deformation increased from 13.5 mm to 16.7, 18.52 and 22.04 respectively and von misses stress increases from 1364MPa to 1391MPa, 1421MPa and 1447MPa.
- ✓ The weight of the carbon polyamide bumper is reduced as we compare with the existing steel bumper by 9.7 kg or 47.5%, with this reduction in weight 38% increase in fuel economy**;** the energy absorption capability of carbon polyamide bumper is improved from the existing steel and aluminum bumper by 11.15% and 16.3% respectively.

6.2 Recommendation

Based on the studies done on this paper the following points are recommended:

- It has been observed that the safety of current vehicles can be changed with minor changes, so owners and manufacturers have some of the safety development concepts described in this document to improve the impact resistance of the vehicle and must be implemented.
- According to the survey, the damage to vehicles is large even at low speeds, so it is better for the government and related organizations to implement accident and safety regulations for vehicles mainly used in the passenger car segment.

6.3 Future work

During the analysis of the bumper, there were a lot of problems to be solved. However, due to the broad applications of the bumper, the analysis is limited to the automobile bumper analysis relating to the effect of impact velocity with a rigid body.

Based on the current and future accident in automobile vehicle and shortage of raw materials throughout the world, the broad study in minimizations of the injury and component failure invites the future works of different researchers. Among the potential area of problems that will be conducted, some of them are:

- Design and analysis of different preventive mechanism
- Redesign of the vehicle structure by considering best geometry of bumper
- Analyzing the effect of carbon polyamide material on environmental impact
- This work does not include how much the front components of the vehicle such as fuel tank, radiator and others affected, so the effect of front collision on front components of the vehicle can be studied
- Impact testing of carbon polyamide experimentally with different velocity.

REFERENCES

Abbood, I. S., aldeen Odaa, S., Hasan, K. F., & Jasim, M. A. (2021). Properties evaluation of fiber reinforced polymers and their constituent materials used in structures–A review. Materials Today: Proceedings, 43, 1003-1008.

Abedini, M., & Zhang, C. (2021). Performance assessment of concrete and steel material models in ls-dyna for enhanced numerical simulation, a state of the art review. Archives of Computational Methods in Engineering, 28(4), 2921-2942.

Al-Graitti, A. (2019). Auto rickshaw impacts with pedestrians-a computational analysis of post-collision kinematics and injury mechanics. Cardiff University,

Amintowlieh, Y., Sardashti, A., & Simon, L. C. (2012). Polyamide 6–wheat straw composites: effects of additives on physical and mechanical properties of the composite. Polymer Composites, 33(6), 976-984.

Anderson, J. M., Nidhi, K., Stanley, K. D., Sorensen, P., Samaras, C., & Oluwatola, O. A. (2014). Autonomous vehicle technology: A guide for policymakers: Rand Corporation.

Andersson, R., Schedin, E., Magnusson, C., Ocklund, J., & Persson, A. (2002). The applicability of stainless steel for crash absorbing components. SAE Transactions, 1918-1922.

Aseer, J., & Sankaranarayanasamy, K. (2017). Effect of fiber content on tensile retention properties of Cellulose Microfiber Reinforced Polymer Composites for Automobile Application. Paper presented at the IOP Conference Series: Materials Science and Engineering.

Begum, S., Ahmed, G. M. S., Badruddin, I. A., Tirth, V., & Algahtani, A. (2019). Analysis of digital light synthesis based flexible and rigid polyurethane for applications in automobile bumpers. Materials Express, 9(8), 839-850.

Belingardi, G., Beyene, A., Koricho, E., & Martorana, B. (2015). Alternative lightweight materials and component manufacturing technologies for vehicle frontal bumper beam. Composite Structures, 120, 483-495.

Bohra, B. A., Pawar, B., & Bargat, S. (2014). Comparative analysis of frontal car bumper during impact. Int J of Appl or Innov in Engg & Management, 3.

Can, B. (2016). Evaluation of tabbed composite specimens for material characterization under medium loading rates: a numerical study. Wichita State University, Costas, M., Díaz, J., Romera, L., & Hernández, S. (2014). A multi-objective surrogate-based optimization of the crashworthiness of a hybrid impact absorber. International Journal of Mechanical Sciences, 88, 46-54.

da Silva, E. P., da Silva, F. M., & Magalh, R. R. (2014). Application of finite elements method for structural analysis in a coffee harvester. Engineering, 2014.

Dange, M. V., Buktar, R. B., & Raykar, N. R. (2015a). Design and analysis of an automotive front bumper beam for low-speed impact. IOSR J. Mech. Civil Eng., 12, 17-27.

Dange, M. V., Buktar, R. B., & Raykar, N. R. (2015b). Design and analysis of an automotive front bumper beam for low-speed impact. IOSR Journal.

Davoodi, M., Sapuan, S., Ahmad, D., Aidy, A., Khalina, A., & Jonoobi, M. (2011). Concept selection of car bumper beam with developed hybrid bio-composite material. Materials & Design, 32(10), 4857-4865.

Ezekwem, D. (2016). Composite Materials Literature review for Car bumber.

Fagnant, D. J., & Kockelman, K. (2015). Preparing a nation for autonomous vehicles: opportunities, barriers and policy recommendations. Transportation Research Part A: Policy and Practice, 77, 167-181.

G Keni, L., Singh, V., Singh, N., Thyagi, A., Kalburgi, S., & KN, C. (2021). Conceptual design and analysis of a car bumper using finite element method. Cogent Engineering, 8(1), 1976480.

Gao, D., Liang, H., Shi, G., & Cao, L. (2019). Multiobjective optimization of carbon fiber-reinforced plastic composite bumper based on adaptive genetic algorithm. Mathematical Problems in Engineering, 2019.

Gholipour, G., Zhang, C., & Mousavi, A. A. (2020). Nonlinear numerical analysis and progressive damage assessment of a cable-stayed bridge pier subjected to ship collision. Marine Structures, 69, 102662.

Gouasmi, M., Ouali, M., Fernini, B., & Meghatria, M. h. (2012). Kinematic modelling and simulation of a 2-R robot using solidworks and verification by MATLAB/Simulink. International Journal of Advanced Robotic Systems, 9(6), 245.

Gulavani, O., Hughes, K., & Vignjevic, R. (2014). Explicit dynamic formulation to demonstrate compliance against quasi-static aircraft seat certification loads (CS25.

561)–part I: influence of time and mass scaling. Proceedings of the Institution of Mechanical Engineers, Part G: Journal of Aerospace Engineering, 228(11), 1982-1995.

GV, A. S., Reddy, P. S., Manoj, M., & Bhaskar, P. (2014). Impact analysis of a car bumper using carbon fiber reinforced PEI and S2 glass/epoxy materials by solid works software. International Journal of Science Engineering and Advance Technology, 2(10), 565-569.

Hu, Y., Liu, C., Zhang, J., Ding, G., & Wu, Q. (2015). Research on carbon fiber–reinforced plastic bumper beam subjected to low-velocity frontal impact. Advances in Mechanical Engineering, 7(6), 1687814015589458.

Jacob, A. B., & Arunkumar, O. (2016). Improving the crashworthiness of an automobile bumper. Paper presented at the International conference on emerging trends in engineering and management.

Jeyanthi, S., Paul ChandraKumar, J., Rajesh Kumar, N., Dhinakaran, S., & Hari Prasad, K. (2014). An investigation on dynamic mechanical analysis and low velocity impact analysis of natural thermoplastic composite frontal beams. International Journal of Applied Engineering Research, 9(22), 13709-13718.

John, A., & Nidhi, M. (2014). Modelling and analysis of an automotive bumper used for a low passenger vehicle. Int. J. Eng. Trend. Tech., 15, 344-353.

Kausar, A. (2019). Advances in carbon fiber reinforced polyamide-based composite materials. Advances in Materials Science, 19(4), 67-82.

KHAN, R. A. (2021). Crashworthiness Characteristics Of Gfrp Overwrapped Pvc Composite Tubes.

Kokate, V., Uttekar, S. S., Karandikar, P., & Holmukhe, R. (2020). Retrofitting of auto rickshaw to e-rickshaw-a feasibility study. Paper presented at the 2020 First International Conference on Power, Control and Computing Technologies (ICPC2T).

Kutz, M. (2011). Applied Plastics Engineering Handbook: Processing and Materials, ; William Andrew. Inc.: New York, NY, USA.

Lad, A. C., & Rao, A. (2014). Design and drawing automation using solid works application programming interface. International Journal of Emerging Engineering Research and Technology, 2(7), 157-167.

Magalhaes, R., Fontes, C., & de Melo, S. V. (2012). Stress analysis of a front bumper fascia using the boundary element method. Engineering analysis with boundary elements, 36(8), 1296-1300.

Marzbanrad, J., Alijanpour, M., & Kiasat, M. S. (2009). Design and analysis of an automotive bumper beam in low-speed frontal crashes. Thin-walled structures, 47(8-9), 902-911.

Meng, N., Ren, X., Santagiuliana, G., Ventura, L., Zhang, H., Wu, J., . . . Bilotti, E. (2019). Ultrahigh β-phase content poly (vinylidene fluoride) with relaxor-like ferroelectricity for high energy density capacitors. Nature communications, 10(1), 1-9.

Mohan, P. (2013). A critical review: the modification, properties, and applications of epoxy resins. Polymer-Plastics Technology and Engineering, 52(2), 107-125.

Motgi, N. S., Naik, S., & Kulkarin, P. (2013). Impact analysis of front bumper. Int. J. Eng. Trends Technol, 6, 287-291.

Muhammad Nasiruddin, S., Hambali, A., Rosidah, J., Widodo, W., & Ahmad, M. (2017). A review of energy absorption of automotive bumper beam. International Journal of Applied Engineering Research, 12(2), 238-245.

Ning, H., Lu, N., Hassen, A. A., Chawla, K., Selim, M., & Pillay, S. (2020). A review of long fibre thermoplastic (LFT) composites. International Materials Reviews, 65(3), 164-188.

Pandey, R., Singh, P., Khanna, M., & Murtaza, Q. (2021). Metal Foam Manufacturing, Mechanical Properties and Its Designing Aspects—A Review. Advances in Manufacturing and Industrial Engineering, 761-770.

Patil, P. R., & Kadam, G. A. (2017). Overview on Comparative Study of Characterization of Properties of Natural Fiber Composites.

Patil, R., Lande, P., Tadamalle, A., & Reddy, Y. (2017). Determination of impact absorbing capacity and toughness of aluminum honeycomb sandwich panel in bumper beam. Materials Today: Proceedings, 4(8), 8816-8826.

Pawlus, W., Karimi, H. R., & Robbersmyr, K. G. (2014). Investigation of vehicle crash modeling techniques: theory and application. The International Journal of Advanced Manufacturing Technology, 70(5), 965-993.

Prabhakaran, S., Chinnarasu, K., & Kumar, M. S. (2012). Design and fabrication of composite bumper for light passenger vehicles. International Journal of Modern Engineering Research, 2(4), 2552-2556.

Purohit, R., Khitoliya, P., & Koli, D. K. (2014). Design and finite element analysis of an automotive clutch assembly. Procedia materials science, 6, 490-502.

Rackauskaite, E., Kotsovinos, P., & Rein, G. (2017). Model parameter sensitivity and benchmarking of the explicit dynamic solver of LS-DYNA for structural analysis in case of fire. Fire Safety Journal, 90, 123-138.

Raj Kumar, G., Balasubramaniyam, S., Senthil Kumar, M., Vijayanandh, R., Raj Kumar, R., & Varun, S. (2019). Crash Analysis on the Automotive Vehicle Bumper. International Journal of Engineering and Advanced Technology, 8(6S3), 1602-1607.

Ramyasree, L., Venkataramaniah, D., & Kumar, G. N. (2015). Impact analysis of frontal car bumper using long fibre reinforced thermoplastics. International Journal of Current Engineering and Technology, 55(33), 2277-4106.

Ryan, S., Hedman, T., & Christiansen, E. L. (2009). Honeycomb vs. foam: evaluating a potential upgrade to international space station module shielding for micrometeoroids and orbital debris. NASA Johnson Space Center, Houston, NASA/TM-2009-214793.

Samuel, R., Asadi, M., Tarda, A., Simbotin, G., & Markopoulos, A. (2021). Validating dynamic crush response of unidirectional carbon fibre tube via finite element analysis method using LS-DYNA. Paper presented at the IOP Conference Series: Materials Science and Engineering.

Sarfraz, M. S., Hong, H., & Kim, S. S. (2021). Recent developments in the manufacturing technologies of composite components and their cost-effectiveness in the automotive industry: A review study. Composite Structures, 266, 113864.

Singh, N. K., & Singh, K. (2015). Review on impact analysis of FRP composites validated by LS-DYNA. Polymer Composites, 36(10), 1786-1798.

Smith, B., Szyniszewski, S., Hajjar, J., Schafer, B., & Arwade, S. (2012). Steel foam for structures: A review of applications, manufacturing and material properties. Journal of Constructional Steel Research, 71, 1-10.

Sonawane, C. R., & Shelar, A. L. (2018). Strength enhancement of car front bumper for slow speed impact by FEA method as per IIHS regulation. Journal of The Institution of Engineers (India): Series C, 99(5), 599-606.

Tay, Y. Y., Papa, A., Koneru, L., Moradi, R., & Lankarani, H. M. (2015). A finite element approach in estimating driver fatality ratio of a fleet of LTVs striking a passenger car based on vehicle's intrusion, acceleration and stiffness ratios in side-impact accidents. Journal of Mechanical Science and Technology, 29(3), 1231-1242.

Uddandapu, P. K. (2013). Impact analysis on car bumper by varying speeds using materials ABS Plastic and Poly Ether Imide by Finite Element Analysis software solid works. Int. J. Mod. Eng. Res, 3, 391-395.

Wang, T., & Li, Y. (2015). Design and analysis of automotive carbon fiber composite bumper beam based on finite element analysis. Advances in Mechanical Engineering, 7(6), 1687814015589561.

Wei, L., Jia, Y., Xiangdong, L., Lei, X., Xingwang, L., & Jing, Y. (2016). Optimization Design of Inner Structure and Material of Cars Front Bumper Based on Finite Element Method.

Yalkın, H. E., Karakuzu, R., & Alpyıldız, T. (2020). Experimental and numerical behaviors of GFRP laminates under low velocity impact. Journal of Composite Materials, 54(21), 2999-3007.

Zhang, X. (2020). Crashworthiness Characterisation of the Car Front Bumper System Based on FEA Analysis.

Zhong, W., Ding, Y.-l., Song, Y.-s., & Geng, F.-f. (2019). Relaxation Behavior of Residual Stress on Deck-to-Rib Welded Joints by Fatigue Loading in an Orthotropic Bridge Deck. Periodica Polytechnica Civil Engineering, 63(4), 1125-1138.

Zhu, G., Liao, J., Sun, G., & Li, Q. (2020). Comparative study on metal/CFRP hybrid structures under static and dynamic loading. International Journal of Impact Engineering, 141, 103509.

Zhu, G., Wang, Z., Cheng, A., & Li, G. (2017). Design optimisation of composite bumper beam with variable cross-sections for automotive vehicle. International journal of crashworthiness, 22(4), 365-376.

APPENDIX

APPENDIX A: LS-DYNA Results

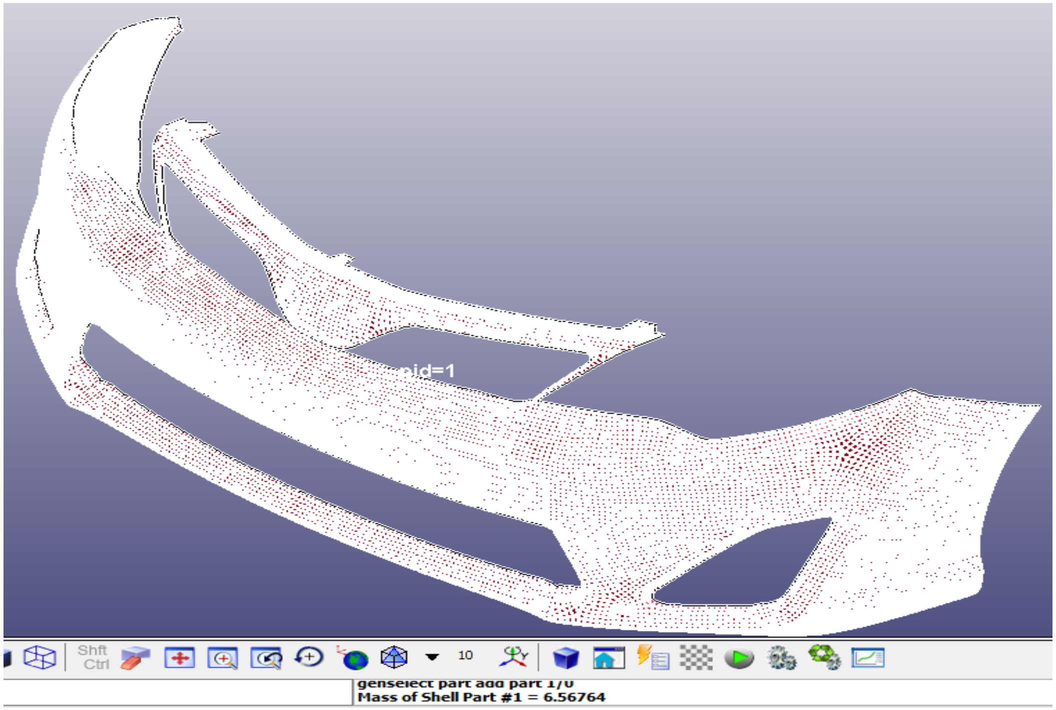

Fig (a) 1 mass of Al 6061 alloy hallow bumper

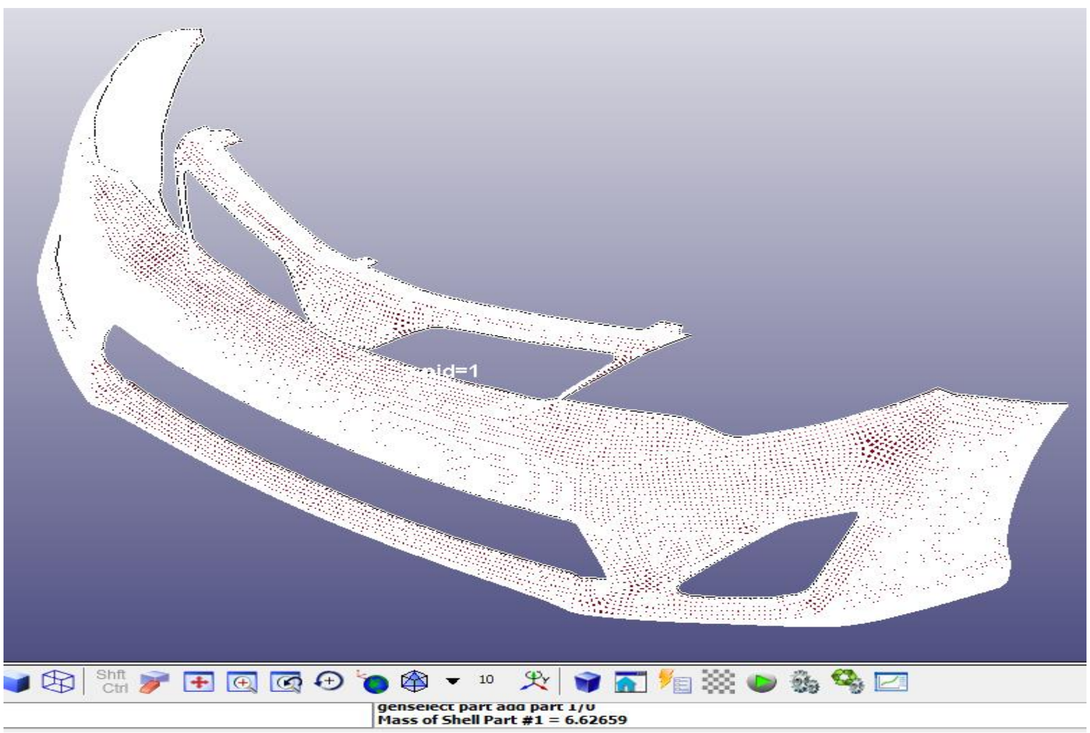

Fig (a) 2 mass of Al 7075 alloy hallow bumper

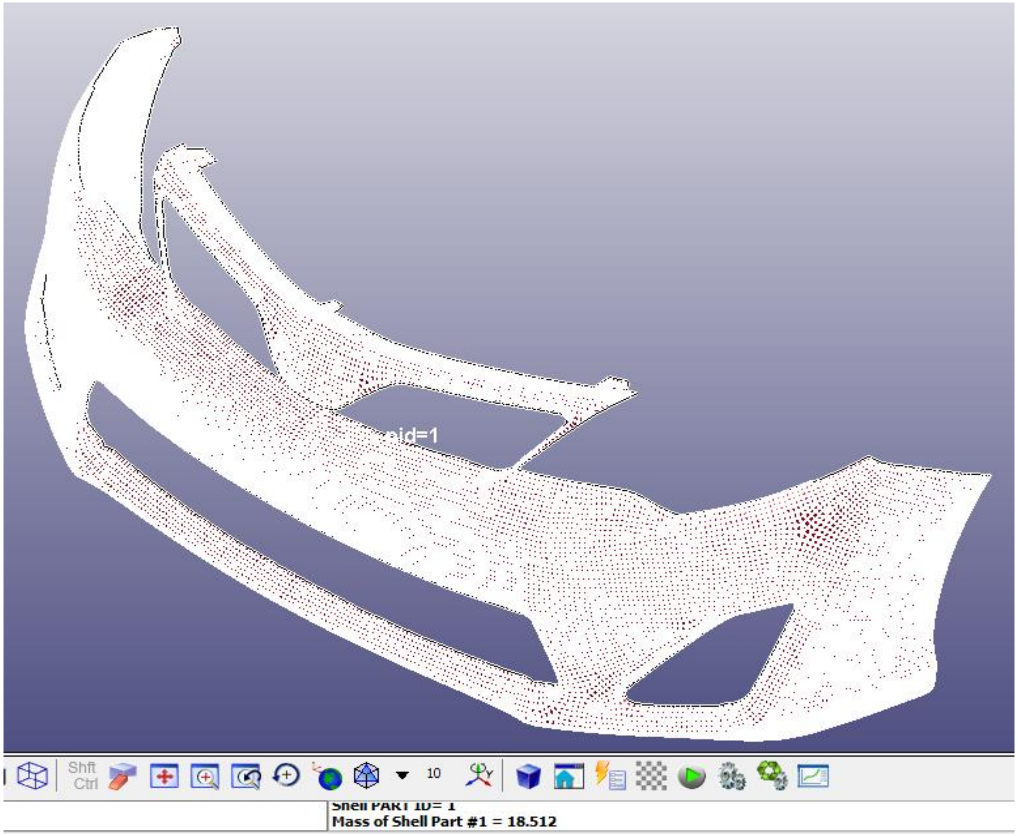

Fig (a) 3 mass of steel hallow bumper

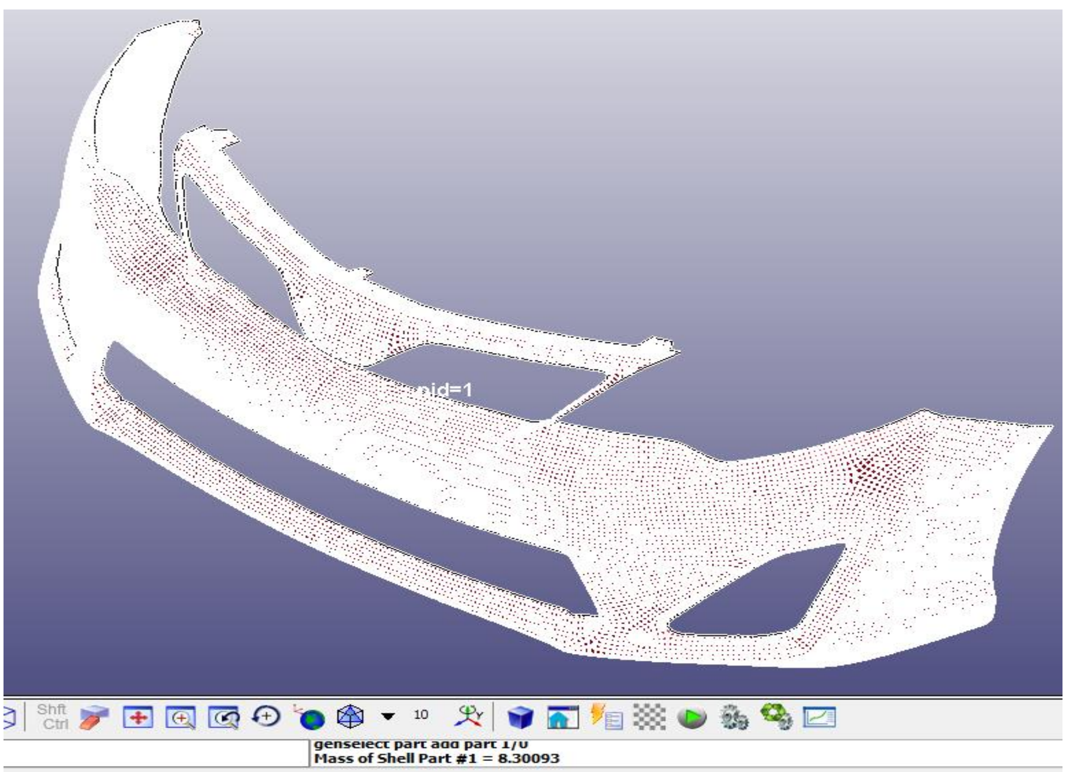

Fig (a) 4 mass of CPA hallow geometry bumper

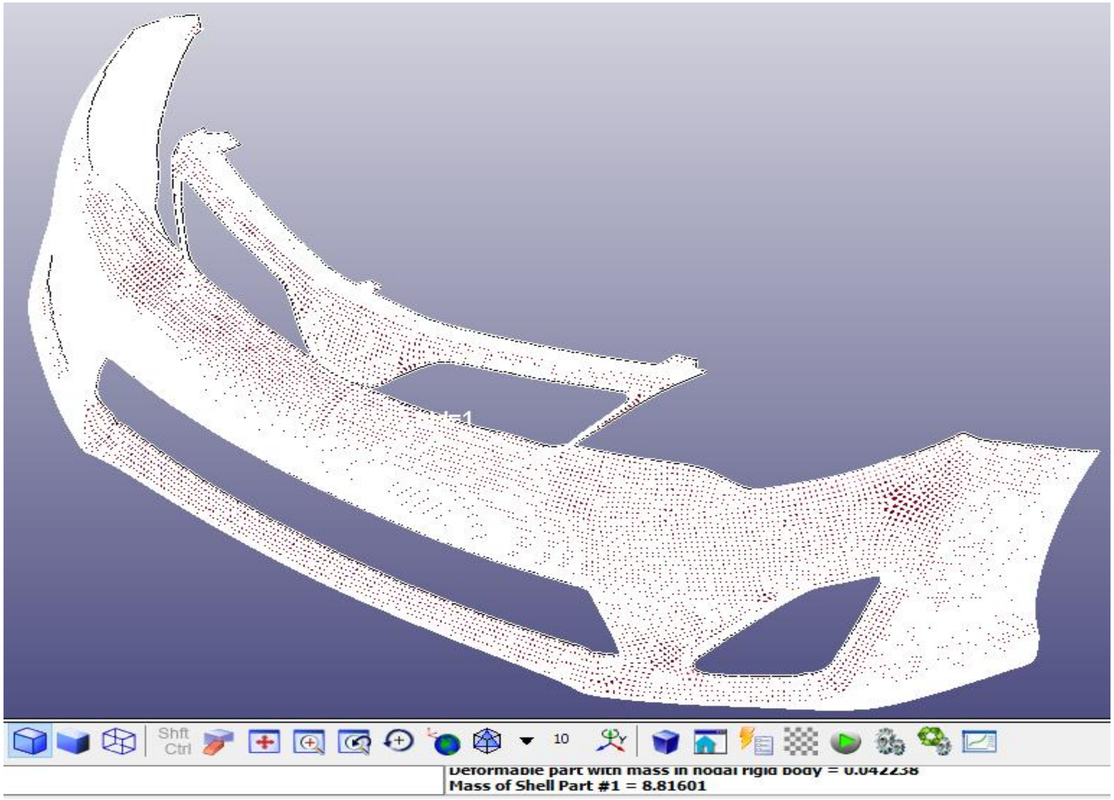

Fig (a) 5 mass of CPA corrugated geometry bumper

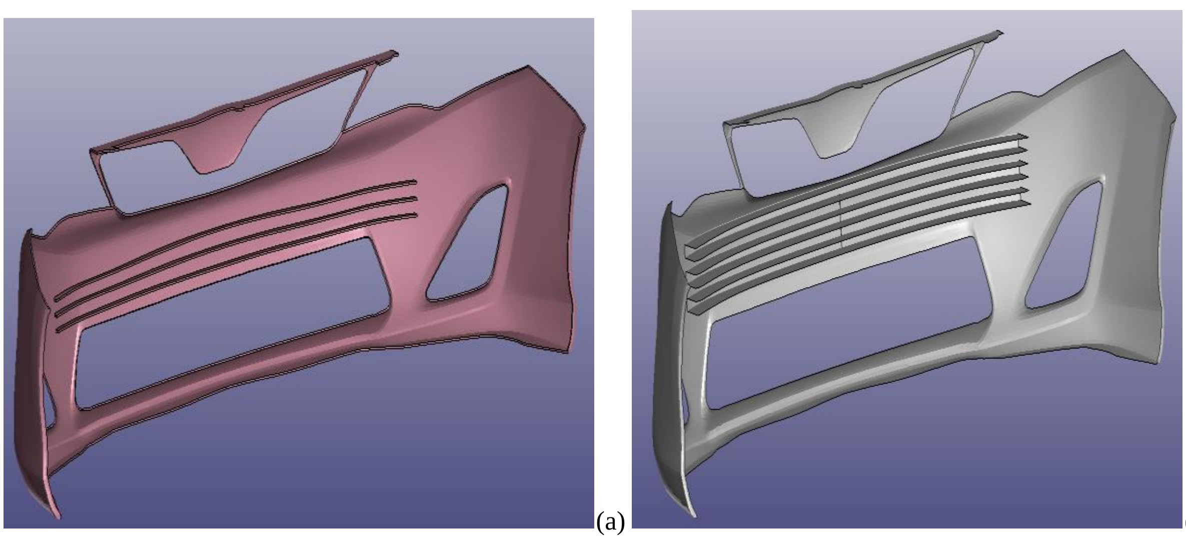

(a) (b)

Fig (a) 6 (a) rectangular section and (b) C-section reinforced bumper

Rectangular cross section is used as cross section of the bumper which is superior in load carrying capacity compared to C-section reinforced bumper. It also provides good fitting space with the bumper structure when making modification.

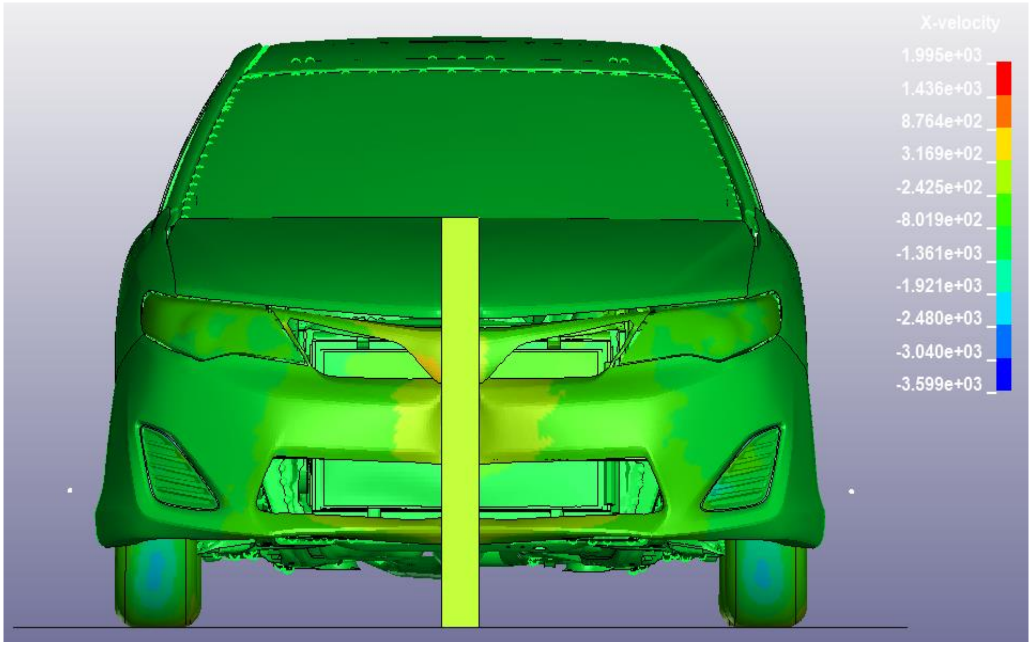

Fig (a) 7 X-velocity of the whole vehicle structure

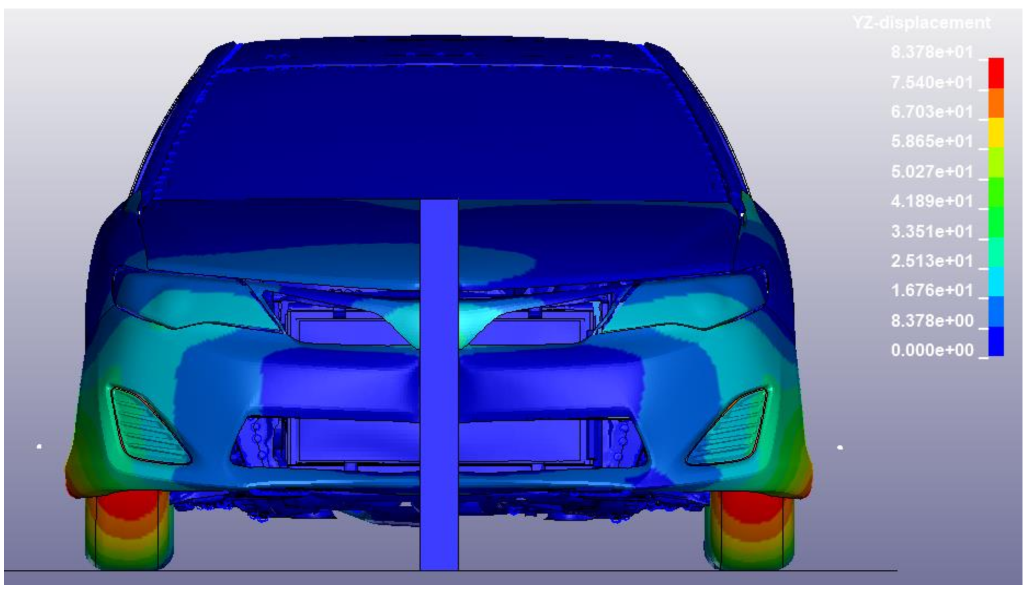

Fig (a) 8 YZ-displacement of the vehicle after collision

Table (a) 1 the quality checks are based on angles (like skew, included angles) while others on side and area ratios and uses as a reference to check the quality of any model (Rahman & Babu, 2019).

Quality Name	Minimum. Value	Maximum. value	Allowable	#Violated(%)
Min side length	0	0	3	0(0%)
Max side length	0	0	30	0(0%)
Aspect Ratio	1	9.77	5	10(0.000818%)
Warpage	0	180	15	331(0.0271%)
Min Quad Angle	20	90	45	214(0.0175%)
Max Quad Angle	0	0	135	0(0%)
Min Tria Angle	0	0	30	0(0%)
Max Tria Angle	0	0	120	0(0%)
Taper	0	0	0.7	0(0%)
Skew	0	58.6	45	44(0.0036%)
Jacobian	-0.0617	1	0.6	643(0.0526%)
Char. length	0	0	1	0(0%)
Area	0	0	5	0(0%)
Feature angle	0	0	30	0(0%)
Time Step	0	0	1.00E-06	0(0%)

APPENDIX B:

Vehicle traffic accident in Ethiopia

Table (b) 1 road traffic accident analysis for different types of vehicles in Ethiopia

year	bicycle	motor cycle	automobile	Small wagon	pickup	truck
2006E.C	150	562	5652	2082	3100	1852
2007E.C	284	747	5,236	2,487	3,220	2,055
2008E.C	128	1,349	4,239	2,309	3,714	1,516
2009E.C	127	881	4,963	2,369	4,950	3,215
2010E.C	113	1,671	6,701	2,375	5,785	3,287
2011E.C	122	1,311	7,299	2,601	4,928	2,745
2012E.C	194	1,146	8,952	2,549	3,799	2,715

year	taxi	bus up to 120	bus 13-45	bus above 46	cart	others
2006E.C	4864	3142	1269	804	288	305
2007E.C	7,588	3,508	1,285	699	468	348
2008E.C	9,443	3,441	1,740	917	379	319
2009E.C	7,927	4,830	2,232	1,048	175	706
2010E.C	6,476	4,702	3,249	667	171	962
2011E.C	8,284	5,082	2,267	966	132	533
2012E.C	6,672	5,449	1,745	1,345	180	491

Table (b) 2 Ten years average traffic accident analysis between private and public means of transports according to Ethiopian federal police commission

Parameters	Private transport vehicles	Public transportation vehicles
Death	403.4	1237.1
Serious injury	978	1576.3
Slight injury	617.7	1371
Property damage	5976.5	7396.5

Table (b) 3 Type of Vehicles and Number in the Regions (up to tahsas 30.2013) Registration

Description	AA	AM	AF	BN	DD	SO	TG	GM	HA	SN	OR	Total
Ambulance	322	0	88	55	6	45	187	0	4	61	525	1293
Automobile	255793	1786	85	54	2413	648	1994	0	1303	102	5670	269848
Bajaji	0	9308	4306	0	3302	0	0	1439	4909	11595	60847	957060
Tri cycle	0	0	0	0	0	0	0	0	0	0	0	0
Bus (<12seats)	31330	9197	492	390	1666	979	5656	2125	80	13431	28513	93859
Bus (>11seats)	19206	13953	698	511	860	871	4473	859	3000	10869	37549	92849
Combiner	106	54	0	0	2	1	5	0	0	0	82	250
Dozer	16	0	0	3	0	1	4	0	0	0	0	24
Dry cargo (<10 Quintal)	52338	3597	347	106	1083	1104	1298	0	0	1659	2069	63601
Dry cargo (>10 Quintal)	139376	3653	262	115	4670	2604	5148	0	0	3731	8119	167678
Dual Purpose	56063	4068	476	342	1704	989	2266	0	56	1453	2968	70385
Field Vehicle	53233	1835	384	161	524	1148	1282	0	300	154	3206	62227
Grader	6	2	0	0	2	1	4	0	0	0	0	17
Forklift	351	0	4	1	10	1	18	0	0	0	2	387
Not Specified	21185	1532	72	58	291	511	397	0	0	126	1251	25423
Gotach	7235	0	0	0	67	5	624	0	0	0	0	7931
Liquid Cargo	8307	313	38	2	244	186	658	0	0	67	183	9998
Liquid Trailer	0	14	0	0	0	0	0	0	0	0	171	185
Motor Bicycle	28235	45137	1389	6920	8111	1651	14405	2643	1076	78463	62129	250159
Other	12526	718	35	39	137	33	485	0	0	44	4277	18294
Three-Wheeler dry load	17	42	0	56	10	250	1874	0	0	0	4	2253
Three-Wheeler public	350	10311	0	2959	0	8523	16647	0	0	0	0	38790
Tractor	1505	401	54	143	21	0	317	0	0	17	526	2984
Trailer	32676	360	8	1	450	1	2913	0	0	1	377	36787
Vehicle with machine	1004	153	20	1	134	27	145	0	0	0	0	1484
Total	721180	106434	8758	11917	25707	19579	60800	7066	10728	121773	218470	1312412